# STATIC, STABILITY AND VIBRATION ANALYSIS OF LAMINATED COMPOSITE PLATES USING HIGHER ORDER THEORY WITH FINITE ELEMENT DISCRETIZATION

ASHOK KUMAR GHOSH

# STATIC, STABILITY AND VIBRATION ANALYSIS OF LAMINATED COMPOSITE PLATES USING HIGHER ORDER THEORY WITH FINITE ELEMENT DISCRETIZATION

A THESIS SUBMITTED TO THE
INDIAN INSTITUTE OF TECHNOLOGY, KHARAGPUR
FOR THE AWARD OF THE DEGREE
OF

**Doctor of Philosophy**

BY

**ASHOK KUMAR GHOSH**

DEPARTMENT OF CIVIL ENGINEERING
INDIAN INSTITUTE OF TECHNOLOGY
KHARAGPUR

1992

# CONTENTS

# CERTIFICATE

This is to certify that the thesis entitled **'Static, Stability and Vibration Analysis of Laminated Composite Plates Using Higher Order Theory With Finite Element Discretization'** that is being submitted by Ashok Kumar Ghosh to Indian Institute of Technology, Kharagpur for the award of the degree of Doctor of Philosophy in Engineering is a record of bona fide research work carried out by him under my supervision and guidance.

Mr. Ghosh has worked on the problem for the last three years and the thesis is, in my opinion, worthy of consideration for the award of the degree of Doctor of Philosophy in accordance with the regulations of the Institute.

The results embodied in this thesis have not been submitted to any other University or Institute for the award of any Degree or Diploma.

Kharagpur
June 25, 1992

(SANTI SEKHAR DEY)
Professor
Civil Engineering Department
Indian Institute of Technology, Kharagpur

# ACKNOWLEDGEMENTS

I take the opportunity to express my sincerest gratitude to my supervisor Professor Santi Sekhar Dey for his interest and guidance throughout the course of this work. It was a great experience working with him from which I learnt precious things about plates and shells, in the broadest sense of the term.

I enjoyed encouragement from all faculty members, especially Prof. P.K.Datta and Prof. N.Mondal. Special thanks are due to Prof. Amalendu Mukherjee and Prof. R.Karmakar for providing facilities of experimental work in the Machine Dynamics Laboratory of Mechanical Deptt. In Prof. A.P.Gupta and Prof. B.B.Pandey I have always found wholehearted appreciation, cooperation and sympathy.

It was a great pleasure to work with Dr. Nishit Mondal, Dr. Ranjan Bhattacherya, Mr. Asoke Bhar, Mr. S.K.Bhattacherya and Mr. Nirjhar Dhang. I benefited greatly sharing ideas, experience and strain at several stages of experimentation with Mr. N.C.Pal. The help rendered by Mr. Tapesh Mukherjee in experimental work is acknowledge with thanks.

Mr. Kishore Biswal was kind enough to go through the manuscript carefully. The author is thankful to him.

Thanks are due to staff of the Structural Laboratory of Civil Engg. Deptt. for preparation of the experimental set-up and the test models and making the experimentation a success.

This leaf would remain incomplete if I do not record the appreciation of the understanding, inspiration and support I received from my wife Mrs. Pritha Ghosh and son Master Rik for whatever I am today.

Ashok kumar Ghosh

(Ashok Kumar Ghosh)

Kharagpur

June 25, 1992

# ABSTRACT

A simple four-noded rectangular element with seven degrees of freedom at each node is developed for the analysis of flexible laminated and sandwich plate structures having a constant thickness of any individual layer. Theoretical formulation is based on simplified higher order shear deformation theory with non-linear displacement distribution through the thickness. The conditions of zero transverse shear stresses are imposed at the outer surfaces of the plate to reduce the number of generalised displacement parameters.

The displacement model is so chosen that it can explain adequately the parabolic distribution of transverse shear stresses and the non-linearity of in-plane displacements across the thickness.

In the finite element modelling, the in-plane displacements and two shear rotations are interpolated over an element by bilinear shape functions. A set of non-comforming shape function is used for the transverse deflection.

The element developed, has been applied to study rectangular plates with following aspects:

(i) static analysis of laminated and sandwich plates;
(ii) free vibration analysis of laminated plates;
(iii) static stability analysis of laminated plates.

A wide range of plates, thick to thin are examined for different loadings and boundary conditions. The results are compared with the existing analytical and numerical solutions.

To further establish the wide range applicability of the element developed, experimental verification of static deflection and free vibration frequencies of laminated plates are conducted in the laboratory.

As a part of the research program, development of a new composite was conceived with a view to fabricate a low cost composite material from locally available materials. Preliminary analysis demonstrates encouraging results.

Keywords:

Bilinear shape function; composite; eigenvalue; eigenvector; free vibration frequency; fiber; finite element method; laminates; low-cost and local material; matrix; mode shapes; non-conforming shape function; nodes; shear deformation theory; stability.

# LIST OF SYMBOLS

| | |
|---|---|
| $x, y, z$ | cartesian coordinates |
| $r, s$ | natural coordinates |
| $a, b$ | plate dimensions |
| $t$ or $h$ | plate thickness |
| $\lambda$ | aspect ratio |
| $U, V, W$ | displacements along x, y and z directions |
| $U_o, V_o, W_o$ | above displacements on mid plane |
| $\varphi_x$, $\varphi_y$ | rotation of normal to the mid plane about y and x axis |

$U_{,z} = \delta U/\delta z$, $U_{,z^2} = \delta^2 U/\delta z^2$ and $N_{1\,,x} = \delta N_1/\delta x$

| | |
|---|---|
| $\theta$ | angle between fiber direction and x axis |
| $E_{11}, E_{22}$ | mod. of elasticity along longitudinal and transverse direction |
| $G_{12}, G_{23}$ | rigidity modulus |
| $\nu_{12}$, $\nu_{21}$ | Poisson's ratios |
| $N_x$, $M_x$, $P_x$ | stress resultants |
| $\sigma$ | normal stress |
| $\tau$ | shear stress |
| $\varepsilon$ | strains |
| $\{\delta\}$ | displacement vector |

| | |
|---|---|
| $[C]$ | constitutive matrix |
| $[D]$ | stress resultant-strain matrix |
| $[B]$ | strain-nodal DOF relations |
| $[K]$ | stiffness matrix |
| $\{N\}$ | stress resultant vector |
| $N_i$ | interpolation functions(i=1,2,3,4) |
| $\|J\|$ | determinant of the Jacobian matrix |
| $w_i, w_j$ | Gaussian weights |
| $\{F\}$ | load vector |
| $q_o$ | load intensity |
| $U_e$ or $\pi$ | total strain energy |
| $\rho$ | mass density |
| K | kinetic energy |
| dt | time increment |
| $[M]$ | mass matrix |
| $I_1$ | normal inertia |
| $I_2$ | rotational inertia |
| U.D.L. | uniformly distributed load |
| F.E. | finite element |
| $[K_E]$ | elastic stiffness matrix |
| $[K_G]$ | geometric stiffness matrix |

# LIST OF FIGURES

# LIST OF TABLES

# LIST OF PHOTOGRAPHS

# CHAPTER 1

# INTRODUCTION

## 1.1 General

Many advanced technology systems demand materials with unusual combination of properties that cannot be achieved with the conventional metal alloys, ceramics and polymeric materials, especially the materials that are needed for aerospace, underwater and transportation applications. For example, Aerospace engineers are increasingly searching for structural members that are : strong, stiff, abrasion and impact resistant, not easily corroded but at the same time possess low densities. This is a rather formidable combination of characteristics. Frequently strong materials are relatively dense; also, increasing the strength or stiffness generally results in a decrease in impact strength.

The concept of using two or more elemental materials combined to form the constituent phases of a composite solid has been employed ever since materials were first used. The earliest use of mud and clay mixed up with hair, straw and chopped vegetable fibers as reinforcement materials is an ideal example of man's endeavour to improve building materials. The goals for composite development have been to achieve a combination of properties not achievable by any of

the elemental materials acting alone; thus a solid could be prepared from constituents so that they can be tailor made to meet specific design requirement.

In fiber reinforced composites, fibers are the principal load carrying elements, while the surrounding matrix keeps them in the desired location and orientation, acts as a load transfer medium between them, and protects them from harsh environment involving elevated temperature and aggressive conditions.

Recognizing the immense potential of composite materials, the last few decades have seen phenomenal advances in research and development of composite materials with new and exciting structural possibilities. Composites have gone far beyond being simply lighter than conventional materials. A weight saving of upto 40 to 50 % over conventional materials can be achieved in some structural components and they can withstand a very high temperature. Composites can no longer be considered as specialised, esoteric materials, only of interest to researchers in material science. Rather they have firmly established themselves as real and viable materials of construction with wide ranging applications.

Composites can occur in nature, and they can also be made artificially. An example of the natural occurance of composites is wood which consists of strong and flexible cellulose fibers surrounded and held together by a stiffer material called lignin. Also, bone is a composite of the strong yet soft protein collagen and the hard, brittle mineral apatite.

In the present context, a composite is a multi-phase material that is artificially made, as opposed to one that occurs or forms naturally.

In designing composite materials, scientists and engineers have ingeniously combined various metals, ceramics and polymers to produce a new generation of extraordinary materials. For example, fiber-reinforced metals may be utilized at higher temperatures than the polymer composites. High specific strengths as well as high specific moduli are possible because the densities of these base metals are relatively low. This combination of properties makes these materials especially attractive for use in some aerospace applications.

The high temperature creep and rupture properties of some of the super alloys (Ni-and Co-based alloys) may be enhanced by fiber reinforcement using refractory metal such as tungsten. Excellent high temperature oxidation resistance and impact strength are also maintained. Designs incorporating these composites permit higher operating temperatures and better efficiencies for turbine engines.

The extensive use of fiber reinforced composite (FRC) materials stimulated interest in predicting accurate response characteristics of the FRCs. With the advent of modern synthetic polymers and high-strength fibers and the continuous depletion of natural resources, composites will certainly get established as real and viable materials of construction.

Commonly, fiber reinforced composites are used in structures in the form of laminated plates and shells. Laminates are characterised by their very high E/G ratio i.e. shear stiffness is very small as compared to their membrane and bending stiffnesses. Transverse shears and the degree of orthotropy can significantly affect the gross plate behaviour for highly anisotropic laminates. To demonstrate the effect of E/G ratio on transverse deflection a simple one-dimensional structure is considered.

### 1.1.1 Influence of $\frac{E}{G}$ ratio on transverse deflection

A single span beam simply supported at both ends is subjected to uniformly distributed load of intensity, p, (Fig. 1.1.a). Fig. 1.1(b) shows the free body diagram of a portion of the beam at a distance x from the reference axis y.

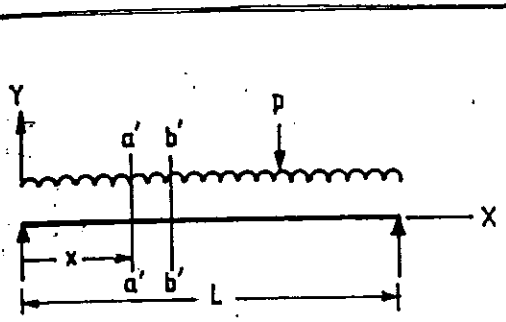


FIG.1.1(a) SIMPLY-SUPPORTED BEAM UNDER U.D.L.

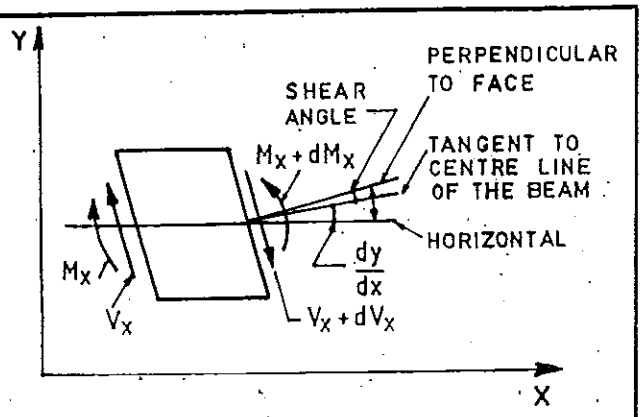


FIG.1.1(b) FREE BODY DIAGRAM OF THE BLOCK BETWEEN SECTION a'a' - b'b'

Fig. 1.2(a) shows an unloaded rectangular beam along with a grid pattern on the side of the beam. Fig. 1.2(b) shows the distorted pattern of the grid. Distortion is maximum at the neutral axis and zero at free surfaces. Transverse shears are responsible for the distortion of the grid.

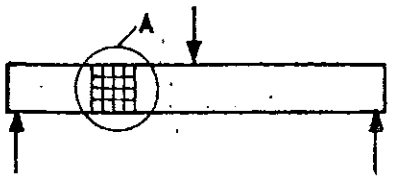


FIG.1.2(a) BEAM WITH A GRID PATTERN BEFORE LOADING

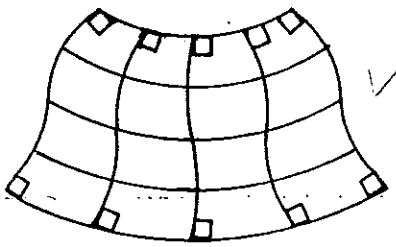

ENLARGED AT 'A' (Fig.1c)

FIG.1.2(b) DISTORTED GRID PATTERN AFTER LOADING

When transverse shear effects are neglected, shear deformation or distortion is nil and the centre line of the beam element will coincide with the perpendicular to the face of the cross section. Due to shear, the rectangular elements tend to distort to diamond shaped ones without rotation of the face and the slope of the centre line will increase by a shear angle ($\psi - \frac{dy}{dx}$) where y is the deflection of the centreline of the beam and $\frac{dy}{dx}$ is the slope of the centreline of the beam; $\psi$ is the slope of the perpendicular to the face.

**Case 1 : With flexure only (i.e. Influence of shear is ignored)**

Equation of equilibrium is given as

$$\frac{d^2y}{dx^2} = \frac{M_x}{EI} \qquad (1.1)$$

where $M_x$ is the moment at the section considered; E is the Young's modulus and I is the moment of inertia of the section. Substituting

$$M_x = \frac{1}{2} ( pLx - px^2 ) \qquad (1.2)$$

in Eq. (1.1), after simplification and applying boundary conditions, one obtains deflection at the middle point of the beam as

$$\Delta_f = \frac{5}{384} \frac{PL^4}{EI} \qquad (1.3)$$

Case 2 : When only shear is accounted

Equation of equilibrium can be given as

$$\psi - \frac{dy}{dx} = \frac{V_x}{KAG} \qquad (1.4)$$

where $V_x$ is the shear at any section at a distance x from the left hand support of the beam; K is the shape factor and is equal to $\frac{5}{6}$ for rectangular section and $\frac{9}{10}$ for a circular section; G is the shear modulus and A is the cross-sectional area.

Substituting

$$V_x = \left( \frac{PL}{2} - px \right) \qquad (1.5)$$

in Eq. 1.4 and after simplification, mid-point deflection can be obtained as

$$\Delta_s = \frac{pL^2}{8KAG} \qquad (1.6)$$

Case 3 : When both flexure and shear are present

Combining Eqs.(1.3) and (1.6), total deflection at middle point of the beam assuming a conservative system is

$$\Delta = \Delta_f + \Delta_s = \frac{5}{384}\frac{pL^4}{EI} + \frac{pL^2}{8KAG} = \Delta_f \left[ 1.0 + 0.96 \left(\frac{h}{L}\right)^2 \frac{E}{G} \right] \qquad (1.7)$$

The term in the bracket is the magnification of flexural deflection due to the effect of transverse shear. For isotropic material the magnification factor can have a maximum value of $[1+0.96 \left(\frac{1}{4}\right)^2 3] = 1.18$ (for $\frac{L}{h} = 4$ and $\frac{E}{G} = 3$) i.e. inclusion of shear will increase flexural

deflection by 18% in the case of an isotropic material. For laminates, this factor can be as high as $(1.0 + .96\ (\frac{1}{4})^2\ 50) = 4.0$ i.e. increase is by 300% (for $\frac{L}{h} = 4$ and $\frac{E}{G} = 50$).

Thus it is clear that in the case of a laminated beam, effect of $\frac{E}{G}$ ratio is much more pronounced than that in the case of an isotropic beam. The effect of shear deflection on gross behaviour of plate is given in Figs. 1.3(a-d).

Two other factors that influence plate behaviour are given in the next section.

### 1.1.2 Effect of degree of orthotropy and coupling

Effect of degree of orthotropy on transverse deflection is given in Figs. 1.3.a-b. The figures reveal that with the increase of degree of orthotropy from 3 to 40, normalized deflection increases by 5 times for $\frac{a}{t} = 4$. Coupling of bending and extension induced by the lamination asymmetry substantially decreases buckling load and vibration frequencies for common composite materials. It has been reported that for anti-symmetric laminates the effect of coupling dies out rapidly as the number of layers is increased.

Prediction of laminate properties is an essential adjunct to the design process. There are several levels of analysis. Most of these methods are based on simplified assumptions to three-dimensional theories. Simplest of all these methods is the one where a laminate is idealized as an isotropic material. In other theories, directional characteristics of layers are accounted for.

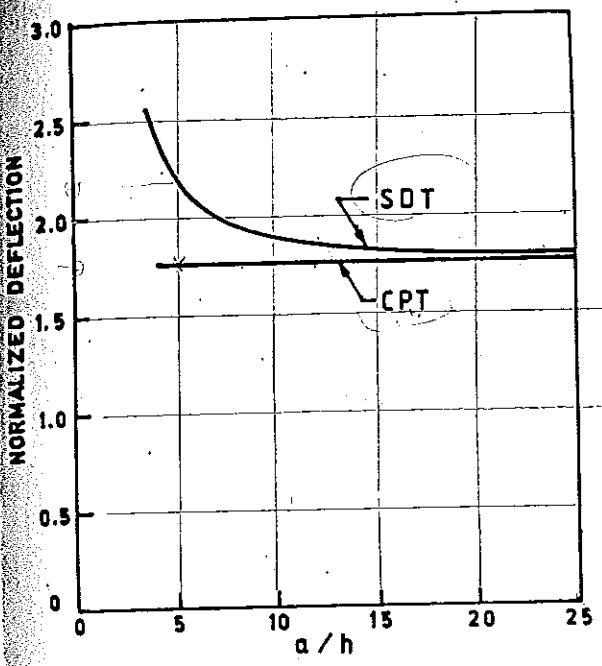


FIG.1.3(a) BENDING OF A 4 LAYER SYMMETRIC CROSS-PLY SQUARE PLATE WITH $E_{11} / E_{22} = 3$ [After Whitney [1] ]

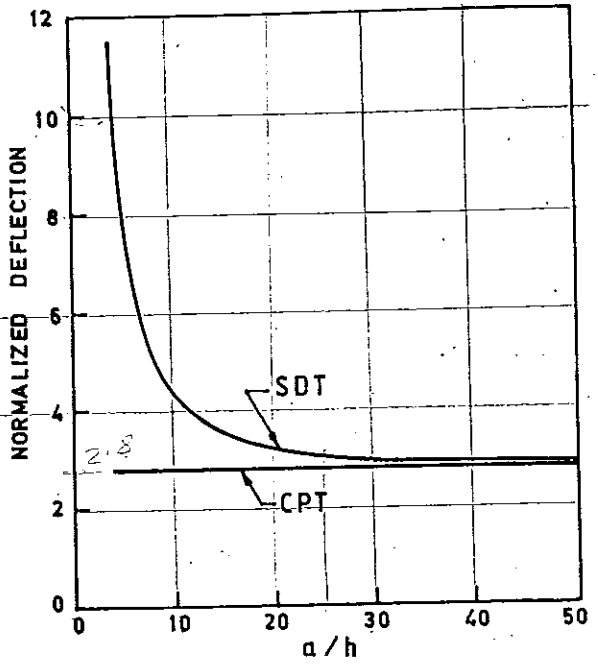


FIG.1.3(b) BENDING OF A 4 LAYER SYMMETRIC CROSS-PLY SQUARE PLATE WITH $E_{11} / E_{22} = 40$ [After Whitney [1] ]

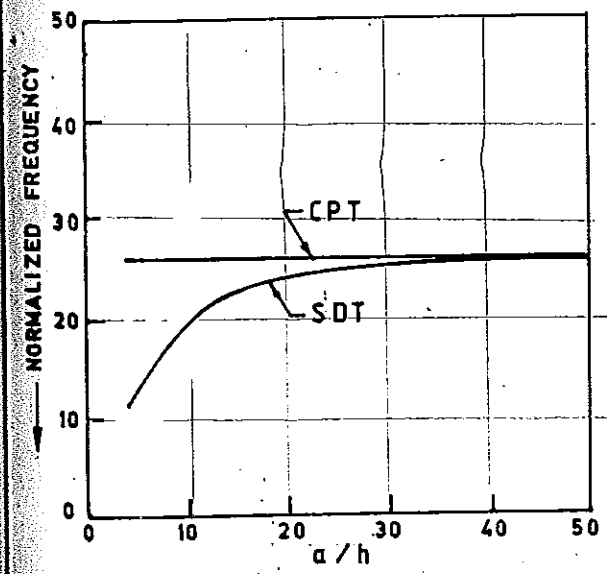


FIG.1.3(c) FUNDAMENTAL FREQUENCY OF FLEXURAL VIBRATION [After Whitney [1] ]

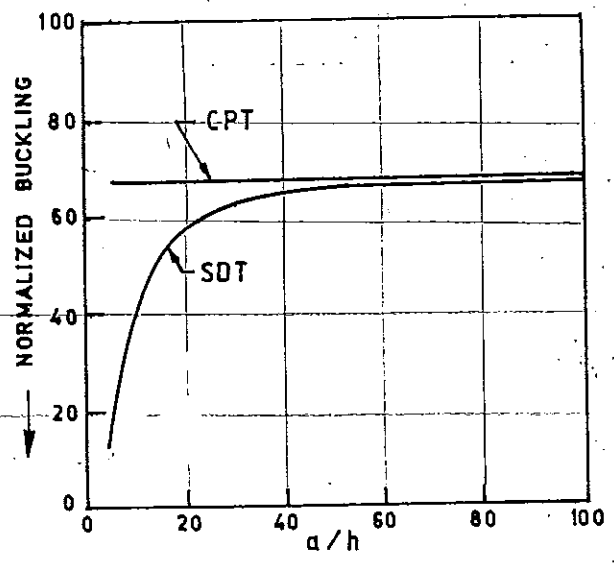


FIG.1.3(d) BUCKLING OF A SQUARE ± 45° PLATE [ After Whitney [1] ]

CPT = CLASSICAL PLATE THEORY
SDT = SHEAR DEFORMATION THEORY

## 1.2 Existing approaches

Several approaches have been proposed to account for the transverse shear effects. Classical laminated plate theory (CLT), which is based on Kirchoff's assumptions, is adequate for predicting thin plate behaviour. With the increase of plate thickness, CLT fails to give acceptable results since it ignores the transverse deflection due to shear. Three-dimensional elasticity models can be applied to predict responses of plates with simple geometry only. But analysis of anisotropic plates with complicated geometry is computationally expensive and therefore is not feasible for practical purposes. Two-dimensional theories are based on introducing a priori probable assumptions regarding the variation of displacements, strain/or stresses in the thickness direction. The simplest of these hypothesis is the linear variation of the displacement components as used in the first order shear deformation theories. An excellent account of the previous research in this area is given by Noor and Burton [2].

Two-dimensional theories are found to be adequate for predicting the gross response of medium thick laminated plates. General approaches for constructing two-dimensional shear deformation theories for multilayered plates can be classified as:

(i)method of hypotheses [3-6];
(ii)method of expansion [7,8];
(iii)asymptotic integration technique [9-11]and
(iv)iterative methods and methods of successive corrections [12].

The first method is an extension of the Kirchoff approach.

The second approach was initiated by Cauchy and Poisson around 1828, and was based on a series expansion, in terms of the thickness coordinate for displacements and/or stresses. For isotropic plates, power series, Legendre polynomials and trigonometric functions have been employed.

In the third approach, appropriate length scales are introduced in the three-dimensional elasticity equations for the different response quantities, followed by parametric (asymptotic) expansions of these quantities. Three dimensional equations are thereby reduced to recursive sets of two-dimensional equations, governing the interior and edge zone responses of the plate.

The fourth approach includes various iterative approximations of the three-dimensional elasticity equations and successive corrections of the two-dimensional equations.

The aforementioned approaches are not mutually exclusive. Some of the theories developed can be classified in more than one catagory. Hybrid methods, combining more than one approach have also been proposed. Examples of these are the global-local laminate model and the two-step approach based on using a two-dimensional theory to evaluate the in-plane stresses and then applying the three-dimensional equilibrium equations to evaluate the transverse shear and normal stresses.

Theory adopted in the present study comes under the method of hypotheses. In this method a suitable displacement model is assumed in the thickness direction.

Finite element analysis of layered composite plates began with Pryor and Barker [13]. Reddy [14] has developed a simple and efficient finite element formulation based on the Young-Norris-Stavsky theory. Di Sciuva [15] presented a finite element formulation based on assumed displacement field using rectangular element with 32 degrees of freedom.

Most of the conventional variational formulation of the classical lamination theory as well as the higher order theory are based on conforming plate elements, which are not only difficult to achieve but with the exception of the higher order elements, they were found to be too stiff.

## 1.3 Scope of present investigation

Current research efforts include theoretical work using both analytical and high-speed digital computer approaches in addition to experimental investigation using advanced materials fabrication, characterization, testing and development of composite out of locally available materials.

Theoretical formulation is based on simplified higher order shear deformation theory with non-linear displacement distribution through the thickness with the conditions of zero transverse shear stresses imposed at the outer surfaces to reduce the number of generalised displacement parameters.

A cubic displacement field (Fig. 1.4.a) is found to be adequate to explain the warping of the cross-section, and account for the parabolic variation of transverse shear along the thickness.

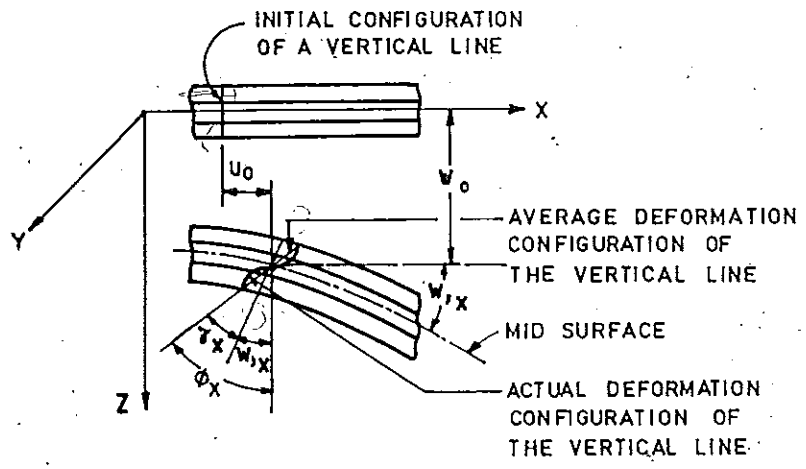


FIG. 1.4 DEFORMATION OF THE NORMAL TO THE MID-PLANE

Applying the condition that the top and bottom surfaces are free from transverse shear stresses, the governing displacement model can be expressed in terms of seven quantities. These are:

(i)two in-plane displacements;

(ii)two shear rotations;

(iii)one transverse displacement and its two first derivatives.

A simple four noded rectangular finite element is developed using strain energy approach. The in-plane displacements and two shear rotations are interpolated over an element by bilinear shape functions. A set of non-conforming shape function as proposed by Zienkiewicz and Cheung [16] is used for the transverse deflection.

A fortran IV program was developed to perform the computations involved in the method.

The element developed, has been applied to study the following aspects of laminated plate:

(i)Static analysis of laminated and sandwich plates.

(ii)Free vibration analysis of laminated plates.

(iii)Experimental investigation of laminated plates.

(iv)Static stability analysis of laminated plates.

An effort has been made for the development of a composite material out of local, low-cost materials and to study a few of its physical and mechanical characteristics and cost effectiveness.

### 1.3.1 Static analysis of laminated and sandwich plates

In order to test and evaluate the present numerical procedure and the related computer program, static analysis (transverse deflection and stresses) of plates have been carried out. Stresses are obtained at Gauss points. Using the technique of local stress smoothening, these stresses are transfered to the corner nodes. The smoothed stress values are then modified by finding the average of the nodal stresses for all elements meeting at a common node.

Before tackling any plate problems, the accuracy of element stiffness matrix is checked for the presence of rigid body modes. Following plate problems are examined under static loading with different boundary conditions.

(i) A three-layer simply supported square plate under sinusoidal loading (Fig. 1.5.a).

(ii) Plates made up of a number of layers viz. 5,7 and 9 (Fig. 1.5.b).

(iii) A three-layer simply supported rectangular plate (Fig. 1.5.c).

(iv) Cylindrical bending of a three-layer symmetric, angle-ply plate under sinusoidal loading.

(v) A three-layer square plate with layers of equal thicknesses.

(vi) A three-ply plate with identical top and bottom plies under uniformly distributed load ( u.d.l.). Effect of modular ratio between plies is also considered.

(vii)A three-ply clamped square plate under u.d.l.

(viii)A three-ply sandwich plate under u.d.l. with three cases (Fig. 1.5.d).

(ix)Finally, accuracy and convergence study was carried out of the proposed finite element model based on the numerical evaluation of some problems and comparision with available analytical solutions. Results on static analysis are compiled in chapter 3.

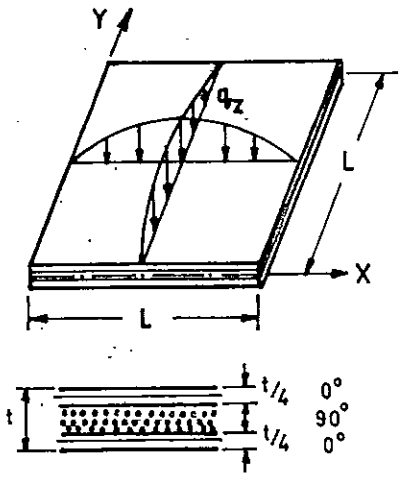


FIG.1.5(a) SIMPLY SUPPORTED CROSSPLY PLATE UNDER SINUSOIDAL DISTRIBUTED LOAD

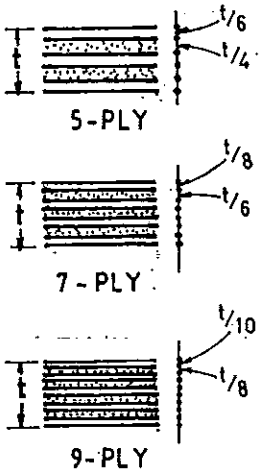


FIG. 1.5(b) MULTIPLE-PLY

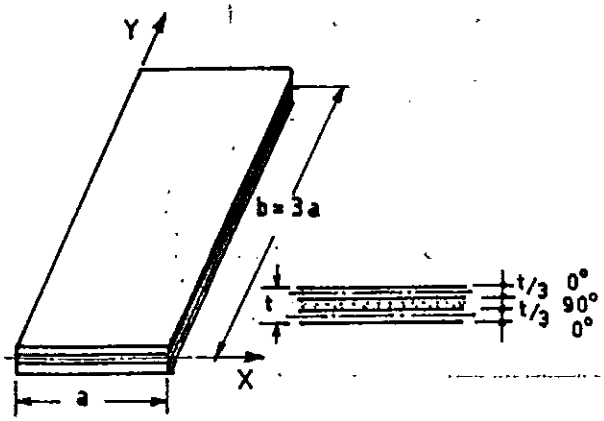


FIG. 1.5(c) SIMPLY-SUPPORTED RECTANGULAR PLATE UNDER SINUSOIDALLY DISTRIBUTED LOAD

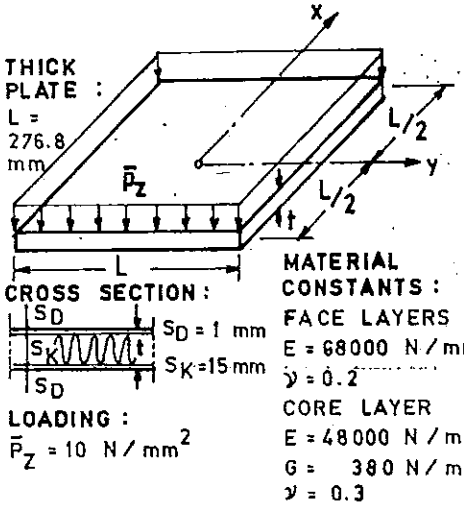


FIG 1.5(d) SANDWICH-PLATE UNDER CONSTANT TRANSVERSE LOAD

### 1.3.2 Free vibration analysis

Determination of deflections and stresses are the commonest of all parameters to be studied while analysing a structure. But to analyse a structure for its integrity, the natural frequencies should be determined in order to compare them with any time dependent loadings to which the structure will be subjected, to ensure that the frequencies imposed and natural frequencies differ considerably. Equations of motion for free vibration are obtained using Hamilton's principle. A consistent mass matrix of the element compatible with the stiffness matrix is developed. Vibration characteristics of the following plates have been examined in chapter 4.

(i) Fundamental frequency for a simply supported bi-directional, multi-layer square plate consisting of a large number of symmetric and anti-symmetric layers and for different degrees of orthotropy (Fig. 1.6.a).

(ii) Effect of in-plane displacements, lamination angle of a four-layer square plate (Fig. 1.6.b).

(iii) Simply supported angle-ply rectangular plates with two different material properties and two lamination angles (Fig. 1.6.c).

(iv) Natural frequency of a square sandwich plate (Fig. 1.6.d).

(v) Convergence of finite element solution for a two-layer square plate with number of Gauss sampling points.

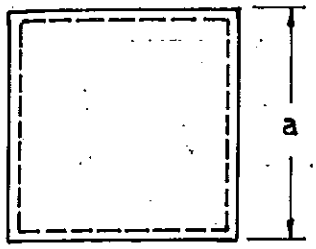


(a) SQUARE PLATE ( Ref. 17 )

MATERIAL PROPERTY :

$G_{12} / E_2 = 0.6$; $G_{23} / E_2 = 0.5$; $\nu_{12} = \nu_{23} = 0.25$

$E_1 / E_2$ = 3, 10, 20, 30, and 40

GEOMETRY :

SKEW-SYMMETRIC WITH LAYERS = 2, 4, 6 and 10

SYMMETRIC WITH LAYERS = 3, 5 and 9

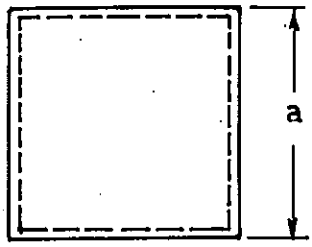


(b) SQUARE PLATE ( θ / -θ / θ ..... / -θ ) ( Ref. 18 )

MATERIAL PROPERTY :

TYPE I : $E_1 / E_2 = 40$; $G_{12} / E_2 = 0.6$; $\nu_{12} = 0.25$

$G_{13} / E_2 = G_{23} / E_2 = 0.5$

TYPE II : $E_1 / E_2 = 25$; $G_{12} / E_2 = 0.5$; $\nu_{12} = 0.25$

$G_{13} / E_2 = G_{23} / E_2 = 0.2$

GEOMETRY :

NO. OF LAYERS = 2, 4, 6, 8, 10, 12, 14 and 16

LAMINATION ANGLE ( θ ) = 30° and 45°

LENGTH-TO-THICKNESS RATIO = 10

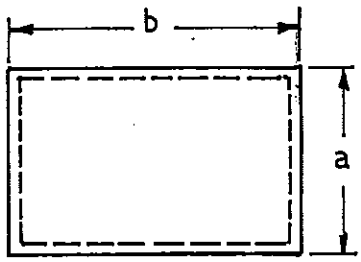


(c) RECTANGULAR PLATE ( Ref. 18 )

MATERIAL PROPERTY : SAME AS OF ABOVE

ASPECT RATIO ( a / b ) = 0.2, 0.4, 0.6, 0.8, 1.0, 1.2, 1.4, 1.6, 1.8 and 2.0

LENGTH-TO-THICKNESS RATIO = 10, 20, 30, 40 and 50

LAMINATION ANGLE ( θ ) = 30° and 45°

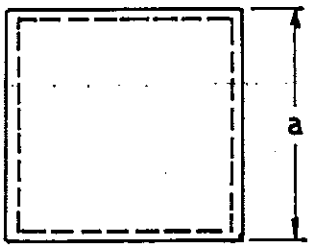


(d) SQUARE SANDWICH PLATE
( 0° / 45° / 90° / CORE / 90° / 45° / 30° / 0° )
( Ref. 19 )

TOP AND BOTTOM LAYER : GRAPHITE / EPOXY

CORE : U. S. COMMERCIAL ALUMINUM

SIMPLY SUPPORTED EDGE ; FREE ; CLAMPED

FIG. 1.6 LAMINATED PLATES FOR VIBRATION ANALYSIS

### 1.3.3 Experimental investigation

To further establish the wide ranging applicability of the element developed, experimental verification of static characteristics of plates with two fiber-matrix volume ratios is taken up in chapter 5. Static analysis involves following experiments:

(i)Coupon tests to determine material properties.

(ii)Clamped square plate under 16-point loading with fiber volume ratios 56%, 59% .

(iii)Clamped square plate under a point load at the centre.

Plates for which natural frequencies and mode shapes have been obtained experimentally and the same are verified against computed values are:

(i)Rectangular plates, clamped on all sides, with various aspect ratios (Figs. 1.7.a-b).

(ii)Square plate with central cut-out with all edges clamped (Fig. 1.7.c).

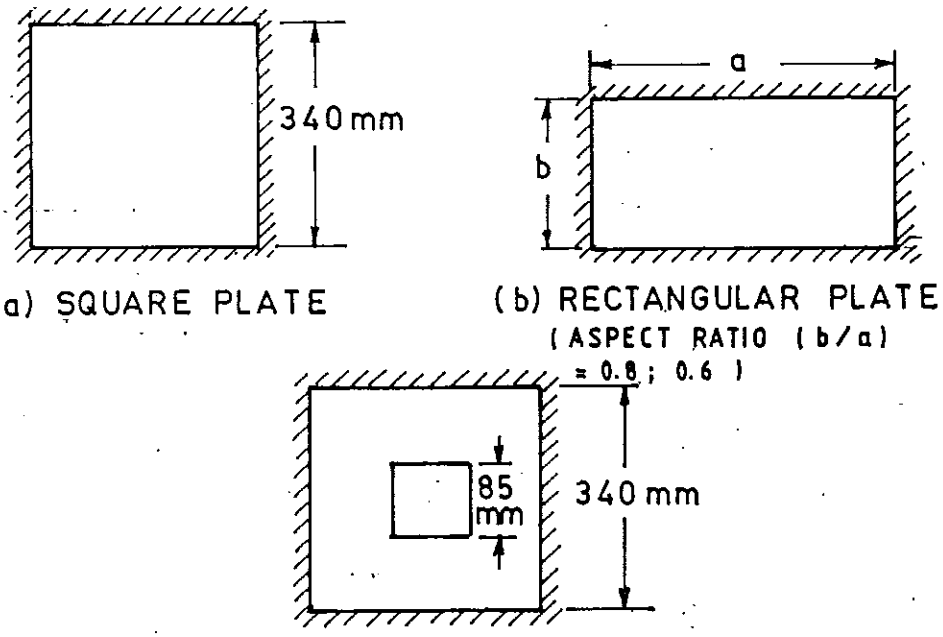


FIG.1.7 LAMINATED PLATES FOR EXPERIMENTAL VERIFICATION

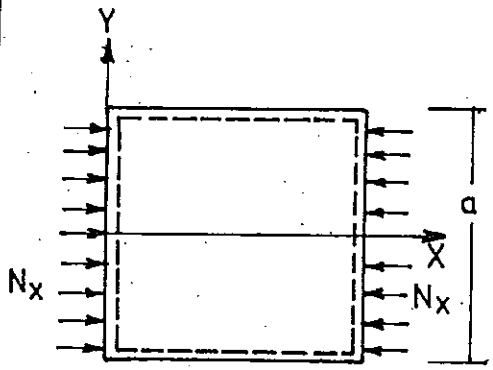


MATERIAL PROPERTY :

$E_y / E_x = 0.543103$ ; $E_{xy} / E_x = 0.23319$

$E_{yz} / E_x = 0.098276$ ; $E_z / E_x = 0.530172$

$E_{xz} / E_x = 0.010776$ ; $G_{xz} / E_x = 0.159914$

$G_{xy} / E_x = 0.262931$ ; $G_{yz} / E_x = 0.26681$

(a) SQUARE ORTHOTROPIC PLATE (Ref. 20)

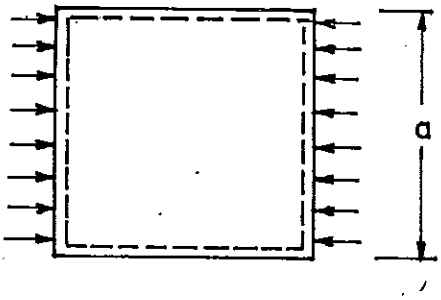


MATERIAL PROPERTY :

SAME AS IN (a)

PLY GEOMETRY :

and $h = 10\, h_1$.

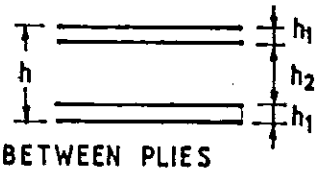


MODULAR RATIO BETWEEN PLIES

$= \beta = E_{x_1} / E_{x_2} = 1, 2, 5, 10$ and 15

(b) THREE-PLY SQUARE LAMINATE (Ref. 20)

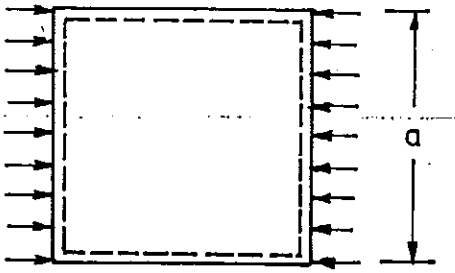


MATERIAL PROPERTY :

$E_1 / E_2 = 40$ ; $G_{12} / E_2 = 0.6$

$G_{23} / E_2 = 0.5$ ; $\nu_{12} = 0.25$

(c) FOUR LAYER SQUARE PLATE
(0° / 90° / 90° / 0°)
(Ref. 21)

FIG.1.8 PLATES AND LOADING FOR STATIC-STABILITY ANALYSIS

Jute is a lignocellulose fiber obtained from the stem of the jute plant (Corochorus Oliltorious). The fiber is obtained after a retting process, where in bundles of the stems are soaked in water for several days to soften the individual filaments and dissolve out water soluble gums and other non-fibrous impurities. Strands of fibers are then separated by a beating and pecting process. After the extraction it is thoroughly dried in the sun.

Phenol formaldehyde is a widely used resin in the manufacture of plastics laminates because of its inherent characteristics as a phenolic resin. Phenolics, when combined with suitable fillers, acquire good chemical and thermal resistance, and have good di-electric strength and dimensional stability. Products made with these resins are inherently low inflamability, and creep resistance, and have low moisture absorption capacity.

The composite plate was fabricated using six layers of jute mat in Phenol formaldehyde( 60% solid content) using the conventional approach of Hot-pressing at $150^{o}C$ and 1.5 $t/in^{2}$ pressure.

Preliminary analysis proves that this laminate has some properties which can be compared with that of glass-reinforced plastics. Following tests were carried out on this new composite

(i)Preliminary cost analysis.
(ii)Ultimate strength and modulus of elasticity.
(iii)Mass density.

Before actually recommending the composite for use as structural member, many more tests are necessary for complete characterization.

Finally in chapter 8, a summary and conclusions based on this study are presented. Recommendations for future works are indicated in this chapter.

# CHAPTER 2

# TWO DIMENSIONAL THEORIES BASED ON METHOD OF HYPOTHESIS

## 2.1 Survey of literature in the field

The need for more accurate computational models for multilayered laminated plates has led to the development of a variety of two-dimensional shear deformation theories. These theories can be classified into two general catagories:

(a)Theories based on replacing the laminated plates by an equivalent single-layer anisotropic plate and introducing global displacement, strain and/or stress approximations in the thickness direction and

(b)discrete layer theories based on piecewise approximations in the thickness direction.

The first catagory includes Classical laminated plate theory (CLT), as discussed by Lekhnitskii [22], using Kirchoff's hypothesis for the analysis of symmetrical laminates.

Following are the assumptions associated with this Classical lamination theory:

(1)Individual layers are assumed to be homogenous,

orthotropic and elastic.

(2)Individual layers are assumed to be in a state of plane stress.

(3)Displacements follow a restrictive class according to Kirchoff's hypothesis and

(4)Individual layers are perfectly bonded to adjacent layers.

The bond layer between any two consecutive laminae is presumed to be infinitesimally thin as well as non-shear-deformable. That is, displacements are continuous across the laminate thickness so that no laminae can slip relative to another. Thus the whole laminate acts as a single layer with very special properties. If a laminate is thin, a line originally straight and normal to the middle surface of the laminate is assumed to remain straight and normal to the middle surface, after bending. This is equivalent to ignoring the shearing strains (i.e. $\gamma_{xz} = \gamma_{yz} = 0$). In additon, the normals to mid-plane are presumed to have constant length so that strain perpendicular to the middle surface is ignored (i.e. $\varepsilon_z = 0$). Thus CLT approximates three-dimensional problem to a plane stress case. Classical Laminated Plate theory ignores the effect of transverse shear deformations. As a result natural frequencies and buckling load calculated using CLT are higher than those obtained from exact theories (Figs. 1.3.c-d). Reissner and Stavsky [23] and Stavsky [24] improved the theory proposed by Lekhnitskii [22] by including the influence of bending-extensional coupling in unsymmetrical laminates. The introduction of shear deflection into laminated plate theory was first accomplished by Stavsky [25] for isotropic layers having identical Poisson's ratios. Ambartsumyan [26] developed a rather cumbersome approach to define transverse shear stresses that satisfy the required continuity conditions at the layer interfaces. Whitney [1] had extended Ambartsumyan's approach to solve certain

specific boundary value problems of more general material and geometric properties than considered in [26]. The most general linear laminate theory, however, is due to Yang et al [6].

The first stress-based shear deformable plate theory was introduced by Reissner [27-29]. The theory is based on the following stress field

$$\sigma_x = \frac{M_x}{(h^2/6)} \frac{z}{(h/2)}$$

$$\sigma_y = \frac{M_y}{(h^2/6)} \frac{z}{(h/2)} \qquad (2.1)$$

$$\tau_{xy} = \frac{M_{xy}}{(h^2/6)} \frac{z}{(h/2)}$$

where $\sigma_x, \sigma_y$ and $\tau_{xy}$ are in-plane normal and shear stresses; $M_x, M_y$ and $M_{xy}$ are the associated moments, z is the thickness coordinate and h is the total thickness of the plate. The distribution of the transverse normal and shear stresses $\sigma_z, \tau_{xz}$ and $\tau_{yz}$ are determined from the equilibrium equations of the three-dimentional elasticity theory.

The origin of displacement based theories is due to Basset [30] who assumed that the displacement components in a shell can be expanded in a series of powers of the thickness coordinate $\zeta$ . For example, the displacement component $u_1$ can be written in the form

$$u_1(\xi_1, \xi_2, \zeta) = u_1^{\circ}(\xi_1, \xi_2) + \Sigma \zeta^n u_1^{(n)}(\xi_1, \xi_2) \qquad (2.2)$$

where $\xi_1$ and $\xi_2$ are the curvilinear coordinates in the middle surface of the shell; $u_1^{(n)}$ has the meaning

$$u_1^{(n)}(\xi_1,\xi_2) = \left.\frac{d^n u_1}{d\zeta^n}\right|_{\zeta = 0} , \quad n = 0,1,2 \ldots \qquad (2.3)$$

Initially Basset's work did not receive much attention. Hildebrand et al [31] and Hencky [32] presented a displaceemnt based shear deformation theory for shells that can be used for flat plates. The following truncated displacement field was assumed

$$\begin{aligned} u_1(\xi_1,\xi_2,\zeta) &= u(\xi_1,\xi_2) + \zeta\, \varphi_x\,(\xi_1,\xi_2) \\ u_2(\xi_1,\xi_2,\zeta) &= v(\xi_1,\xi_2) + \zeta\, \varphi_y\,(\xi_1,\xi_2) \\ u_3(\xi_1,\xi_2,\zeta) &= w(\xi_1,\xi_2)\,. \end{aligned} \qquad (2.4)$$

For plate equivalent of Eq. (2.4) in Cartesian coordinate system is referred to as the Mindlin's plate theory which has the form of Eq. (2.5).

$$\begin{aligned} u &= u^o + z\,\varphi_x \\ v &= v^o + z\,\varphi_y \\ w &= w^o \end{aligned} \qquad (2.5)$$

Mindlin [33] employed kinematic assumptions to obtain the governing differential equations. In this derivation, it was necessary to introduce a correction factor which was introduced in order to adjust the transverse shear stresses and match the response predicted by using Eq. (2.5) with that of the three-dimensional elasticity theory.

Shear deformation theory based on the displacement field given by Eq. (2.5) is referred to as first order shear deformation theory (FSDT). This theory assumes constant shear rotation through out the plate thickness. It may be pointed out that Classical Plate Theory is merely a special case of the First Order Shear Deformation Theory. The range of validity of FSDT is strongly dependent on the factors used in adjusting the transverse shear stiffnesses of the plate.

Several approaches have been proposed by various investigators for calculating the shear correction factors for different laminates. Most of these approaches were based on matching certain gross response characteristics as predicted by the First Order Theory, with the corresponding characteristics of the three-dimensional elesticity theory. Gross response characteristics include transverse shear strain energy, natural frequency associated with the thickness shear vibration mode, and velocity of propagation of a flexural wave. Chow [34] used energy approach to evaluate this correction factor for symmetric laminates and Whitney [35], that for general laminates. Bert [36] obtained this factor by equating the shear strain energy for the actual non-homogenous beam to that in an equivalent member having an uniform shear strain as assumed in Timoshenko Beam Theory. All the shear correction factors in use to date are calculated a priori and are, therefore, functions of the lamination parameters only. They do not account for the differences in the distribution of the transverse shear strains in the thickness direction resulting from different loading conditions.

First Order Shear Deformation Theories do not consider the warping of the cross-section which is quite important in composite construction. As an improvement over this, the effect of warping of cross-section was accounted by assuming

a piece-wise linear distribution of in-plane displacements across the thickness of each layer separately. This approach can be classified under discrete layer theory. The continuity of the transverse stresses at layer interfaces can be satisfied by either:

(a) imposing the continuity conditions as constrain conditions or by;

(b) using explicit approximations for the transverse stresses within each layer(semi-inverse approach).

But even this improvement did not eliminate the use of shear correction co-efficients which for composite structures depended upon laminate construction details. In order to avoid the use of shear correction co-efficients, theories have been developed based on complete three-dimensional approach [20,37-39] or based on higher order displacement models leading to realistic parabolic variation of transverse shear stresses through the plate thickness.

First Order Shear Deformation Theory has the deficiency that it fails to predict warping of cross-section and does not predict parabolic shear stress distribution across the thickness. Three-dimensional theory on the other hand treats each layer as an elastic continuum with possibly distinct material properties from adjacent layers, which give rise to a large number of differential equations. In order to obviate the deficiencies of both First Order Shear Deformation Theory and three-dimensional elasticity theory, more refined theories that account more realistic variation of transverse shear stresses across the plate thickness as well as warping of the cross-section were developed.

Higher order refined theories, based on non-linear distribution of displacements and/or strains in the thickness

direction can predict plate behaviour more accurately. In order to reduce the number of displacement parameters used in some of these theories, following simplifications have been proposed. The first simplification is referred to as the semi-inverse method. It is based on assuming the distribution of the transverse shear stresses and either (a) or (b):

(a) using the constitutive relations to derive expressions for the in-plane displacements which are non-linear in the thickness coordinate. This approach was used by Ambartsumyan, Reissner and many others;

(b) using the mixed variational principle in terms of displacements and transverse stresses, which is a modification of the mixed principle to derive the governing equation of the plate [40].

The second type of simplification is based on imposing the transverse shear stress (and strain) conditions at top and bottom surfaces of the plate. This approach was introduced for isotropic plates by Panc [41] and later applied by a number of researchers to laminated plates. Theory presented in this thesis is based on this type of simplification.

There have been several theories proposed by various researchers which involve terms higher than those for the First Order Shear Deformation Theory.

Next to the theory given in Eq. (2.5) is a higher order theory that involves displacement field of the type

$$\begin{aligned} u &= u^{o} + z\varphi_{x} \\ v &= v^{o} + z\varphi_{y} \\ w &= w^{o} + z\varphi_{z} + z^{2}\,\xi_{z} \end{aligned} \tag{2.6}$$

This theory includes the effect of transverse normal strain. Displacement field as given in Eq. (2.6), along with corresponding stress distribution assumptions have been used by Naghdi [42] to derive a general theory of shells and by Essenburg [43] to derive the corresponding one-dimensional plate theory. In case of contact problems, Essenburg demonstrated that the utility and advantages of the theory based on Eq. (2.6) over other lower order theories. Whitney and Sun [44] had developed a theory on laminated cylindrical shells based on displacement field of the same level as that of Eq. (2.6). They wrongly used a shear correction factor of the same type as that employed by Mindlin in deriving the stress resultants.

Next higher level is based on the displacement field of the form

$$\begin{aligned} u &= u^{o} + z\varphi_{x} + z^{2}\xi_{x} \\ v &= v^{o} + z\varphi_{y} + z^{2}\xi_{y} \\ w &= w^{o} + z\varphi_{z} + z^{2}\xi_{z} \end{aligned} \tag{2.7}$$

A theory derived from Eq. (2.7) has been given by Nelson and Lorch [45] for laminates. They had incorporated a shear correction factor which is inconsistent with the level of approximation in Eq. (2.7). Hildebrand, et al [31] briefly examined a theory given by Eq. (2.7) and concluded that the inclusion of the quadratic terms in the in-plane displacements do not provide a significant improvement over the lower order theories, for certain problems. Reissner [46] had developed a theory on a displacement model where in-plane displacements varying cubically and transverse displacements parabolically as

$$u = z\varphi_x + z^3\zeta_x$$
$$v = z\varphi_y + z^3\zeta_y \qquad (2.8)$$
$$w = w^o + z^2\xi_z$$

This model does not have in-plane displacement components at the mid surface. Reissner showed that this theory predicts results accurately when compared with the elasticity solution for pure bending of an isotropic plate with a circular hole. Lo et al [47] presented a theory for homogenous isotropic plates which is of the same order of approximation as that of Reissner's Eq. (2.8) ,but included the terms contributing to the in-plane mode of deformations.

$$u = u^o + z\varphi_x + z^2\xi_x + z^3\zeta_x$$
$$v = v^o + z\varphi_y + z^2\xi_y + z^3\zeta_y \qquad (2.9)$$
$$w = w^o + z\varphi_z + z^2\xi_z$$

Thus, the theory accounts for the parabolic variation of transverse shear stresses, linear variation of transverse normal strains and a cubic variation of the in-plane displacements across the plate thickness. The principle of stationary potential energy has been used to derive the governing differential equations. Further, Lo et al [48] have extended their works for the analysis of laminated composite plates. Lo et al [49] have also demonstrated that the best method for evaluating the stresses is by determining the in-plane stresses directly from the displacement solution and then determining the transverse stresses through integration of equilibrium equations utilizing the in-plane stress solutions therein. Levinson [50] and Murthy [51] have presented higher order theories in which in-plane

displacements are expanded as cubic functions of the thickness coordinate with the transverse displacement kept constant across the thickness. Nine independent variables were reduced to five by conditioning that the transverse shear stresses vanish on the top and bottom surfaces. The theory given by Levinson is applicable for static and dynamic analysis of homogenous isotropic plates where as that given by Murthy is applicable for flexural analysis of laminated plates. They both used the equilibrium equations of the First Order Shear Deformation Theory which are variationally inconsistent for the higher order displacement fields. Reddy [14] presented a consistent derivation of the associated equilibrium equations. The displacement field used by Reddy and Levinson are identical and they contain the same number of dependent variables.

In a recent paper, Reissner [52] presented a state of art of various plate theories and showed how they can be derived from three-dimensional elasticity theory.

The displacement model adopted in the present thesis is based on simplified higher order shear deformation theory with non-linear distribution of displacements through out the thickness. To reduce the number of generalised displacement parameters, the conditions of zero transverse shear stresses were imposed at the outer surfaces. The displacement model can be given as

$$\begin{aligned} u &= u^{o} + z\varphi_x + z^2\xi_x + z^3\zeta_x \\ v &= v^{o} + z\varphi_y + z^2\xi_y + z^3\zeta_y \\ w &= w^{o} \end{aligned} \qquad (2.10)$$

In-plane displacements are expanded as cubic functions of the thickness coordinate and transverse displacements are

constant through out the plate thickness.

For most practical problems, the effect of transverse shear deformation is more pronounced on the response of multi-layered composite plates than that of transverse normal strain and stress. That is why, in the present model transverse displacement is taken constant across the thickness.

This model satisfies conditions of zero transverse shear stresses at top and bottom surfaces of the plate and be non-zero elsewhere. The accuracy of the response predicted by different shear deformation theories is strongly dependent on the significance of the transverse shear deformation, which in turn, depends on a number of plate parameters. Due to large number of these parameters closed form solutions are only obtainable for plates with simple geometries, loading and boundary conditions. Symmetric laminate has no coupling between bending and stretching and may be treated on the basis of orthotropic or anisotropic plate theory, involving only a fourth order differential equation of equilibrium. Unsymmetric laminates yield bending-stretching coupling and are governed by higher order equations. In a relatively few cases, this can be solved analytically. For most of the problems, approximate techniques such as the Ritz, Galerkin, Series solution, Finite Difference or Finite Element methods may be used.

The finite element method has the versatility of dealing with complex geometrics, arbitrary loadings and general material properties. A great deal of work involves the development and application of finite element method to plates and shells. Present study is based on the application of this method to predict the behaviour of lamianted plate structures. A brief review of finite element on plate bending is presented in the next section.

## 2.2 Finite element in plate bending

Finite element method has undergone an extremely active development stage since its beginning in the late 1950s. During the first 10-15 years of this activity, research efforts centred on element development. More recently there has been a shift of interest towards work focusing on applications of the method. A brief review of literature on plate bending using finite elements which have direct relevance with the present work is presented here. An extensive review of existing literatures on plate bending elements is given in tabular form in [53].

Interest in plate bending elements came very early in the history of the finite element method. At the beginning of 1960s, a number of elements were proposed by researchers such as Clough [54], Adini [55], Melosh [56], and Tocher [57]. By the middle of 1960's, variational basis for the finite element method had become better understood and coupled with this came the realization that interelement compatibility or conformity was an important property, without which, element convergence might not always be obtained.

Most of the early plate bending elements were of the non-conforming type. Success in achieving full conformity came easiest in the case of rectangular elements. Derivation of suitable triangular elements proved to be considerably more difficult than rectangular elements. Conforming plate elements were not only difficult to obtain, but with the exception of the higher order elements, they were found to be too stiff. There was considerable scepticism about the need to meet the $C^1$ continuity requirement.

Many researchers sought elements based on alternative variational principles. One logical choice is the principle

of minimum complementary potential energy resulting in an equilibrium formulation. The chosen functions would be required to satisfy equilibrium at every point in the structure and the stress conditions on the boundaries. Stress based theories are in general, very complex. Considerable clarification and simplification in the use of the equilibrium (stress based) method can be attributed to Morley [58] and Elias [59], who implemented the use of elements stress functions. Severn and Taylor [60] had employed similar theory for deducing the stiffness matrix for rectangular and triangular plate elements. Herrmann's [61] mixed method was based on a modified Reissner variational principle. He relaxed the continuity requirements for displacements but imposed continuity conditions on the stress field. The decade of the 1970's witnessed the development of research in the field of finite element with the introduction of new techniques such as reduced integration and penalty number formulations, substitute shape functions and derivative smoothening. To determine the stiffness characteristics of the entire assembled structure which are required for analysis, one must find the stiffness properties of individual un-assembled elements. A number of alternative methods are available for determining the stiffness characteristics of structural elements, they are:

(1)strain energy approach;

(2)principle of works;

(3)solution of differential equation for the element displacements;

(4)inversion of flexibility matrix.

Strain energy method is based on direct application of Castigliano's theorem. The strain energy is first calculated in terms of element displacements and on differentiation with

respect to each displacement in turn the complete set of force-displacement equations are obtained; these equations can be formulated in matrix notations.

In the second method, the principle of work applied through the unit displacement theorem leads directly to the required matrix equation relating element forces to their associated displacements.

In the third method, the solution of the differential equation for displacement is used to derive the required stiffness relationships. The application of this method is limited to structural elements for which, solutions for displacement is available.

The above methods can also be utilised for the determination of flexibility matrix which on inversion leads to the stiffness matrix. In some problems this procedure has been found to be relatively simpler.

The strain energy method based on direct application of Castigliano's theorem is adopted in the present thesis for the derivation of element stiffness matrix.

Stiffness matrix for a laminated plate element is developed in the next chapter. Once the stiffness matrix for an element has been established, the other steps follow logically towards the solution of the plate problem.

## 2.3 Summary

Gradual development of two-dimensional plate theories is given in the Table below:

Table 2.1

| | | | |
|---|---|---|---|
| Basset [30] | 1890 | $u = u^o + \sum_n z^n \frac{d^n u}{d\zeta^n}$ | n=0,1,2... Eq. (2.2) |
| Lekhnitskii [22] | 1968 | $u = -zw_{,x}$ ; $v = -zw_{,y}$ ; $w = w^o$ | |
| Reissner [27-29] | 1944,1945 & 1947 | $\sigma_x = \frac{M_x}{(h^2/6)} \frac{z}{(h/2)}$ ; $\sigma_y = \frac{M_y}{(h^2/6)} \frac{z}{(h/2)}$ <br> $\tau_{xy} = \frac{M_{xy}}{(h^2/6)} \frac{z}{(h/2)}$ | Eq. (2.1) |
| Hencky [32] | 1947 | $u = z\varphi_x$ ; $v = z\varphi_y$ ; $w = w^o$ | |
| Hildebrand [31] | 1949 | $u = z\varphi_x$ ; $v = z\varphi_y$ ; $w = w^o + z^2 w_2$ | |
| Mindlin [33] | 1951 | $u = u^o - z\varphi_x$ ; $v = v^o - z\varphi_y$ ; $w = w^o$ | Eq. (2.5) |
| Naghdi & [42] <br> Essenburg [43] | 1957 <br> 1975 | $u = u^o + z\varphi_x$ ; $v = v^o + z\varphi_y$ <br> $w = w^o + z\varphi_z + z^3 \xi_z$ | Eq. (2.6) |
| Reissner & Stavsky [23,24] | 1961 | $u = u^o - zw_{,x}$ ; $v = v^o - zw_{,y}$ <br> $w = w^o$ | |
| Whitney & Sun [44] | 1974 | $u = u^o + z\varphi_x$ ; $v = v^o + z\varphi_y$ <br> $w = w^o + z\varphi_z + z^3 \zeta_z$ | |

Continuation from previous page

| | | |
|---|---|---|
| Nelson & Lorch [45] | 1974 | $u = u^o+z\varphi_x+z^2\xi_x$ ; $v = v^o+z\varphi_y+z^2\xi_y$<br>$w = w^o+z\varphi+z^2\xi$ Eq. (2.7) |
| Reissner [46] | 1975 | $u = z\varphi_x+z^3\zeta_x$ ; $v = z\varphi_y+z^3\zeta_y$<br>$w = w^o+z^2\xi_z$ Eq. (2.8) |
| Lo et el [47,48] [49] | 1977 1978 | $u=u^o+z\varphi_x+z^2\xi_x+z^3\zeta_x$ ; $v=v^o+z\varphi_y+z^2\xi_y+z^3\zeta_y$<br>$w = w^o+z\varphi_z+z^2\xi_z$ Eq. (2.9) |
| Reddy [14] | 1984 | $u=u^o+z\varphi_x+z^2\xi_x+z^3\zeta_x$ ; $v=v^o+z\varphi_y+z^2\xi_y+z^3\zeta_y$<br>$w = w^o$ Eq. (2.10) |

# CHAPTER 3

# FINITE ELEMENT FORMULATION AND STATIC ANALYSIS

## 3.1 Introduction

Theoretically one can model laminates by breaking up each ply into usual prism type finite elements with the thickness of each element representing the thickness of each ply. Moreover to avoid a wide variation among the elements, a certain minimum value of aspect ratios are to be maintained from the computational and accuracy point of view. To achieve this a large number of elements are necessary to discritize a single layer of the composite. If the composite plate is composed of m number of plys, then automatically total number of elements is just m fold of the number of elements in each ply. In certain practical problem it ranges more than few thousand elements for a moderately accurate solution. As a result the analysis will be very time consuming and expensive. But, with the assumption of two-dimensional theory, the number of elements can be reduced drastically by representing displacement/stress/strain by a single function rather than several ones through the thickness.

In the present thesis, a laminate is discritized into finite elements such that the thickness of each element is the same as that of the laminate. A short review on FE

analysis of laminated composite plates under static loading is given below.

## 3.2 Finite element analysis of laminated composite plates

Finite element analysis of layered composite plates began with Pryor and Barker [13] and Barker et al [62], who formulated a rectangular element for the analysis of thick laminated plates, including transverse shear effect. Mau et al [63,64] used the so called hybrid stress finite element method to analyse thick composite plates. Noor and Mathers [65] used finite element models based on Reissner's plate theory i.e. mixed formulation, to study the effects of shear deformation and anisotropy. Mawenya and Devis [66] and Panda and Natarajan [67] used the quadratic shell element given by Ahmad et al [68] and analysed the bending of thick plate. Spilker et al [69] used two hybrid stress elements to study the static bending of layered composite plates. Reddy [70] had developed a simple and efficient finite element based on the Young-Norris-Stavsky (YNS) theory. The element had been successfully used for the free vibration and thermo-elastic analysis of ordinary and laminated composite plates [71,72]. Pryor [73] gave a detailed description of the finite element formulation of the first order shear deformation theory in which the transverse shear effects are included in a manner similar to that of Reissner's [28] theory.

Di Sciuva [15] had presented a finite element formulation based on assumed displacement field using rectangular element with 32 degrees of freedom. The theory accounts for piecewise linear interpolation of inplane displacements across the thickness and allows continuity of displacements at the interfaces between the layers.

Phan and Reddy [21] had given a displacement finite element model based on higher order shear deformation theory to analyse laminates under bending, vibration and stability. Rao [74] had presented the formulation of a rectangular laminated anisotropic shallow shell finite element which can be conveniently degenerated to plate element. Displacements were taken as the products of one-dimensional first order Hermite interpolation polynomials. Moser et al [75] used quadratic and cubic finite elements to analyse laminated composite plates and shells having plane or curved surfaces. Plate elements were based on the shear deformation theory and the shell elements were on the kinematically equivalent degenerated three dimensional concept.

Ghosh and Dey [76] have given an explicit derivation of displacement based simple finite element using 7 degrees of freedom to analyse laminated and sandwich plates under various loading conditions.

Conventional variational formulation of the classical lamination theory [4] as well as the third order theory [14] involves higher order (i.e. 2nd order) derivatives of the transverse displacement. Therefore, in the finite element modelling of such theories, the continuity of not only the transverse displacement should be imposed but also its derivatives along the element boundary. In other words, a conforming plate bending element based on a displacement formulation of these theories requires the continuity of transverse displacements and their derivatives across the interelement boundaries. The construction of such an element is algebraically complicated, requiring for example, a quintic polynomial with 21 degrees of freedom for a six-noded triangular element. An extensive review on finite element method in laminated plates and shells is given by Reddy (77).

Aim of present study is to analyse laminated plates both thick and thin, using a four-noded rectangular bilinear element. For bilinear element, compatibility is guaranteed because element sides remain straight even after the deformation.

## 3.3 Process of analysis

Static analysis of laminated plate involves following steps:

(i) idealization of the structure, choice of shape function and evaluation of stiffness matrix for each element;

(ii) determining the element load vector;

(iii) assembling the stiffness matrices and load vectors for the complete structure;

(iv) solving the set of resulting equations for nodal displacements subjected to boundary conditions;

(v) evaluation of element displacements and stresses.

### 3.3.1 Strain energy formulation

The elastic strain energy in a loaded element is given by

$$U_e = \frac{1}{2} \int \sigma_{ij} \, \varepsilon_{ij} \, d(vol) \qquad (3.1)$$

where the integration is performed over the volume of the element. The stresses and strains in an element are related through Hooke's law, which may be written as

$$\{\sigma_{ij}\} = [C] \{\varepsilon_{ij}\} \qquad (3.2)$$

The strains in an element are defined in terms of the displacements as

$$\{\varepsilon_{ij}\} = [L]\{u\} \tag{3.3}$$

where [L] is a suitable linear operator. However, the displacements themselves are usually defined in terms of a set of basis functions valid only within the element. It is customary to write

$$u = \sum_{i=1}^{k} N_i u_i \tag{3.4}$$

where $u_i$ represents specified displacements at nodes on the element, and $N_i$ represents the shape functions associated with each node. So the strain-displacement matrix may be written as

$$\{\varepsilon_{ij}\} = [B]\ \{u_i\} \tag{3.5}$$

Substituting Eqs. 3.2-3.5, in Eq.3.1 and since $\{u_i\}$ is constant, it may be taken outside of the integral sign. The strain energy expression then becomes

$$U_e = \frac{1}{2}\{u_i\}^T \left[ \int_V [B]^T [C]\ [B]\ d(vol) \right] \{u_i\}$$

$$\equiv \frac{1}{2}\{u_i\}^T \left[ \int_A [B]^T [D]\ [B]\ d(area) \right] \{u_i\} \tag{3.6}$$

The term in the square brackets represents the element stiffness matrix. Here [C] is the stress-strain constitutive matrix and [D] is the stress resultant-strain matrix.

The first step towards the formulation of element stiffness matrix is to define the governing displacement field. This is taken up in the next section.

### 3.3.1.1 Displacement function

A higher order shear deformation theory is considered in the present study. The theory includes effects of transverse shear strains/stresses as well as warping of the cross-section. We begin the formulation by defining a local coordinate system (x,y,z) at any point on the mid surface of the plate element, with (x,y) axes lie in the plane of the plate while z axis normal to mid surface as shown in Fig. 3.1.

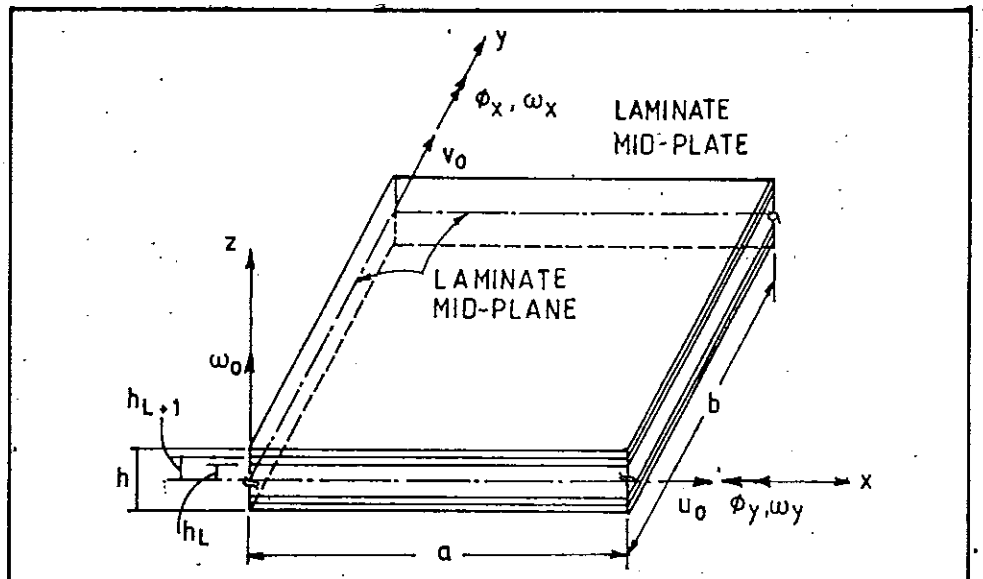


FIG. 3.1 LOCAL COORDINATE SYSTEM

Displacement field is assumed as

$$U(x,y,z) = U(x,y,0) + z\varphi_x(x,y,0) + z^2\xi_x(x,y,0) + z^3\zeta_x(x,y,0) \cdots$$

$$\equiv U_o + z\,\varphi_{xo} + z^2\xi_{xo} + z^3\zeta_{xo}$$

$$V(x,y,z) = V(x,y,0) + z\varphi_y(x,y,0) + z^2\xi_y(x,y,0) + z^3\zeta_y(x,y,0)$$

$$\equiv V_o + z\,\varphi_{yo} + z^2\xi_{yo} + z^3\zeta_{yo}$$

$$W(x,y,z) = W(x,y,0) \equiv W_o \tag{3.8}$$

where $U_o, V_o$ and $W_o$ are the displacements of the corresponding point on the reference surface with coordinates $(x_o, y_o, z_o)$, $\varphi_{xo}$, $\varphi_{yo}$ are the average rotations about y and x axes respectively of the normals to the midsurface of the undeformed plate. The remaining terms correspond to the higher order rotations. Fig. 1.4 gives the deformation of a section of the plate by a plane parallel to xz plane. Conditions of zero transverse shearing stresses at the top and bottom surfaces of the plate may be written in the form

$$\tau_{xz}(x,y,\pm\frac{t}{2})=0 \quad \text{and} \quad \tau_{yz}(x,y,\pm\frac{t}{2})=0 \tag{3.9}$$

where t is the thickness of the plate. For an orthotropic plate, this means

$$\varepsilon_{xz}(x,y,\pm\frac{t}{2})= 0 \quad \text{and} \quad \varepsilon_{yz}(x,y,\pm\frac{t}{2})= 0 \tag{3.10}$$

Differentiating Eq. 3.8 and substituting in Eq. 3.10, one obtains the following relations

$$\xi_{xo}=0 \; ; \quad \zeta_{xo}= -\frac{4}{3t^2}\left(\frac{\partial w}{\partial x} + \varphi_{xo}\right) \quad \text{and}$$

$$\xi_{yo}=0 \; ; \quad \zeta_{yo}= -\frac{4}{3t^2}\left(\frac{\partial w}{\partial y} + \varphi_{yo}\right) \tag{3.11}$$

Substituting Eq. 3.11 in Eq. 3.8, and on simplification yields the displacement functions as

$$\left.\begin{aligned} U(x,y,z) &= U_o + z\left[\varphi_{xo} - \frac{4z^2}{3t^2}\left(\frac{\partial w}{\partial x} + \varphi_{xo}\right)\right] \\ V(x,y,z) &= V_o + z\left[\varphi_{yo} - \frac{4z^2}{3t^2}\left(\frac{\partial w}{\partial y} + \varphi_{yo}\right)\right] \\ W(x,y,z) &= W_o \ . \end{aligned}\right\} \qquad (3.12)$$

Thus, displacement at any point in the plate can be expressed in terms of seven unknown quantities as $u_o, v_o, \varphi_x, \varphi_y, w, w_{,x}$ and $w_{,y}$.

The angles $\varphi_x$ and $\varphi_y$ are the total rotations of section x = constant and y = constant respectively and are given by

$$\left.\begin{aligned} \varphi_x(x,y) &= \frac{\partial w}{\partial x} + \gamma_x\,(x,y) \\ \varphi_y(x,y) &= \frac{\partial w}{\partial y} + \gamma_y\,(x,y) \end{aligned}\right\} \qquad (3.13)$$

where $\gamma_x$ and $\gamma_y$ are average transverse shear strains. It can be shown that a shear co-efficient is an estimate of the warping of the cross-section.

### 3.3.1.2. Strain-displacement relations

The strain displacement relations in the Cartesian coordinate system can be obtained by substituting Eq. 3.12 into the strain-displacement relation and is given by

$$\{\varepsilon\} =$$

$$\begin{Bmatrix} \varepsilon_x \\ \varepsilon_y \\ \varepsilon_{xy} \\ \varepsilon_{xz} \\ \varepsilon_{yz} \end{Bmatrix} = \begin{Bmatrix} U_{o,x} + z\left[\varphi_{xo,x} - \frac{4z^2}{3t^2}\left(\varphi_{xo,x} + \frac{\partial^2 w}{\partial x^2}\right)\right] \\ V_{o,y} + z\left[\varphi_{yo,y} - \frac{4z^2}{3t^2}\left(\varphi_{yo,y} + \frac{\partial^2 w}{\partial y^2}\right)\right] \\ U_{o,y}+V_{o,x} + z\left[\varphi_{xo,y}+\varphi_{yo,x} - \frac{4z^2}{3t^2}\left(\varphi_{xo,y}+\varphi_{yo,x}+2\frac{\partial^2 w}{\partial x \partial y}\right)\right] \\ \varphi_{xo} - 4\frac{z^2}{t^2}\left(\frac{\partial w}{\partial x} + \varphi_{xo}\right) + \frac{\partial w}{\partial x} \\ \varphi_{yo} - 4\frac{z^2}{t^2}\left(\frac{\partial w}{\partial y} + \varphi_{yo}\right) + \frac{\partial w}{\partial y} \end{Bmatrix}$$

$$\text{or,} \quad \{\varepsilon\} = \begin{Bmatrix} \varepsilon_x^o \\ \varepsilon_y^o \\ \varepsilon_{xy}^o \\ \varepsilon_{xz}^o \\ \varepsilon_{yz}^o \end{Bmatrix} + z\begin{Bmatrix} K_x^1 \\ K_y^1 \\ K_{xy}^1 \\ o \\ o \end{Bmatrix} + z^2\begin{Bmatrix} o \\ o \\ o \\ K_{xz}^2 \\ K_{yz}^2 \end{Bmatrix} + z^3\begin{Bmatrix} K_x^3 \\ K_y^3 \\ K_{xy}^3 \\ o \\ o \end{Bmatrix} \qquad (3.14)$$

where

$$\varepsilon_x^o = U_{o,x} \quad ; \quad K_x^1 = \varphi_{xo,x} \quad ;$$

$$\varepsilon_y^o = V_{o,y} \quad ; \quad K_y^1 = \varphi_{yo,y} \quad ;$$

$$\varepsilon_{xy}^o = U_{o,y}+V_{o,x} \quad ; \quad K_{xy}^1 = \varphi_{xo,y}+\varphi_{yo,x} \quad ;$$

$$\varepsilon_{xz}^o = \varphi_{xo} + W_{o,x} \quad ; \quad K_{xz}^2 = -\frac{4}{t^2}\left(\frac{\partial w}{\partial x} + \varphi_{xo}\right) \quad ;$$

$$\varepsilon^{o}_{yz} = \varphi_{yo} + W_{o,y} \quad ; \qquad K^{2}_{yz} = -\frac{4}{t^2}\left(\frac{\partial w}{\partial y} + \varphi_{yo}\right) \quad ;$$

$$K^{3}_{x} = -\frac{4}{3t^2}\left(\frac{\partial^2 w}{\partial x^2} + \varphi_{xo,x}\right) \quad ;$$

$$K^{3}_{y} = -\frac{4}{3t^2}\left(\frac{\partial^2 w}{\partial y^2} + \varphi_{yo,y}\right) \quad ;$$

$$K^{3}_{xy} = -\frac{4}{3t^2}\left(2\frac{\partial^2 w}{\partial x \partial y} + \varphi_{xo,y} + \varphi_{yo,x}\right). \qquad (15)$$

Here, strain includes linear strains, curvatures, twists and other higher order curvatures. It may be noted that the transverse shear stresses are represented parabolically over the thickness and therefore, there is no need for any shear correction factor.

### 3.3.1.3 Stress-Strain relation

Each orthotropic layer of the plate has known elastic properties. The stress-strain relation of any particular layer, with one of the axes of orthotropy coinciding with one of the principal axis, is given by

$$\begin{Bmatrix} \sigma_x \\ \sigma_y \\ \sigma_z \\ \tau_{xy} \\ \tau_{xz} \\ \tau_{yz} \end{Bmatrix} = \begin{bmatrix} c_{11} & c_{12} & c_{13} & c_{14} & o & o \\ c_{21} & c_{22} & c_{23} & c_{24} & o & o \\ c_{31} & c_{32} & c_{33} & c_{34} & o & o \\ c_{41} & c_{42} & c_{43} & c_{44} & o & o \\ o & o & o & o & c_{55} & c_{56} \\ o & o & o & o & c_{65} & c_{66} \end{bmatrix} \begin{Bmatrix} \varepsilon_x \\ \varepsilon_y \\ \varepsilon_z \\ \varepsilon_{xy} \\ \varepsilon_{xz} \\ \varepsilon_{yz} \end{Bmatrix} \qquad 3.15$$

Since normal stress $\sigma_z$ is small it can be neglected. The corresponding strain $\varepsilon_z$ can be eliminated from Eq. 3.15 by equating $\sigma_z$ equal to zero. This results in reduced stress-strain relationship as

$$\begin{Bmatrix}\sigma_x\\ \sigma_y\\ \tau_{xy}\\ \tau_{xz}\\ \tau_{yz}\end{Bmatrix}=\begin{bmatrix}c'_{11} & c'_{12} & c'_{14} & o & o\\ c'_{21} & c'_{22} & c'_{24} & o & o\\ c'_{41} & c'_{42} & c'_{44} & o & o\\ o & o & o & c'_{55} & c'_{56}\\ o & o & o & c'_{65} & c'_{66}\end{bmatrix}\begin{Bmatrix}\varepsilon_x\\ \varepsilon_y\\ \varepsilon_{xy}\\ \varepsilon_{xz}\\ \varepsilon_{yz}\end{Bmatrix}$$

where

$c'_{ij} = c_{ij} - c_{i3}c_{j3}/c_{33}$ for i,j = 1,2 4 and

$c'_{ij} = c_{ij}$ for i,j = 5,6

(3.16)

For a particular case when fibers are oriented at an angle $\theta$ with the x-axis, the transformed stress-strain relation for a laminae will be

$$\begin{Bmatrix}\sigma_x\\ \sigma_y\\ \tau_{xy}\\ \tau_{xz}\\ \tau_{yz}\end{Bmatrix}=\begin{bmatrix}Q_{11} & Q_{12} & Q_{14} & o & o\\ Q_{21} & Q_{22} & Q_{24} & o & o\\ Q_{41} & Q_{42} & Q_{44} & o & o\\ o & o & o & Q_{55} & Q_{56}\\ o & o & o & Q_{65} & Q_{66}\end{bmatrix}\begin{Bmatrix}\varepsilon_x\\ \varepsilon_y\\ \varepsilon_{xy}\\ \varepsilon_{xz}\\ \varepsilon_{yz}\end{Bmatrix}, \text{where} \qquad (3.17)$$

$$Q_{11} = C'_{11}\cos^4\theta + 2(C'_{12} + 2C'_{44})\cos^2\theta \sin^2\theta + C'_{22}\sin^4\theta$$

$$Q_{12} = (C'_{11} + C'_{22} - 4C'_{44})\cos^2\theta \sin^2\theta + C'_{12}(\cos^4\theta + \sin^4\theta)$$

$$Q_{22} = C'_{11}\sin^4\theta + 2(C'_{12} + 2C'_{44})\cos^2\theta \sin^2\theta + C'_{22}\cos^4\theta$$

$$Q_{44} = (C'_{11} + C'_{22} - 2C'_{12} - 2C'_{44})\cos^2\theta \sin^2\theta + C'_{44}(\cos^4\theta + \sin^4\theta)$$

$$Q_{14} = (C'_{11} - 2C'_{44} - C'_{12})\cos^3\theta \sin\theta + (C'_{12} - C'_{22} + 2C'_{44})\cos\theta \sin^3\theta$$

$$Q_{24} = (C'_{11} - 2C'_{44} - C'_{12})\cos\theta \sin^3\theta + (C'_{12} - C'_{22} + 2C'_{44})\cos^3\theta \sin\theta$$

$$Q_{55} = C'_{55}\cos^2\theta + C'_{66}\sin^2\theta \; ; \; Q_{56} = (C'_{55} - C'_{66})\cos\theta \sin\theta$$

$$Q_{66} = C'_{55}\sin^2\theta + C'_{66}\cos^2\theta \; . \qquad (3.18)$$

### 3.3.1.4 Stress resultant-Strain relation

Combining Eq. 3.14 with Eq. 3.17 and on integrating layer by layer over the thickness, one obtains the stress resultants-strain relation in the matrix form as

$$\begin{Bmatrix} N_x \\ N_y \\ N_{xy} \\ Q_{xz} \\ Q_{yz} \\ M_x \\ M_y \\ M_{xy} \\ R_{xz} \\ R_{yz} \\ P_x \\ P_y \\ P_{xy} \end{Bmatrix} = \begin{bmatrix} A_{11} & A_{12} & A_{14} & 0 & 0 & B_{11} & B_{12} & B_{14} & 0 & 0 & E_{11} & E_{12} & E_{14} \\ & A_{22} & A_{24} & 0 & 0 & B_{21} & B_{22} & B_{24} & 0 & 0 & E_{21} & E_{22} & E_{24} \\ & & A_{44} & 0 & 0 & B_{41} & B_{42} & B_{44} & 0 & 0 & E_{41} & E_{42} & E_{44} \\ & & & A_{55} & A_{56} & 0 & 0 & 0 & D_{55} & D_{56} & 0 & 0 & 0 \\ & & & & A_{66} & 0 & 0 & 0 & D_{65} & D_{66} & 0 & 0 & 0 \\ & & & & & D_{11} & D_{12} & D_{14} & 0 & 0 & F_{11} & F_{12} & F_{14} \\ & & & & & & D_{22} & D_{24} & 0 & 0 & F_{21} & F_{22} & F_{24} \\ & & & & & & & D_{44} & 0 & 0 & F_{41} & F_{42} & F_{44} \\ & & & & & & & & F_{55} & F_{56} & 0 & 0 & 0 \\ & & & & & & & & & F_{66} & 0 & 0 & 0 \\ & & & & & & & & & & H_{11} & H_{12} & H_{14} \\ & & \text{Symmetric} & & & & & & & & & H_{22} & H_{24} \\ & & & & & & & & & & & & H_{44} \end{bmatrix} \begin{Bmatrix} \varepsilon_x^o \\ \varepsilon_y^o \\ \varepsilon_{xy}^o \\ \varepsilon_{xz}^o \\ \varepsilon_{yz}^o \\ K_x^1 \\ K_y^1 \\ K_{xy}^1 \\ K_{xz}^2 \\ K_{yz}^2 \\ K_x^3 \\ K_y^3 \\ K_{xy}^3 \end{Bmatrix}$$

or in compact notation, $\{N\} = [D]\{\varepsilon^o\}$, (3.19)

where,

$$(N_x, M_x, P_x) = \int_{-t/2}^{t/2} \sigma_x(1, z, z^3)dz \; ; \quad (Q_{xz}, R_{xz}) = \int_{-t/2}^{t/2} \tau_{xz}(1, z^2)dz \; ;$$

$$(N_y, M_y, P_y) = \int_{-t/2}^{t/2} \sigma_y(1, z, z^3)dz \; ; \quad (Q_{yz}, R_{yz}) = \int_{-t/2}^{t/2} \tau_{yz}(1, z^2)dz \; ;$$

and

$$(N_{xy}, M_{xy}, P_{xy}) = \int_{-t/2}^{t/2} \tau_{xy}(1, z, z^3)dz \; ; \qquad (3.20)$$

Elements of membrane stiffness matrix [A], membrane-bending coupling matrix [B], bending stiffness matrix [D] and other higher order matrices [E], [F], and [H] are definied as follows

$$(A_{ij}, B_{ij}, D_{ij}, E_{ij}, F_{ij}, H_{ij}) = \int_{-t/2}^{t/2} Q_{ij}(1, z, z^2, z^3, z^4, z^6)\, dz \qquad (3.21)$$

where i, j takes the values 1 to 6.

Eq. 3.19 contains higher order moment of stress resultants that are difficult to interpret physically.

### 3.3.1.5 Finite element formulation

Based on above theory, a rectangular flat plate element with seven degrees of freedom as given in Eq. 3.12 at each nodal point is formulated. The local element coordinate system is chosen to be parallel to the global coordinate system of the plate. Within the element, displacements can be interpolated in terms of the nodal degrees of freedom by adopting

(a) Interpolation functions for element coordinates x and y ; in-plane displacements $U_o$ and $V_o$ and the two rotations $(\varphi_{xo}, \varphi_{yo})$ by

$$p = \Sigma N_i p_i \; , \; (i = 1 \text{ to } 4 \qquad (3.22)$$

where p is the value of the above mentioned variables at any point in the element and $p_i$ is its value at node i of that particular element and $N_i$ is the interpolation function. $N_i$ can be expressed in the natural coordinate system (r and s) as

$$N_i = \frac{1}{4} * (1+rr_i) * (1+ss_i) \qquad (3.23)$$

where i is the number of function and $r_i$=-1,1,1,-1 ; $s_i$=-1,-1,1 1,for i=1,2,3 and 4 respectively.

(b)The transverse displacement is interpolated using a non-conforming shape function as proposed by Zienkiewicz and Cheung [16], which can be written in explicit form as

$$w(x;y)=[f_1\ g_1\ h_1\ f_2\ g_2\ h_2\ f_3\ g_3\ h_3\ f_4\ g_4\ h_4] \begin{Bmatrix} w_{o1} \\ w,_{x1} \\ w,_{y1} \\ w_{o2} \\ \vdots \\ w,_{x4} \\ w,_{y4} \end{Bmatrix}$$

where

$$f_i = \frac{1}{8} * (1+rr_i)*(1+ss_i)*(2+rr_i+ss_i-s^2-r^2) \qquad (3.24)$$

$$g_i = \frac{a}{16} * r_i*(1+rr_i)^2*(1+ss_i)*(rr_i-1)$$

$$h_i = \frac{b}{16} * s_i*(1+ss_i)^2*(1+rr_i)*(ss_i-1) \qquad (3.25)$$

and i varies from 1 to4.

Here,

$$r = \frac{2}{a}(x_c - x)$$

$$s = \frac{2}{b}(y_c - y)$$

and $(x_c, y_c)$ are the coordinates of the centroid of the plate; a, b are the sides of the rectangle. The non-dimensional coordinates for nodes 1,2,3 and 4 are (-1,-1),(1,-1),(1,1) and (-1,1) respectively.

Nodal displacement vector $\{\delta_1\}$ of the first node on the reference surface is given by

$$\{\delta_1\} = [U_{o1} \quad V_{o1} \quad \phi_{xo1} \quad \phi_{yo1} \quad w_{o1} \quad w_{,x1} \quad w_{,y1}]^T \tag{3.26}$$

and the element displacement vector $\{\delta_e\}$ is given by

$$\{\delta_e\} = [\delta_1 \quad \delta_2 \quad \delta_3 \quad \delta_4]^T \tag{3.27}$$

Generalised displacement vector at a point is

$$\{\delta\} = [U_o \quad V_o \quad \phi_{xo} \quad \phi_{yo} \quad w_o \quad w_{,xo} \quad w_{,yo}]^T \tag{3.28}$$

Substituting Eq. 3.22, Eq.3.24 and Eq. 3.28 in Eqs. 3.14, one obtains the relation between strain versus nodal d.o.f. as

$$
\begin{Bmatrix} \varepsilon_x^o \\ \varepsilon_y^o \\ \varepsilon_{xy}^o \\ \varepsilon_{xz}^o \\ \varepsilon_{yz}^o \\ K_x^1 \\ K_y^1 \\ K_{xy}^1 \\ K_{xz}^2 \\ K_{yz}^2 \\ K_x^3 \\ K_y^3 \\ K_{xy}^3 \end{Bmatrix} = \begin{bmatrix} N_{1,x} & & & & & \cdots & \cdots \\ & N_{1,y} & & & & \cdots & \cdots \\ N_{1,y} & N_{1,x} & & & & \cdots & \cdots \\ & & N_1 & f_{1,x} & g_{1,x} \; h_{1,x} & \cdots & \cdots \\ & & & N_1 & f_{1,y} \; g_{1,y} \; h_{1,y} & \cdots & \cdots \\ & & N_{1,x} & & & \cdots & \cdots \\ & & & N_{1,y} & & \cdots & \cdots \\ & & N_{1,y} & N_{1,x} & & \cdots & \cdots \\ & & \bar{N}_1 & \bar{f}_{1,x} & \bar{g}_{1,x} \; \bar{h}_{1,x} & \cdots & \cdots \\ & & & \bar{N}_1 & \bar{f}_{1,y} \; \bar{g}_{1,y} \; \bar{h}_{1,y} & \cdots & \cdots \\ & & \bar{\bar{N}}_{1,x} & \bar{\bar{f}}_{1,xx} & \bar{\bar{g}}_{1,xx} \; \bar{\bar{h}}_{1,xx} & \cdots & \cdots \\ & & & \bar{\bar{N}}_{1,y} & \bar{\bar{f}}_{1,yy} \; \bar{\bar{g}}_{1,yy} \; \bar{\bar{h}}_{1,yy} & \cdots & \cdots \\ & & \bar{\bar{N}}_{1,y} & \bar{\bar{N}}_{1,x} & 2\bar{\bar{f}}_{1,xy} \; 2\bar{\bar{g}}_{1,xy} \; 2\bar{\bar{h}}_{1,xy} & \cdots & \cdots \end{bmatrix} \begin{Bmatrix} U_{o1} \\ V_{o1} \\ \varphi_{xo1} \\ . \\ . \\ . \\ . \\ U_{o4} \\ V_{o4} \\ \varphi_{xo4} \\ \varphi_{yo4} \\ W_{o4} \\ W_{o4,x} \\ W_{o4,y} \end{Bmatrix}
$$

where,

$c_1 = -\frac{4}{t^2}$ ; $c_2 = -\frac{4}{3t^2}$ ; and terms with single bar and double bar mean multiplying with $c_1$ and $c_2$ respectively i.e. $\bar{N}_1 = C_1 N_1$ ; $\bar{\bar{N}}_1 = C_2 N_1$ and so on.

In compact form,

$$\{ \varepsilon^o \} = [ B ] \{ \delta_e \} \qquad (3.29)$$

Once all the relations are evaluated, internal strain energy of an element due to bending and shear can now be determined from Eq. 3.1. Integrating the products of strains and stress resultants over the area of an element i.e..

$$\Pi = \frac{1}{2} \int_A \{\varepsilon\}^T [N] \, dA \, , \tag{3.30}$$

where $\{\varepsilon\}$ includes all strains including those for shear and [N] is the vector of all stress resultants including higher order terms. Substituting Eq. 3.19 and Eq. 3.29 for $\{\varepsilon\}$ and [N] into Eq. 3.30, one obtains

$$\Pi = \frac{1}{2} \int_A \{\delta\}^T [B]^T [D][B] \{\delta\} \, dA \tag{3.31}$$

In a concise form

$$\Pi = \frac{1}{2} \{\delta_e\}^T [K_e] \{\delta_e\} \tag{3.32}$$

$$\text{where} \quad [K_e] = \int_A [B]^T [D][B] \, dA \tag{3.33}$$

is the stiffness matrix for an element which includes membrane, bending and transverse shear stresses. Evaluation of this stiffness matrix involves integration of functions over the domain represented by the element as

$$[K_e] = \int_{-1}^{1} \int_{-1}^{1} [B]^T [D][B] \det[J] \, dr \, ds \tag{3.34}$$

Where r, s are the natural coordinate system. This integral is evaluated numerically using Gauss Quadrature. Thus, the stiffness matrix is evaluated as a double summation over the domain and is given by

$$[K_e] = \sum_{s}^{gps} \sum_{r}^{gpr} (\vartheta_{rs}) w_r \, w_s \qquad (3.35)$$

where gpr, gps are the number of integration points and $w_r$ and $w_s$ are the weights in the r, s directions respectively.

$$\vartheta_{rs} = [B]^T [D] [B] \det [J] \qquad (3.36)$$

Once the element stiffness matrix is evaluated, next step is to determine the element load vector.

### 3.3.2 Consistent load vector

In the finite element analysis of structures by the displacement method, the only permissible form of loading, other than initial stressing is by the prescription of concentrated loads at the nodal points. All forms of loading such as gravity action, pressures assigned to element surfaces, must be converted into equivalent nodal forces.

Now, if a distributed load q is acting per unit area of an element in the direction of w, than the contribution of these forces to each of the nodes is

$$\left\{ F_i \right\} = \int\int N^T q \, dx \, dy \qquad (3.37)$$

For the present element with 7 d.o.f., the load vector is considered as ( assuming component of load along first four d.o.f. is nil) i.e.

$$\left\{ F_i \right\} = \begin{Bmatrix} F_{xi} \\ F_{yi} \\ F_{\varphi xi} \\ \vdots \\ F_{w_{yi}} \end{Bmatrix} = q \sum_i \sum_j w_i \, w_j \, |J| \begin{Bmatrix} o \\ o \\ o \\ o \\ f_i \\ g_i \\ h_i \end{Bmatrix} \qquad (3.38)$$

Combining the nodal load vectors $\{F_i\}$s, the element load vector $\{F_e\}$ can be obtained as:

$$\{F_e\} = [\ F_1\ F_2\ F_3\ F_4\ ]^T \qquad (3.39)$$

### 3.3.3 Formulation of global matrix

Stiffness matrix for the entire structure is assembled in half band form after accounting the boundary conditions. Load vector is also formed. Global displacement vector is determined by solving the equilibrium equations by standard Gauss elimination technique.

### 3.3.4 Solution

The stiffness matrix of the plate structure is symmetric and banded. In the development of finite element program, the symmetric and banded nature of the stiffness matrix [K] is effectively made use of, for reducing the main storage requirement. Only elements between bandwidth and main diagonal are stored as an one-dimensional array. Numbering of nodes are done so as to keep the half band width to a minimum. The stiffness and load matrices of the structure have been formed only for those degrees of freedom which are unrestrained. By this process boundary conditions are imposed implicitly and equations of equilibrium corresponding to specified boundary displacements are not formed.

Table 3.1 gives the type of boundary conditions which are to be incorporated on edges where x is constant. Similar statements can be made for edges where y is constant by interchanging the subscripts for x and y.

Table: 3.1 Boundary conditions for various edge conditions, x = constant.

| Simply supported | Clamped | Free |
|---|---|---|
| $U_o \neq 0$ ; $V_o \neq 0$ | $U_o = 0$ ; $V_o = 0$ | $U_o \neq V_o \neq 0$ |
| $\varphi_{xo} \neq 0$; $\varphi_{yo} = 0$ | $\varphi_{xo} = 0$ ; $\varphi_{yo} = 0$ | $\varphi_{xo} \neq \varphi_{yo} \neq 0$ |
| $w_o = 0$ ; $w,_x \neq 0$ | $w_o = 0$ ; $w,_x = 0$ | $w_o \neq 0$ ; $w,_x \neq 0$ |
| $w,_y = 0$ | $w,_y = 0$ | $w,_y \neq 0$ |

Standard Gauss elimination method is used for the solution of algebraic equations.

## 3.4. Stress formulation

Generalised strain at a point is related to the reference surface strains as

$$\{\varepsilon\} = \begin{Bmatrix} \varepsilon_x \\ \varepsilon_y \\ \varepsilon_{xy} \\ \varepsilon_{xz} \\ \varepsilon_{yz} \end{Bmatrix} = \begin{bmatrix} 1 & o & o & o & o & z & o & o & o & o & z^3 & o & o \\ o & 1 & o & o & o & o & z & o & o & o & o & z^3 & o \\ o & o & 1 & o & o & o & o & z & o & o & o & o & z^3 \\ o & o & o & 1 & o & o & o & o & z^2 & o & o & o & o \\ o & o & o & o & 1 & o & o & o & o & z^2 & o & o & o \end{bmatrix} \begin{Bmatrix} \varepsilon_x^o \\ \varepsilon_y^o \\ \vdots \\ K_{xy}^3 \end{Bmatrix}$$

In short $\{\varepsilon\} = [B_1]\{\varepsilon^o\}$ (3.40)

Substituting Eq. 3.29 in Eq. 3.40, one obtains

$$\{\varepsilon\} = [B_1][B]\{\delta_e\} = [B_2]\{\delta_e\} \quad (3.41)$$

The global displacement vector $\{\delta_e\}$ is substituted in Eq. 3.41, to get the strain vector which in turn will be substituted in Eq. 3.17 to get the stress vector at any point in the structure. Stresses are obtained at the 2X2 Gauss sampling points. Using the technique of local stress smoothening [78], these stresses are transfered to the corner nodes. The smoothed stress values are then modified by finding the average of the nodal stresses of all elements meeting at a common node.

## 3.5 Numerical examples and discussion

To demonstrate the accuracy and the reliability of the finite element procedure, various plate problems with different boundary conditions and loading cases are selected for comparison with the available theoritical and experimental results of other research workers. This also provides a scope to verify the computer program developed in this connection.

Before tackling any plate problems, the accuracy of element stiffness matrix is checked for the presence of rigid body modes.

Static analysis of both laminated as well as sandwich plates were considered in this chapter.

### 3.5.1 Eigenvalue analysis

It is well known that proper representation of rigid body modes in the functional representation of the displacements leads to accurate results with relatively coarse mesh and consequently less computational effort. To check the accuracy of the element formulation, eigenvalue

analysis is performed for a three layer square laminated plate element with the following geometrical and material parameters. Numerical integration is carried out at 2X2 Gauss-Quadrature points.

**Geometrical parameters:**

Plate : 3-ply ($0^{o}$-$90^{o}$-$0^{o}$) laminate

Side-to-thickness ratio = a/t = $\lambda$ = 100

**Material constants:**

$E_{11}$= 172.4 GPa ($25x10^{6}$psi) ;

$E_{22}$= 6.9 GPa ($10^{6}$psi) ;

$G_{12}$= $G_{13}$= 3.45 GPa ($.5x10^{6}$psi) ; $G_{23}$= 1.38 GPa ($.2x10^{6}$psi) ;

$\nu_{12}$= $\nu_{13}$= 0.25 ; $\nu_{21}$= $(E_2/E_1)x\ \nu_{12}$

Table 3.2 shows the 28 eigenvalues obtained from single element. It can be seen that six of the eigenvalues are nearly zero as compared to other ones. These correspond to six rigid body motions of the plate element.

**Table 3.2:** Eigenvalues obtained for a plate element.

| | | | |
|---|---|---|---|
| -0.77912278E-08 | 0.27600276E+05 | 0.29544430E+06 | 0.90768363E+06 |
| -0.40987838E-08 | 0.68667099E+05 | 0.35255376E+06 | 0.93755961E+06 |
| -0.11788449E-08 | 0.69911146E+05 | 0.36239458E+06 | 0.14184858E+06 |
| -0.10396425E-08 | 0.12365673E+06 | 0.38348547E+06 | 0.16613569E+07 |
| 0.14309289E-08 | 0.12385595E+06 | 0.48886279E+06 | 0.27565006E+07 |
| 0.36080886E-08 | 0.15267839E+06 | 0.56254239E+06 | 0.28413074E+07 |
| 0.11385220E+03 | 0.15703389E+06 | 0.86710803E+06 | 0.452325679+07 |

### 3.5.2 Static analysis of laminated plates

**EXAMPLE 3.1:** Analysis of a three layer $(0^{\circ}\text{-}90^{\circ}\text{-}0^{\circ})$, simply-supported square plate with side-to-thickness ratios as 10, 20 and 100 with material constants are the same as that in above. Fig. 1.5.c gives the loading condition. Table 3.3 gives the comparison of present solution with existing literature values.

Notations used in the table are:

R indicates sources of reference;

A: Exact/Pagano and Hatfield [39]; B: FE1/J. N. Reddy[70];

C: FE2/Panda and Natarajan [67]; D: FE3/Mawenya and Davis[66];

E: ISPQ/Moser, Lehar and Schmid [75]; F: FE4/Phan and Reddy[21];

G: Author's values.

**Loading:** $q = q_o \sin(\pi x/a)\sin(\pi y/b)$; here $a = b = L$

Results are presented in terms of normalized quantities as :

$$(\bar{\sigma}_x, \bar{\sigma}_y, \bar{\tau}_{xy}) = (1/q_o\lambda^2)(\sigma_x, \sigma_y, \tau_{xy}),$$

$$\bar{w} = \pi^4 Q w/12\lambda^4 t q_o, \quad \lambda = a/t, \quad \bar{z} = z/t \text{ , where}$$

$$Q = 4G_{12} + [\, E_{11} + E_{22}(1+2\,\nu_{12})]/(1-\nu_{12}\,\nu_{21})$$

$\delta_{max} = \bar{w}(a/2, a/2, 0)$ ; $E_\delta$ = % Error in $\delta_{max}$ from exact value;

$\sigma_1 = \bar{\sigma}_x(a/2, a/2, \pm 1/2)$ ; $E_{\sigma_1}$ = % Error in $\sigma_1$ from exact value ;

$\sigma_2 = \bar{\sigma}_y(a/2, a/2, \pm 1/4)$ ; $E_{\sigma_2}$ = % Error in $\sigma_2$ from exact value;

$\tau = \bar{\tau}_{xy}(0, 0, \pm 1/2)$ ; $E_\tau$ = % Error in $\tau$ from exact value.

Table 3.3: A three layer cross ply square plate under sinusoidal loading

| λ | R | $\delta_{max}$ | $E_\delta$ | $\sigma_1$ | $E_{\sigma_1}$ | $\sigma_2$ | $E_{\sigma_2}$ | $\tau$ | $E_\tau$ |
|---|---|---|---|---|---|---|---|---|---|
| | A | 1.709 | - | .559 | - | .403 | - | 0.0276 | - |
| | B | 1.534 | -10.24 | .484 | -13.4 | .350 | -13.2 | - | - |
| 10 | C | 1.448 | -15.27 | .532 | -4.43 | .307 | -23.8 | 0.0250 | -9.4 |
| | D | 2.034 | 19.02 | .542 | -3.04 | - | - | 0.0292 | +5.8 |
| | E | 1.727 | 1.04 | .493 | -11.8 | .407 | 0.99 | - | - |
| | F | 1.714 | 0.31 | .554 | -0.88 | .397 | -1.42 | 0.0273 | -1.1 |
| | G | 1.468 | -14.0 | .577 | +3.29 | .318 | -21.1 | 0.0247 | -11. |
| | A | 1.189 | - | .543 | - | .309 | - | 0.0230 | - |
| | B | 1.136 | -4.48 | .511 | -5.89 | .287 | -7.12 | - | - |
| 20 | C | 1.114 | -6.31 | .557 | 2.58 | .307 | -0.65 | 0.0231 | 0.4 |
| | D | 1.273 | 7.07 | .546 | .55 | - | - | 0.0239 | 3.9 |
| | E | 1.191 | 0.14 | .533 | -1.84 | .312 | 0.97 | - | |
| | F | 1.191 | +.16 | .538 | -0.96 | .3085 | -1.61 | 0.0230 | -1.3 |
| | G | 1.119 | -5.90 | .556 | 2.76 | .284 | -8.22 | 0.0224 | -2.6 |
| | A | 1.008 | - | .539 | - | .271 | - | 0.0214 | |
| | B | 1.005 | -.298 | .523 | -2.97 | .263 | -2.95 | - | |
| 100 | C | 1.003 | -.496 | .566 | 5.01 | .284 | 4.80 | 0.0223 | 4.2 |
| | D | 1.015 | .694 | .551 | 2.23 | - | - | 0.0219 | 2.3 |
| | E | 0.999 | -.899 | .537 | -0.37 | .265 | -2.20 | - | |
| | F | 0.997 | -1.11 | .523 | -2.89 | .263 | -2.81 | 0.0209 | -2.4 |
| | G | 1.004 | - 0.4 | .543 | 0.7 | .267 | -1.48 | 0.0215 | 0.3 |
| CPT | | 1.000 | | 0.539 | | 0.269 | | 0.0213 | |

**EXAMPLE 3.2:** Most studies deal with laminates consisting of only a few layers, while in reality, there can be many layers, and at times upto 100 or more. It is necessary to examine the response of the present element to multi-ply laminates. Square laminates with edge dimension a and thickness t consisting of 5,7 and 9 layers under the same loading and material constants as given in example 3.1. are

investigated. Results are compared with the exact values [39]. All the laminates considered are symmetric w.r.t. the central plane, with fiber orientations alternatively $0^{o}$ and $90^{o}$ w.r.t the x axis, and $0^{o}$ layers are at the outer surfaces of the laminate. Total thicknesses of $0^{o}$ and $90^{o}$ layers are the same. Layers at the same orientation have equal thicknesses (Fig. 1.5.b). Material properties are as given in example 3.1.

Results are given in table 3.4(a-c) in terms of the same normalized quantities as given above. In table below 1 stands for exact value [39] and 2 for Author's value. For all tables, quantities are found at the same location except for $\sigma_y$ , for which locations are given in each table separately. Here, $\tau_1 = \tau_{xy}(0,0,\pm 1/2)$ ; $\tau_2 = \tau_{xz}(0,a/2,0)$ ; $\tau_3 = \tau_{yz}(a/2,0,0)$.

Table 3.4(a-b): Maximum deflection and stresses in 5 and 7 ply plates

| For 5-ply laminate and $\sigma_2 = \sigma_y(a/2,a/2,\pm 1/3)$ | | | | | | | | | | | | |
|---|---|---|---|---|---|---|---|---|---|---|---|---|
| $\lambda$ | $\delta_{max}$ | | $\sigma_1$ | | $\sigma_2$ | | $\tau_1$ | | $\tau_2$ | | $\tau_3$ | |
| | 1 | 2 | 1 | 2 | 1 | 2 | 1 | 2 | 1 | 2 | 1 | 2 |
| 10 | 1.57 | 1.42 | .545 | .574 | .430 | .389 | .0246 | .0236 | .258 | .160 | .223 | .289 |
| 20 | 1.15 | 1.10 | .539 | .557 | .380 | .369 | .0222 | .0221 | .268 | .161 | .212 | .281 |
| 100 | 1.01 | .994 | .539 | .535 | .360 | .356 | .0213 | .0214 | .272 | .140 | .205 | .236 |
| CPT | 1.00 | | .539 | | .359 | | .0213 | | .272 | | .205 | |
| 3.4.b. 7-ply laminate and $\sigma_2 = \sigma_y(a/2,a/2\ \pm 3/8)$ | | | | | | | | | | | | |
| 10 | 1.53 | 1.41 | .548 | .577 | .457 | .434 | .0237 | .0234 | .255 | .384 | .219 | .123 |
| 20 | 1.13 | 1.10 | .539 | .557 | .419 | .415 | .0219 | .0221 | .267 | .386 | .210 | .121 |
| 100 | 1.01 | .993 | .539 | .535 | .405 | .400 | .0213 | .0214 | .272 | .337 | .205 | .103 |
| CPT | 1.00 | | .539 | | .404 | | .0213 | | .272 | | .205 | |

Table 3.4.c: Maximum deflection and stresses in 9 ply plate

| 9-ply laminate and $\sigma_2 = \sigma_y(a/2, a/2, \pm 2/5)$ | | | | | | | | | | | | |
|---|---|---|---|---|---|---|---|---|---|---|---|---|
| 10 | 1.51 | 1.41 | .551 | .580 | .477 | .462 | .0233 | .0233 | .247 | .150 | .226 | .318 |
| 20 | 1.13 | 1.10 | .541 | .558 | .444 | .444 | .0218 | .0221 | .255 | .151 | .221 | .313 |
| 100 | 1.01 | .993 | .539 | .535 | .431 | .427 | .0213 | .0214 | .259 | .131 | .219 | .268 |
| CPT | 1.00 | | .539 | | .431 | | .0213 | | .259 | | .219 | |

Fig. 3.2 gives the distribution of in-plane displacement $u(0, b/2, z)$ and $\sigma_x(a/2, b/2, z)$ across the depth in a 9-ply square laminate.

**EXAMPLE 3.3:** A three layer $(0^o, 90^o, 0^o)$ of equal, simply supported rectangular plate with b=3a as shown in Fig. 1.5(c). Material properties are same as that of example 3.1. Results of this case is given in Table 3.5.

Notations used are:

Loading is $q = q_o \sin(\frac{\pi x}{a}) \sin(\frac{\pi y}{3a})$ and $\lambda = \frac{a}{t} = 100, 20$ and 10.

$\bar{w} = w * 100.E_{22}/q_o t\lambda^4$ ; $\lambda = a/t$, $\bar{z} = z/t$ ,

$\delta_{max} = \bar{w}\ (a/2, a/2, 0)$ ; $E_\delta$= % Error in $\delta_{max}$ from exact value;

$\sigma_1 = \bar{\sigma}_x(a/2, a/2, \pm 1/2)$ ; $E_{\sigma_1}$= % Error in $\sigma_1$ from exact value ;

$\sigma_2 = \bar{\sigma}_y(a/2, a/2, \pm\ 1/6)$ ; $E_{\sigma_2}$ = % Error in $\sigma_2$ from exact value ;

$\tau = \bar{\tau}_{xy}(0, 0, \pm\ 1/2)$ ; $E_\tau$ = % Error in $\tau$ from exact value.

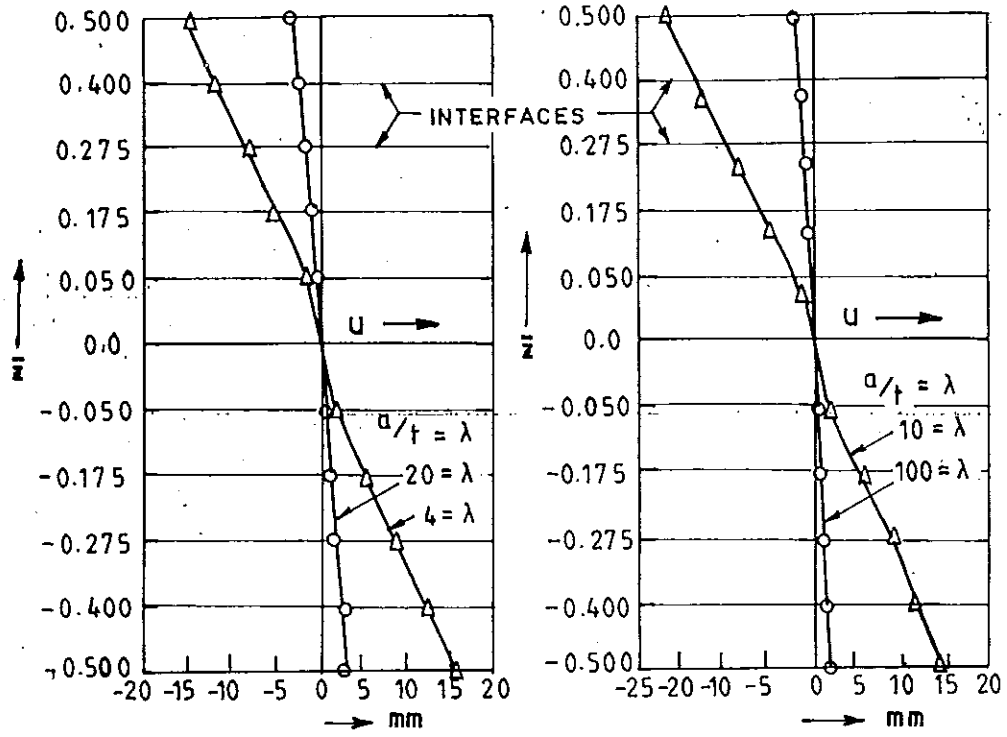


(a) IN-PLANE DISPLACEMENT ( $\bar{u}$ ) AT ( 0, $\frac{b}{2}$ , $\bar{z}$ )

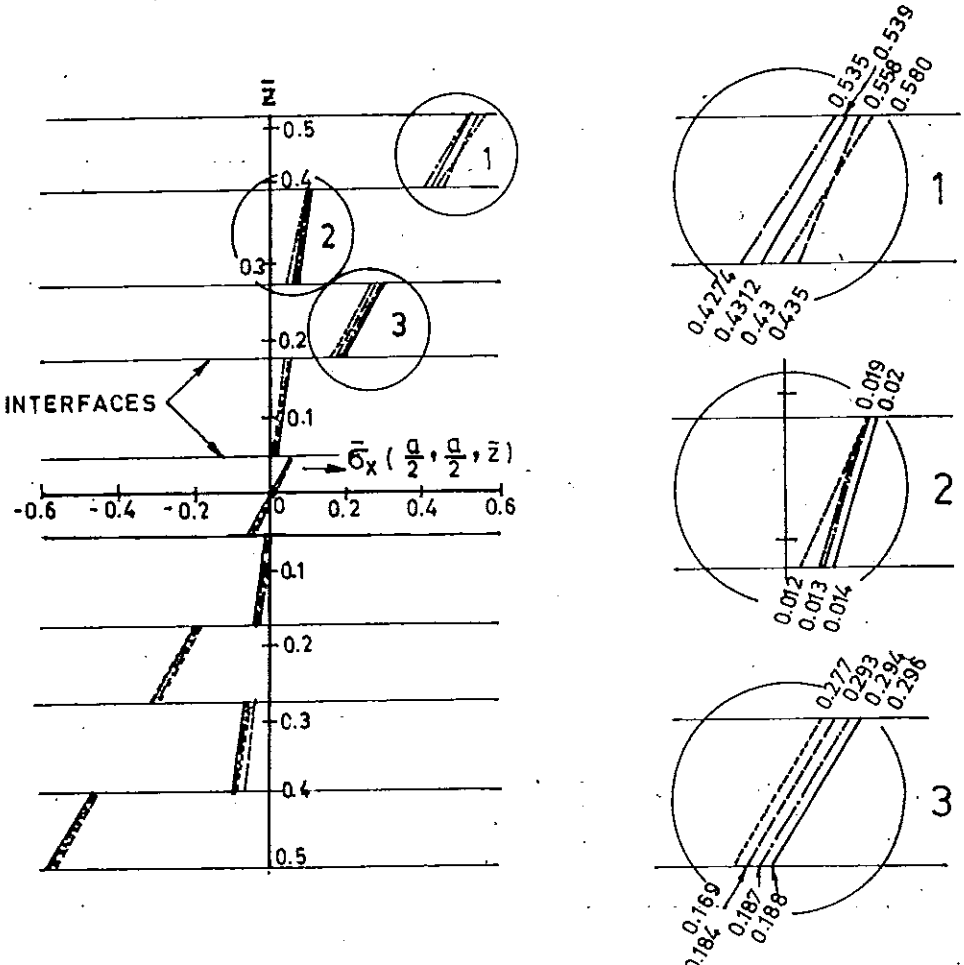


(b) NORMAL STRESS $\sigma_x$ ( $\frac{a}{2}$ , $\frac{a}{2}$ , z ) IN 9-PLY LAMINATE

FIG. 3.2

R for reference sources

A : Exact/Pagano and Hatfield [39]; B: Panda and Natarajan[67]

C : FE/Mawenya and Davis [66]; D : Author's value ;

Table 3.5: Three layer, cross-ply rectangular plate under sinusoidal loading (b=3a).

| λ | R | $\delta_{max}$ | $E_\delta$ | $\sigma_1$ | $E_{\sigma_1}$ | $\sigma_2$ | $E_{\sigma_2}$ | $\tau$ | $E_\tau$ |
|---|---|---|---|---|---|---|---|---|---|
| | A | 0.919 | - | .725 | - | .044 | - | 0.0123 | - |
| | B | 0.752 | -18.17 | .653 | - 9.90 | .037 | 15.60 | 0.0105 | 14.6 |
| 10 | C | 1.141 | -24.16 | .685 | - 5.50 | - | - | 0.0141 | 14.6 |
| | D | 0.834 | - 9.24 | .704 | - 2.86 | .037 | 14.71 | 0.0113 | +8.50 |
| | A | 0.610 | - | .650 | - | .030 | - | 0.0093 | - |
| | B | 0.565 | -7.40 | .654 | 0.62 | .029 | 4.01 | 0.0091 | 2.15 |
| 20 | C | 0.664 | 8.85 | .651 | 0.154 | - | - | 0.0099 | - |
| | D | 0.594 | -2.64 | .655 | 0.70 | .0278 | 7.02 | 0.0091 | 2.0 |
| | A | 0.508 | - | .624 | - | .0253 | - | 0.0083 | - |
| | B | 0.505 | .590 | .654 | 4.80 | .0261 | 3.16 | 0.0086 | 3.6 |
| 100 | C | 0.510 | .390 | .638 | 2.24 | - | - | 0.0085 | 2.4 |
| | D | 0.511 | .530 | .614 | 1.63 | .0244 | 3.55 | 0.0083 | 0.2 |
| CPT | | 0.503 | | 0.623 | | 0.0252 | | - | |

**EXAMPLE 3.4:** Cylindrical bending of a three layer symmetric angle-ply laminate where ply orientation and thickness respectively are $(+\theta^o, -\theta^o, +\theta^o)$ and (t/4, t/2, t/4). Angles are measured clockwise from the x-axis. Material properties of layers are same as that of example 3.2. The plate is under sinusoidal loading $p_z = q_o \sin(\pi x/a)$. Table 3.6 gives the results for $\lambda = 10$.

Notations used are

$\bar{w}$ = central deflection x $(\pi^4 Q)/(12 q_o t \lambda^4)$;

$\bar{\sigma}_x = \sigma_x(a/2, t/2) \times (\pi^2/6 q_o \lambda^2)$; $E_w$ and $E_\sigma$ are % errors in deflection and stress from exact values [79].

References:

A: Exact elasticity solution [79]; B: Panda and Natarajan [67]

C: Author's solution.

**Table 3.6:** Cylindrical bending of three layer angle ply $(\phi^o, -\phi^o, -\phi^o)$ plate under sinusoidal loading ($\lambda$ = 10).

| $\theta^o$ | $\bar{Q}$ | $\bar{w}$ | | | $\bar{\sigma}_x$ | | | $E_w$ | $E_\sigma$ |
|---|---|---|---|---|---|---|---|---|---|
| | | A | B | C | A | B | C | | |
| 15 | 1.5456 | 1.532 | 1.495 | 2.159 | 1.09 | 1.170 | 0.96 | 49 | 11.9 |
| 30 | 1.0288 | 1.532 | 1.534 | 1.757 | 1.06 | 1.194 | 0.91 | 14 | 15.9 |
| 45 | 0.5022 | 1.375 | 1.470 | 1.518 | 1.03 | 1.117 | 0.98 | 10 | 4.8 |
| 60 | 0.1822 | 1.164 | 1.271 | 1.271 | 1.02 | 1.078 | 1.03 | 9 | 1.5 |
| 75 | 0.0803 | 1.035 | 1.062 | 1.114 | 1.00 | 1.054 | 0.94 | 7 | 6.0 |
| CPT | | 1.000 | | | | | | | |

**EXAMPLE 3.5:** Three ply square laminate with layers of equal thickness and subjected to a uniformly distributed load of intensity $q_o$. This load is expanded in terms of the double-fourier series as

$$q = \sum Q_{mn} \sin\alpha x \sin\beta y \; ; \text{ where } \alpha = m\pi/a \text{ and } \beta = n\pi/b \; ; \text{ and}$$

$$Q_{mn} = \frac{16q_o}{mn\pi^2} \; ; \; m,n = 1,3,5,\ldots.$$

$$= 0 \; ; \; m,n = 2,4,\ldots.$$

Material properties are same as that in example 3.2. Midpoint deflection with different number of terms in the fourier series are given in table 3.7, where FSDT means First Order Shear Deformation Theory.

**Table 3.7:** Non-dimensionalized deflection $\bar{w}$ with different m,n values

| | Reddy [14] | | | FSDT | | | Author's theory | | |
|---|---|---|---|---|---|---|---|---|---|
| $\lambda$ | N=9 | N=29 | N=49 | N=9 | N=29 | N=49 | N=9 | N=29 | N=49 |
| 10 | 1.090 | 1.090 | 1.090 | 1.022 | 1.022 | 1.022 | 0.968 | 0.961 | 0.965 |
| 20 | 0.776 | 0.776 | 0.776 | .7574 | .7573 | .7573 | .7588 | .7553 | .7572 |
| 100 | .6705 | .6705 | .6705 | .6697 | .6697 | .6697 | .6834 | .6861 | .6823 |

$\bar{w} = (w\, E_{22} t^3) \times 100/(q_o a^4)$ and $m = n = N$ .

**EXAMPLE 3.6:** Numerical results for a 3-ply square laminated plate with identical top and bottom plies under uniformly distributed load with material properties as given below. Effect of modular ratio between plies is presented. The relative values of the moduli are the same in all the plies i.e. $(E_x : E_y : E_z : E_{xy} : E_{xz} : E_{yz} : G_{xy} : G_{xz} : G_{yz})$ are identical.

Geometric and material properties are given in Fig. 1.8(a).

Following notations are used in the table below

$w = w(a/2, b/2)$ ; $\sigma_x$ and $\sigma_y$ at $(a/2, b/2)$ ; $\tau_{xz}$ is at $(0, b/2)$

**Table 3.8:** A 3-ply laminate under u.d.l.

| Ref. | $\beta$ | $wEx_2/h$ | $\sigma_x/q_o$ at | | | $\sigma_y/q_o$ at | | | $\tau_{xz}/q_o$ | |
|---|---|---|---|---|---|---|---|---|---|---|
| | | centre | 11 | 12 | 13 | 21 | 22 | 23 | 31 | 32 |
| P | 1 | 679.33 | 36.98 | 29.23 | 29.23 | 21.93 | 17.35 | 17.35 | 1.97 | 5.46 |
| | 5 | 256.17 | 60.88 | 47.26 | 9.45 | 38.64 | 30.34 | 6.07 | 3.120 | 4.84 |
| | 10 | 154.02 | 65.85 | 50.22 | 5.022 | 43.39 | 33.71 | 3.371 | 3.438 | 4.4 |
| | 15 | 114.10 | 67.34 | 50.55 | 3.37 | 45.75 | 35.24 | 2.35 | 3.541 | 4.053 |
| TPT | 1 | 640.39 | 36.10 | 28.88 | 28.88 | 21.62 | 17.30 | 17.30 | 2.003 | 5.564 |
| | 5 | 216.94 | 61.14 | 48.91 | 9.783 | 36.62 | 29.30 | 5.86 | 3.386 | 4.59 |
| | 10 | 118.77 | 66.95 | 53.56 | 5.356 | 40.10 | 32.08 | 3.208 | 3.708 | 4.367 |
| | 15 | 81.77 | 69.14 | 55.31 | 3.69 | 41.41 | 33.13 | 2.21 | 3.83 | 4.283 |
| S&R | 1 | 688.58 | 36.02 | 28.54 | 28.54 | 22.21 | 17.67 | 17.67 | 2.40 | 5.34 |
| | 5 | 258.97 | 60.35 | 46.62 | 9.34 | 38.49 | 30.10 | 6.16 | 3.72 | 4.36 |
| | 10 | 159.38 | 65.33 | 48.86 | 4.90 | 43.57 | 33.41 | 3.50 | 3.93 | 4.096 |
| | 15 | 121.72 | 66.79 | 48.30 | 3.24 | 46.42 | 34.96 | 2.494 | 3.956 | 3.964 |

P=Author's ; TPT=Thin plate theory ; S&R=Srinivas et al [20]

11 ≡ Top ply at top surface ; 12 ≡ Top ply at interface ;
13 ≡ Mid ply at upper interface ; 21 ≡ Top ply at top surface ;
22 ≡ Top ply at interface ; 23 ≡ Mid ply at upper interface ;
31 ≡ At upper interface and 32 ≡ At mid surface.

### 3.5.3 Static analysis of sandwich plates

**EXAMPLE 3.7:** A three ply sandwich plate under uniformly distributed loading with cross-section and material constants are as given in Fig. 1.5(d). Three typical cases are taken up from [75].

case1: Thin, simply-supported plate;
case2: thick, simply-supported plate and
case3: thick, clamped plate.

Results given in table 3.9 are taken from Ref.[75] for comparison.

**Table 3.9:** Sandwich plate under uniform load : comparison of results for different aspect-ratios.

| | Element | NET | D.O.F. | $w_{max}$ | $Q_{max}$ | $M_{max}$ |
|---|---|---|---|---|---|---|
| Simply-Supported Thin Plate | TRIM 32 | 5X5 | 425 | 7802.4 | 4039 | 700040 |
| | ISPQ | 5X5 | 300 | 7780.2 | 5305 | 691510 |
| | ISPC | 5X5 | 675 | 7782.7 | 4118 | 689650 |
| | Author's | 4x4 | 120 | 8144.8 | 3391 | 654266 |
| | Shear deformation Theory | | | 7801.9 | 4050 | 689560 |
| | Classical Plate Theory | | | 7615.8 | 4050 | 689560 |
| Simply-Supported Thick Plate | TRIM 32 | 5X5 | 425 | 31.455 | 934 | 372300 |
| | ISPQ | 5X5 | 300 | 30.441 | 948 | 368210 |
| | ISPC | 5X5 | 675 | 30.440 | 935 | 366870 |
| | Author's | 4x4 | 120 | 31.320 | 810 | 349750 |
| | Shear deformation Theory | | | 31.454 | 935 | 366830 |
| | Classical Plate Theory | | | 21.553 | 935 | 366830 |
| Clamped Thick Plate | TRIM 32 | 5X5 | 425 | 17.069 | 1009 | 331900 |
| | ISPQ | 5X5 | 300 | 16.036 | 1042 | 334080 |
| | ISPC | 5X5 | 675 | 16.037 | 1017 | 341200 |
| | Author's | 4x4 | 120 | 15.270 | 984 | 438680 |
| | Shear deformation Theory | | | | | |
| | Classical Plate Theory | | | 6.7130 | | 393210 |

**EXAMPLE 3.8:** Response of a square sandwich plate under uniformly distributed loading is considered. The material of the face sheets and core are as given below. Thickness of each face sheet is h/10. Table 3.10 gives the mid-point deflection and maximum stresses in the normalised quantities. Results are compared with that in Ref.[79].

Notation used in the table are

R for reference source where

P : Author's analysis ; E : Exact/Pagano [79]

Results are given in normalized quantities as :

$$(\bar{\sigma}_x, \bar{\sigma}_y, \bar{\tau}_{xy}) = (1/q_o\lambda^2)(\sigma_x, \sigma_y, \tau_{xy}),$$

$\lambda = a/t$ ; $\sigma_{11} = \bar{\sigma}_x(a/2, b/2, \pm 0.5)$ ; $\sigma_{12} = \bar{\sigma}_x(a/2, b/2, \mp 0.4)$;

$\sigma_2 = \bar{\sigma}_y(a/2, b/2, \mp 0.5)$ ; $\sigma_3 = \bar{\tau}_{xz}(0, b/2, 0)$ ; $\sigma_4 = \bar{\tau}_{yz}(a/2, 0, 0)$;

$\sigma_5 = \bar{\tau}_{xy}(0, 0, \mp 0.5)$ ;

Material properties of face layers are same as that in example 3.1.

Core layer has properties as :

$E_{11} = E_{22} = 275.79$ N/mm$^2$ ; $E_{33} = 3447.4$ N/mm$^2$ ; $G_{13} = G_{23} = 413.69$ N/mm$^2$ ;

$G_{12} = 110.3$N/mm$^2$ ; $\nu_{31} = \nu_{32} = \nu_{12} = 0.25$

Table 3.10: Maximum stresses in square Sandwich Plate

| $\lambda$ | R | $\sigma_{11}$ | $\sigma_{12}$ | $\sigma_2$ | $\sigma_3$ | $\sigma_4$ | $\sigma_5$ |
|---|---|---|---|---|---|---|---|
| 4 | P | 1.450 | 0.183 | 0.226 | 0.281 | 0.1175 | 0.1464 |
| | E | 1.510 | 0.196 | 0.253 | 0.239 | 0.1072 | 0.1481 |
| 10 | p | 1.168 | 0.719 | 0.956 | 0.342 | 0.0567 | 0.0703 |
| | E | 1.152 | 0.629 | 0.1099 | 0.300 | 0.0527 | 0.0717 |
| 20 | P | 1.141 | 0.851 | 0.0615 | 0.357 | 0.0394 | 0.0515 |
| | E | 1.11 | 0.810 | 0.070 | 0.317 | 0.0361 | 0.0511 |
| 100 | P | 1.109 | 0.882 | 0.0483 | 0.345 | 0.0256 | 0.0443 |
| | E | 1.098 | 0.875 | 0.055 | 0.324 | 0.0297 | 0.0437 |
| CPT | | 1.097 | 0.878 | 0.0543 | 0.324 | 0.0295 | 0.0433 |

Figs. 3.3.a-f give the distribution of in-plane displacement (u) and all the stresses through the thickness of the sandwich plate.

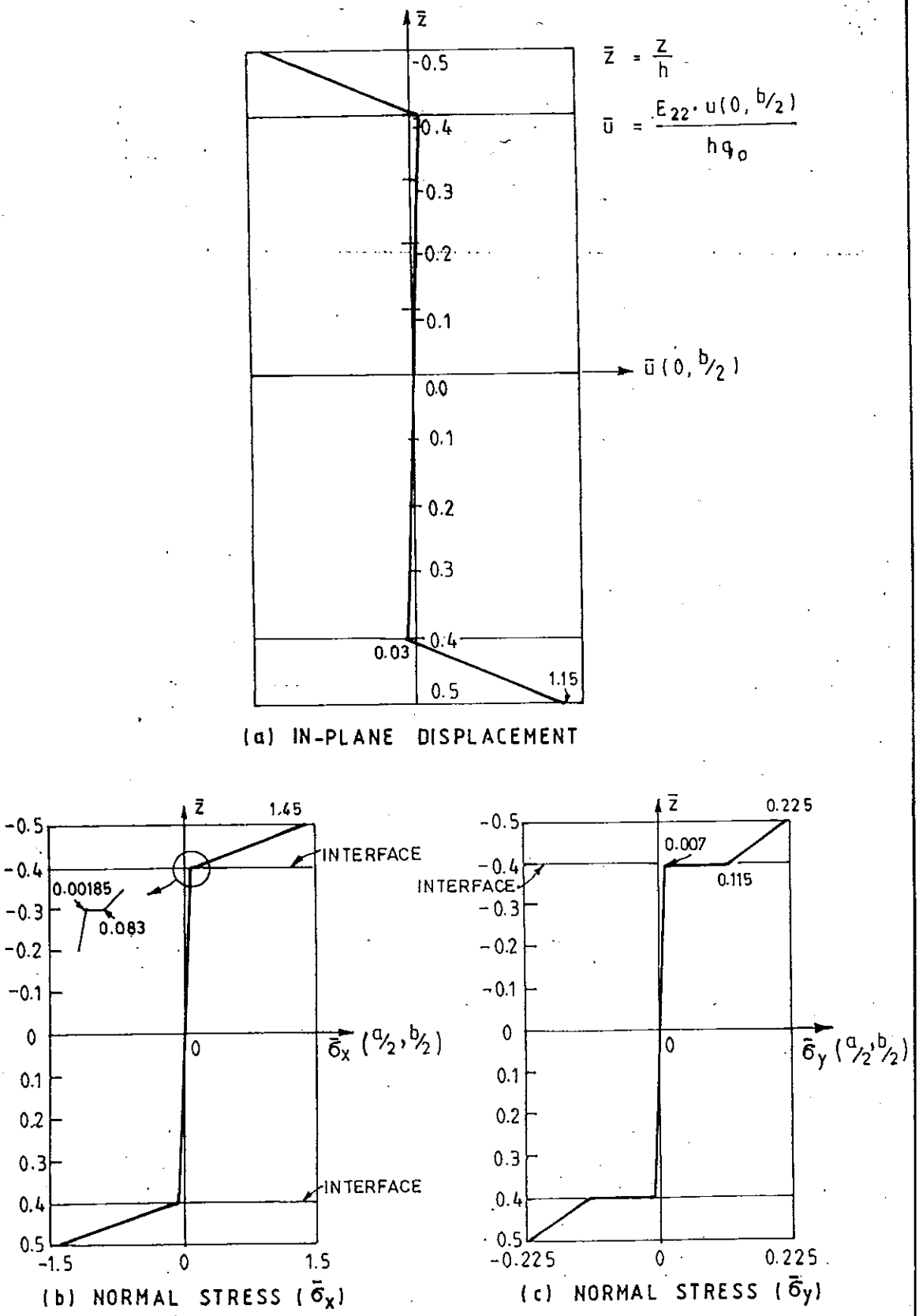


FIG.3.3 DISTRIBUTION OF DEFLECTION AND NORMAL STRESSES IN A 3-PLY SANDWICH PLATE ($\lambda = 4$)

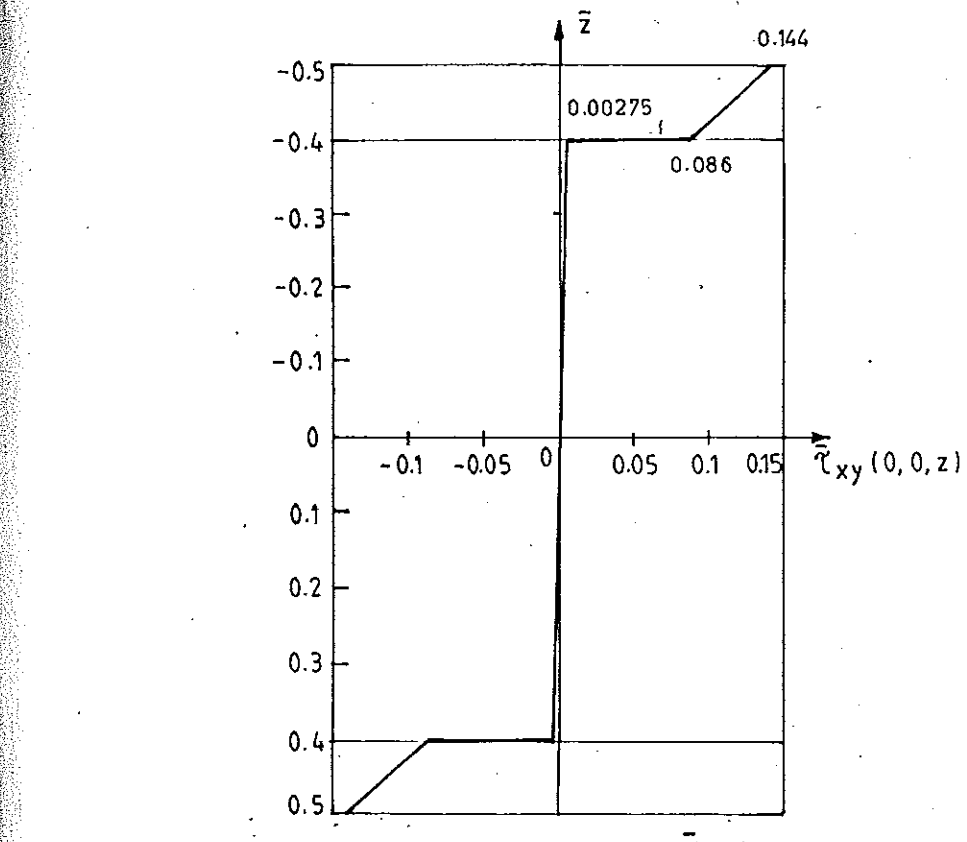


(d) SHEAR STRESS ( $\bar{\tau}_{xy}$ )

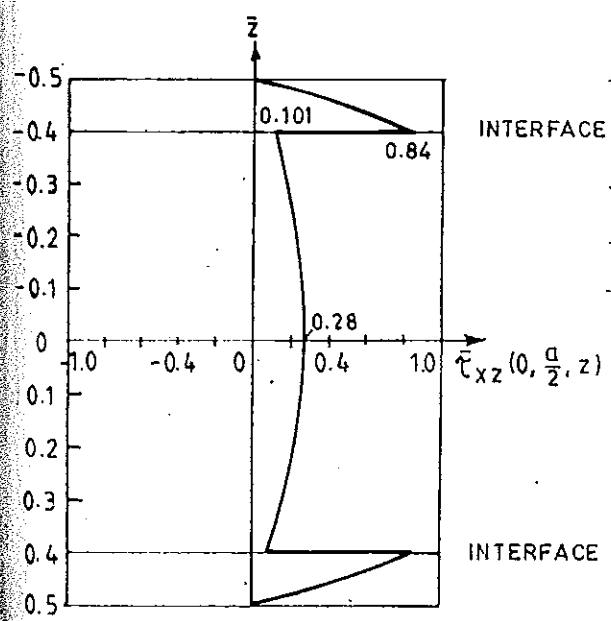


(e) TRANSVERSE SHEAR STRESS ( $\bar{\tau}_{xz}$ )

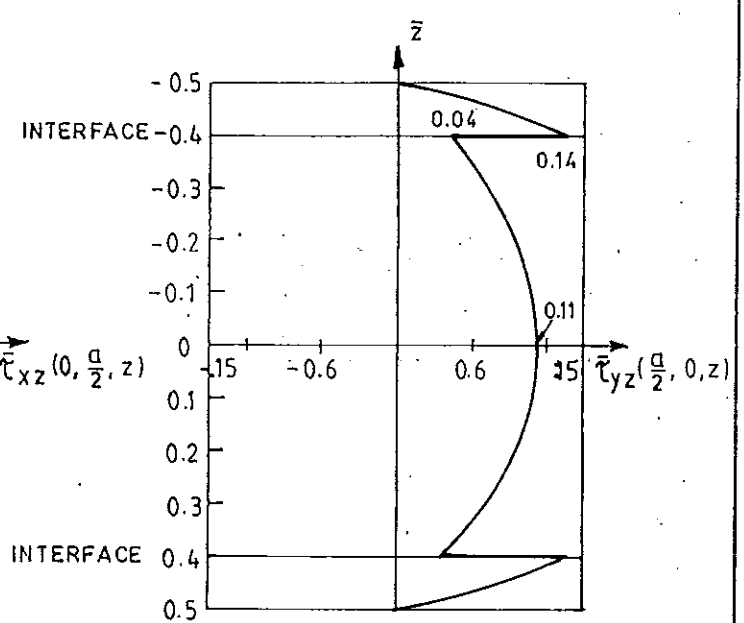


(f) TRANSVERSE SHEAR STRESS ( $\bar{\tau}_{yz}$ )

FIG. 3.3 DISTRIBUTION OF IN-PLANE AND TRANSVERSE SHEAR STRESSES ( $\lambda = 4$ )

### 3.5.4 Convergence test

**EXAMPLE:3.9:** Convergence of the finite element solutions to the exact values [39] for quantities like middle point deflection (w), and stresses ($\sigma_x, \sigma_y, \tau_{xy}$) are given in Figs. 3.4.a-d respectively for a square plate with parameters as given in example 3.1. Different mesh sizes (total structural degrees of freedom) versus percentage error from the exact values were plotted.

## 3.6 DISCUSSION

To check the accuracy of the element formulation, eigenvalue analysis was performed in the element level. These eigenvalues are presented in Table 3.2. Six, out of twenty-eight eigenvalues are found to be nearly zero indicating the presence of as many rigid body modes. On the basis of results presented in this chapter, the following observations can be made:

It is clear from Table 3.3, Reddy's [70] linear and quadratic elements perform better for thick plates. Elements developed by Panda et al [67] ,Mawenya [66] and Moser [75], which either have too many structural degrees of freedom or have performance not as satisfactory as that of the present element. Phan's [21] element behaves excellent for thick plate, but the error increases with the increase of aspect ratio. It is also clear that the numerical values of all quantities converge to the CPT solutions as aspect ratio ($\lambda$) is increased.

In the case of multi-layered laminates (Table 3.4.a-c), results obtained for deflection and in-plane stresses are quite close to the exact [39] values. But a wide variation is noticed in case of transverse shear. In the case of a

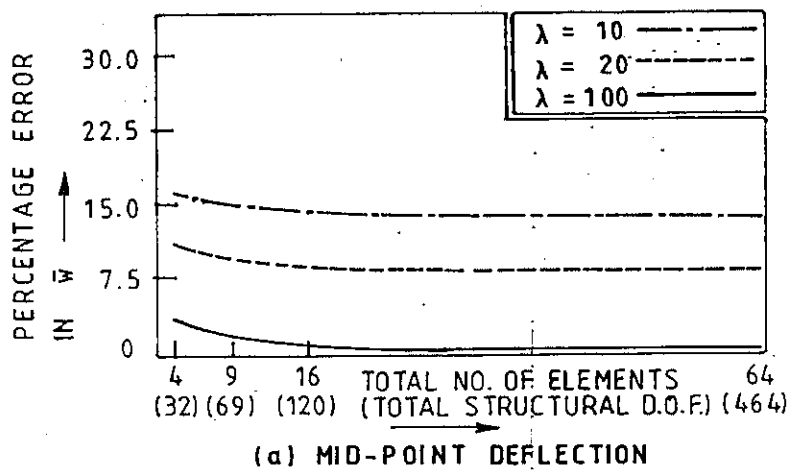


(a) MID-POINT DEFLECTION

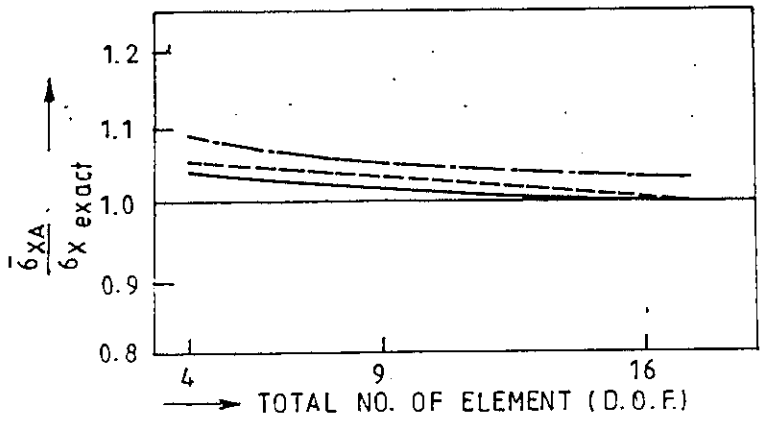


(b) SIGMA X AT (a/2, b/2, t/2)

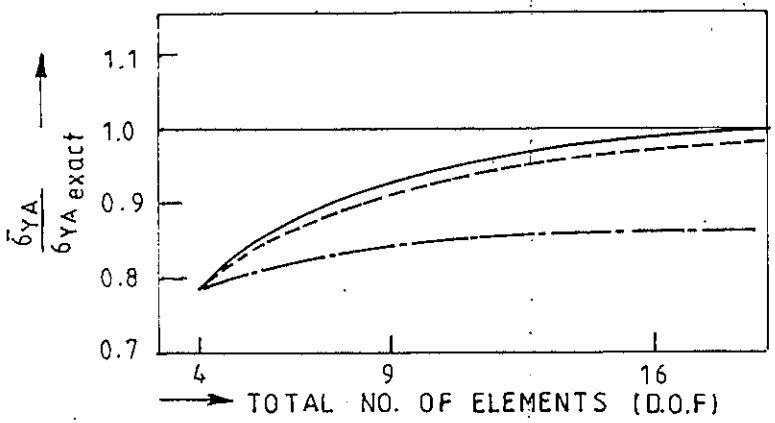


(c) SIGMA Y AT (a/2, b/2, t/4)

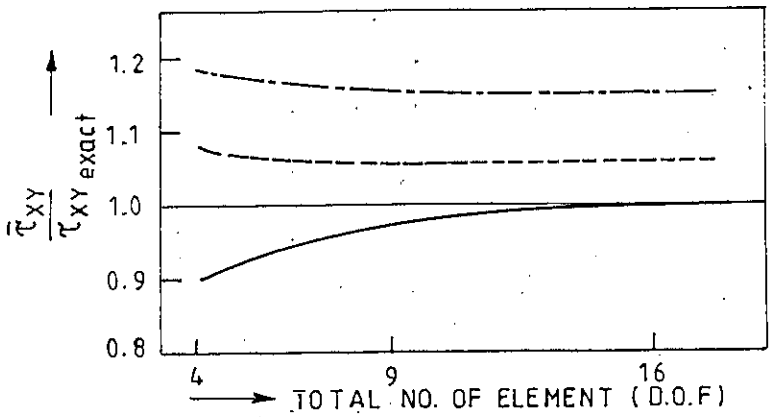


(d) SHEAR STRESS XY (0,b/2,0)

FIG. 3.4 CONVERGENCE OE MID POINT DEFLECTION AND STRESSES

rectangular plate (Table 3.5), results obtained using present element are more accurate than that of presented by other researchers. This remark holds good for thick as well as thin plates. Table 3.6 gives the cylindrical bending of angle-ply laminates. Error in deflection gradually decreases with the increase of $\theta$ values till $\theta = 60^{\circ}$. But the errors in stress values flactuate with increasing $\theta$ values.

Mid point deflection of a square plate under uniformly distributed load is given in Table 3.7. Results are found to be acceptable when compared to Reddy's values [14].

In Table 3.8, effects of modular ratio between plies are presented for three-ply square laminate with identical top and bottom plies. It can be observed from the Table that thin plate theory underestimates maximum deflection. The error in predicting transverse shear stress at the upper interface of the plate is higher than that at mid surface.

Results on sandwich plate with different boundary conditions are given in Table 3.9. In the case of a thick plate with clamped boundary conditions, maximum moment value differs from other literature values more than other quantities. Present finite element predicts the behaviour of simply supported sandwich plate very accurately.

As a final example on static analysis, response of a square sandwich plate under distributed loading is considered. Selected results of the analysis are presented in Table 3.10. Distribution of in-plane displacement and stresses through the thickness of the plate are given in Fig.3.3(a-f). Distribution of transverse shear stress through the thickness of the plate does not compare well with exact results. Reddy [14] has demonstrated that transverse shear stress distribution can be different if instead of

constitutive relation, equilibrium equations are used. In the present study, costitutive relations are used and the stress distribution compares that in ref. [14].

Convergence test shows clearly that the errors of the finite element solution with respect to analytical values are highest for lowest $\lambda$ value and the error decreases rapidly as $\lambda$ value increases. It may be noted that the variation of errors is rather slow with regard to progressive mesh refinement.

## 3.7 Conclusion

A standard four-noded reactangular element with seven degrees of freedom at each node is developed for the analysis of laminated and sandwich plates with different boundary conditions and static loading environments. Quarter of a plate is discretized into 4X4 elements. A wide variety of laminated and sandwich plates are considered. The present element predicts more accurate results in the case of simply supported than in the clamped case. This is clear from Table 3.9. Transverse shear stresses obtained for multi-ply laminates (Table 3.4) are, at places, more than 50% from exact values. But, in-plane normal as well as shear stresses are very accurate. Thus a better prediction of transverse shear stresses can be obtained using equilibrium equation and these in-plane stresses.

# CHAPTER 4

# FREE VIBRATION ANALYSIS OF LAMINATED PLATES

## 4.1 Survey of literature in the field

The first correct statement of the governing differential equation of plate vibrations is attributed by Rayleigh [81] to Sophie Germain, a French Mathematician of the early 19th century. In the same work, Rayleigh presented his well known general method of solution for the natural frequencies of vibration of any system. Timoshenko, had given [82] an analytical solution for the case of the simply-supported rectangular plates. In 1950, Young [83], used the Rayleigh-Ritz method to compute the first six eigenvalues for the square clamped plate, using beam mode shapes to represent the plate deflections. Hearmon [84] published the results obtained by Iguchi for the fundamental mode of vibration of rectangular plates with various aspect ratios. In 1954, Warburton [85], published his simple approximate solutions using characteristic beam functions in Rayleigh's method.

The first vibrational analysis of laminated plate was carried out by Pister [86] for a thin plate, arbitrarily laminated of isotropic layers. Stavsky [87] formulated a coupled bending-stretching dynamic theory for thin laminated plates of composite-material, but he did not present any

numerical results. Apparently the first published results of the vibrational analysis of such plates is due to Ashton and Waddoups [88]. They used the Rayleigh-Ritz method to analyse rectangular plates. They demonstrated that their results compare reasonably well with the experimental results for the completely free and cantilever cases. Whitney and Leissa [89], presented closed-form solutions for the natural frequencies of simply supported plates with cross-ply and angle-ply lamination schemes. Ashton and Anderson [90] and Bert and Mayberry [91] had carried out Rayleigh-Ritz and experimental investigations of clamped plates independently.

The first vibrational analysis of laminated plates including thickness-shear flexibility was made by Ambartsumuyan [92]. Ambartsumyan did not give any numerical results for vibration of laminated plates; however, Whitney [1] did so, using Ambartsumyans basic theory.

Yang, et al [6] extended Mindlin's homogenous, isotropic, dynamic plate analysis to the laminated anisotropic case. They assumed a thickness-shear angle which is independent of the thickness coordinates (z) and then integrated the stress equations of motion to obtain the governing differential equations. After integration, they introduced a thickness-shear co-efficient in an ad-hoc fashion to correlate the predicted frequencies with known results.

Solution of three-dimensional equations of elasticity has been attempted by Srinivas et al [38] and Jones [93,94] for composite plates with rectangular plan form as well as for plates with one dimension infinitely long. It has been shown by various investigators [95,20] that YNS (Yang-Norris-Stavsky) theory is adequate for predicting gross structural behaviour in the first few 'flexural' modes but

not the higher 'shear' modes.

The first extensive application of the YNS theory to commonly encountered laminate configurations was due to Whitney and Pagano [4], who considered cylindrical bending of anti-symmetric cross-ply and angle-ply plate strips under sinusoidal load distribution and free vibration of anti-symmetric angle-ply plate strips. Fortier and rossettos [96] analysed free vibration of thick rectangular plates of unsymmetric cross-ply construction while Sinha and Rath [97] considered both vibration and buckling for the same type of plates.

The use of high-damping polymeric materials in the form of a thin layer or tape has come into widespread use as a structural damper to reduce the vibrational response of aircraft panels, especially in high noise regions such as in the vicinity of jet engines. Dong [98] has given the solution for the dynamic response of a simply supported rectangular plate arbitrarily laminated of orthotropic, viscoelastic plies which was modelled as a standard linear solid. Bert and Chen [99] presented, using the YNS theory, a closed-form solution for the free vibration of simply supported, rectangular, anti-symmetric, angle-ply laminates.

Reddy and his colleagues [18,70,100-104] presented finite element analysis of the bending, vibration and transient response of laminated anisotropic composite plates. Chandra Shekhara [105] had successfully applied the method of state space approach, formulated by Vlasov and Leontev [106], to study the travelling waves in layered media. The free vibration in cross-ply and angle-ply laminates has also been studied by Chandra Shekhara and Santosh [107] and Chandra Sekhara and Chander [108]. In these studies good correlation has been found with the exact solutions of three-dimensional

equations of elasticity.

Noor [17] has studied the reliability and range of validity of two-dimensional plate theories when applied to the low-frequency free vibration analysis of simply supported, bi-directional, multilayered plates consisting of a large number of layers.

Jones [93] has discussed the buckling and vibration of un-symmetrically laminated cross-ply rectangular plates. Transverse vibration of hybrid laminated plates have been investigated by Iyenger and Umaretiya [109]. The effects of kinematic and material characteristics on the fundamental frequency calculations of composite plates have been presented by Ochoa et al [110]. Hinton [111] used the so called finite strip method to study the free vibration of layered cross-ply laminated plates.

In recent years, many higher-order theories have been presented to improve the predictions of laminate static and dynamic behaviour [112,113]. However, some of the improved models are capable of only predicting the global responses i.e. the transverse displacement, free vibration frequencies and buckling loads. Owen et al [114] attempted to give a simple refined model which is suitable for both the global response and local response. Kant et al [19] has presented a refined higher order plate model with a simple $C^o$ finite element formulation for free vibration of anisotropic laminated plates.

Dynamics of laminated composite plates with a higher order theory and finite element discretisation have been investigated by Mallikarjuna and Kant [115]. Vibration analysis of laminated plates and shells by a hybrid stress element have been reported by Mau et. al. [64].

## 4.2 Governing differential equation

For an oscillating body with displacements $u_i$ so small that the acceleration is given by $\frac{\partial^2 u_i}{\partial t^2}$ in Eulerian coordinates, the equation of small motion

$$\sigma_{ij,j} + F_i = \rho \frac{\partial^2 u_i}{\partial t^2} \tag{4.1}$$

where $\rho$ is the mass density of the material and $F_i$ is the body force per unit volume. The boundary surface S shall be assumed to consist of two parts, $S_\sigma$ and $S_u$, with the following boundary conditions.

Over $S_\sigma$ : The surface traction $T_i$ is prescibed
Over $S_u$ : The displacement $u_i$ is prescribed

Let us consider virtual displacement $\delta u_i$. The variations $\delta u_i$ must vanish over the boundary surface $S_u$ ; but are arbitrary over the rest of the boundary surface $S_\sigma$, where surface tractions are prescribed.

Virtual work done by the body and surface forces are

$$\int_v F_i \, \delta u_i \, dv + \int_s T_i \, \delta u_i \, ds \tag{4.2}$$

where $T_i$ is the surface traction.

The variational equation of motion is given as

$$\int_v \sigma_{ij} \, \delta\varepsilon_{ij} \, dv = \int_v (F_i - \rho \frac{\partial^2 u_i}{\partial t^2}) \delta u_i \, dv + \int_s T_i \delta u_i \, ds \tag{4.3}$$

For an elastic body where strain energy function exists, the variational equation of motion can be witten as

$$\delta \int_v W \, dv = \int_v [F_i - \rho \frac{\partial^2 u_i}{\partial t^2}] \, \delta u_i \, dv + \int_s T_i \, \delta u_i \, ds \qquad (4.4)$$

Since the variations $\delta u_i$ are assumed to vanish over the part of the boundary $S_u$ where surface displacements are prescribed, the limit for the surface integral can be replaced by $S_\sigma$ . If the variation $\delta u_i$ were identified with the actual displacements $(\frac{\partial u_i}{\partial t})dt$, then the result above states that, in an arbitrary time interval, the sum of the energy of deformation and the kinetic energy increase by an amount that is equal to the work done by the external forces during the same time interval.

If the virtual displacements $\delta u_i$ are regarded as functions of time and space, not to be identified with the actual displacements, and the variational equation of motion Eq. 4.4 is integrated w.r.t. time between two arbitrary instants $t_o$ and $t_1$, an important variational principle for the moving body can be derived

$$\int_{t_o}^{t_1} \int_v \delta W \, dv \, dt = \int_{t_o}^{t_1} dt \int_v F_i \delta u_i dv + \int_{t_o}^{t_1} dt \int_s T_i \, \delta u_i ds - \int_{t_o}^{t_1} dt \int_v \rho \frac{\partial^2 u_i}{\partial t^2} \delta u_i \, dv$$

where $\delta u_i(t_o) = \delta u_i(t_1) = 0$ , simplifying (4.5)

$$\int_{t_o}^{t_1} \delta \, (U - K) \, dt = \int_{t_o}^{t_1} \int_v F_i \, \delta u_i dv \, dt + \int_{t_o}^{t_1} \int_{S_\sigma} T_i \, \delta u_i ds \, dt \qquad (4.6)$$

where

U represents the total strain energy of the body, $U = \int_v W dv$ and

$K = \frac{1}{2} \int_v \rho (\partial u_i / \partial t)^2 \, dv$ = Kinetic energy of the moving body.

(4.7.a-b)

Substituting $\int_v F_i \, \delta u_i \, dv + \int_{s_\sigma} T_i \, \delta u_i \, ds = - \delta A$ (4.8)

in the above equation,

$$\delta \int_{t_o}^{t_1} ( U - K + A ) dt = 0, \qquad (4.9)$$

then term $L \equiv U - K + A$ is called Lagrangian function and Eq. 4.9 represent Hamilton's principle.

For free vibration, $- \delta A = 0$ as no surface traction or body force exist.

In finite element modelling,

$$U = \int_v \{d\}^T [B]^T [C][B] \{d\} dv \quad \text{and} \quad K = 1/2 \int_v [\rho \{\dot{d}\}^T [N]^T [N] \{\dot{d}\}] \, dv$$

(4.10.a-b)

where $\{u\} = [N] \{d\}$ and $\{\varepsilon\} = [B] \{d\}$ (4.11.a-b)

The Hamilton's principle states that the variation of the Lagrangian during any time interval $t_o$ and $t_1$ must be zero. Substituting Eqs. 4.10.a-b into Eq. 4.6, we get

$$\int_{t_o}^{t_1} [\{\delta d\}^T \rho \int_v [N]^T [N] \, dv \{\ddot{d}\} - \{\delta d\}^T \int_v [B]^T [C][B] \, dv \{d\}] = 0$$

(4.12)

1st term of Eq. 4.12 $= \int_{t_o}^{t_1} \{\delta d\}^T \int_v \rho \, [N]^T \, [N] \, dv \{\ddot{d}\} \, dt =$

$$\rho\ [\{\delta d\}^T \int_v [N]^T[N]\ dv\ \{\dot{d}\}]_{t_o}^{t_1} - \int_{t_o}^{t_1} \{\delta d\}^T \int_v \rho\ [N]^T[N]\ dv\ \{\ddot{d}\}dt \tag{4.13}$$

According to Hamilton's principle, the displacement configuration must satisfy the conditions given at time $t_o$ and $t_1$. Hence

$\{\ \delta d(t_1)\ \} = \{\ \delta d(t_2)\ \} = 0 \Rightarrow$ 1st term of Equ. 4.12 vanishes.

Substituting the other term , we get

$$-\int_{t_o}^{t_1} \{\delta d\}^T \left[ \int_v \rho\ [N]^T[N]\ dv\ \{\ddot{d}\}\ dt - \int [B]^T[C][B]dv\ \{d\} \right] dt = 0 \tag{4.14}$$

Since the displacement variations $\{\delta d\}$ are arbitrary, the terms within the brackets must vanish. Thus, we get the undamped dynamic equations of motion for multiple degrees of freedom system as

$$[M]\ \{\ddot{d}\} + [K]\ \{d\} = 0 \quad \text{where,} \tag{4.15}$$

$[K]$ is the stiffness matrix $= \int_v [B]^T\ [C]\ [B]\ dv$ and

$[M]$ is mass matrix $= \int_v \rho\ [N]^T\ [N]\ dv$ (4.16. a-b)

The element mass matrix is developed below.

## 4.3 Formulation of consistent mass matrix

Element mass matrix is usually accomplished by the physical lumping of the structural mass at points where the influence co-efficients are defined. The resulting mass matrix is diagonal and tends to a simple technique of formulation and solution. However, the computed natural frequencies and mode shapes may differ greatly from the solution of the exact problem.

Archer [116] improved the accuracy of the dynamic analysis by considering a mass distribution scheme which is as the actual distribution of mass throughout the structure in a manner similar to Rayleigh Ritz's formulation. The natural frequencies obtained by the use of the consistent mass matrix are upper bounds to the exact solution.

Hinton et al [117]have presented a scheme for mass lumping for parabolic isoparametric elements. Kant et al [19] have used bi-directional square element and used a special mass matrix based on Hinton's model and obtained reasonably accurate results. Rock and Hinton [118] have given several different alternative schemes for deriving element mass matrices.

In the present investigation, a mass matrix $[M^e]$ as given in [19] is used.

$$[M^e] = \int_A [\underline{N}^T]\ [m]\ [\underline{N}]\ d(\text{area}) \qquad (4.17)$$

where

[N] can be given as

$$\sum_{i=1}^{4} \begin{vmatrix} N_i & 0 & 0 & 0 & 0 & 0 & 0 \\ 0 & N_i & 0 & 0 & 0 & 0 & 0 \\ 0 & 0 & N_i & 0 & 0 & 0 & 0 \\ 0 & 0 & 0 & N_i & 0 & 0 & 0 \\ 0 & 0 & 0 & 0 & f_i & g_i & h_i \\ 0 & 0 & 0 & 0 & f_{i,x} & g_{i,x} & h_{i,x} \\ 0 & 0 & 0 & 0 & f_{i,y} & g_{i,y} & h_{i,y} \end{vmatrix}$$

and

$$[m] = \begin{bmatrix} I_1 & & & & & & \\ & I_1 & & & & & \\ & & I_2 & & & & \\ & & & I_2 & & & \\ & & & & I_1 & & \\ & & & & & I_2 & \\ & & & & & & I_2 \end{bmatrix}$$

in which $I_1$, $I_2$ are normal inertia, rotational inertia respectively

$$( I_1 , I_2 ) = \sum_{1}^{n} \int_{h_i}^{h_{i+1}} \rho^i [ 1, z^2 ] \, dz, \qquad (4.18)$$

where $\rho^i$ is the material density of the i th layer

## 4.4 Solution

Eqs. 4.15 have the solution of the form

$$\{d\} = a \, e^{ipt} \, \{\bar{d}\} \qquad (4.20)$$

where

a is a scalar of dimension L, p is a scalar of dimension 1/t, t=time, $i = \sqrt{-1}$ and $\{\bar{d}\}$ is a non dimensional vector, which is independent of t.

On sustituting Eq. 4.20 in Eq. 4.15, we get

$$[K]\{\bar{d}\} - p^2 [M]\{\bar{d}\} = 0 \qquad (4.21)$$

or, $[K]\{\bar{d}\} = p^2 [M]\{\bar{d}\}$

or, $[M]\{\bar{d}\} = \lambda [K]\{\bar{d}\}$ ; where $\lambda = \frac{1}{p^2}$ (4.22)

This is a generalised real symmetric eigenvalue problem of the form

$[A]\{z\} = \lambda [B]\{z\}$ , with [B] is symmetric positive definite.

International Mathematical and Statistical Libraries (IMSL) routine GVCSP is used to calculate eigenvalues and eigenvectors of the system

$$\left[ [M] - \lambda [K] \right] \left\{ \bar{d} \right\} = 0 \qquad (4.23)$$

Having determined $\lambda$, natural frequencies and mode shapes can be obtained.

## 4.5 Numerical examples (free vibration)

In order to illustrate the applicability of the element developed, undamped transverse vibration of anisotropic simply supported laminated and sandwich plates are considered. Numerical examples are chosen to demonstrate the effect of

(i)degree of orthotropy;
(ii)number of layers;
(iii)transverse shear deformation;
(iv)span-to-thickness ratio;
(v)coupling between stretching and bending and
(vi)lamination angle

on dimensionless fundamental frequencies.

**EXAMPLE 4.1:** Fundamental frequency of simply supported bi-directional, multi-layered square laminated plates consisting of a large number of symmetric and anti-symmetric layers. The effects of varying degree of orthotropy and number of layers are considered. Fiber orientations of different lamina alternate between $0^{o}$ and $90^{o}$ w.r.t. x-axis. In the symmetrical case the $0^{o}$ layers are at the outer surfaces of the laminate. Total thickness of the $0^{o}$ and $90^{o}$ layers in each laminate are the same.

Degree of orthotropy is varied between 3 and 40;
No. of layers used are 2,3,4,5,6,9 and 10;

Material properties of the individual layers are

$$G_{LT}/E_T = 0.6 \; ; \; G_{TT}/E_T = 0.5 \; ; \; \nu_{LT} = \nu_{TT} = 0.25$$

Where subscript L refers to the direction of fibers and T refers to the transverse direction. $\nu_{LT}$ is the major Poisson's ratio and $\frac{h}{L}$ is varied between 0.05 to 0.50.

Results are presented in Table 4.1 in terms of non-dimensional $\lambda'$ value, where $\lambda' = 10\lambda$ and $\lambda = \omega(\rho h^2/E_T)^{1/2}$

**Table 4.1:** Effect of degree of orthotropy of the individual layers on the fundamental frequency of simply supported square multi-layered composite plates with h/L = 0.20

**(skew symmetric case)**

| Source | No. of layers | $E_1/E_2$ = 3 | 10 | 20 | 30 | 40 |
|---|---|---|---|---|---|---|
| Noor [17]* | | 2.5031 | 2.7938 | 3.0698 | 3.2705 | 3.4250 |
| Author's | 2 | 2.48 | 2.82 | 3.17 | 3.45 | 3.69 |
| Owen [114] | | 2.5601 | 2.8712 | 3.1558 | 3.3610 | 3.5185 |
| CPT | | 2.7082 | 3.0968 | 3.5422 | 3.9335 | 4.2884 |
| Noor [17] | | 2.6182 | 3.2578 | 3.7622 | 4.0660 | 4.2719 |
| Author's | 4 | 2.60 | 3.32 | 3.90 | 4.27 | 4.53 |
| Owen [114] | | 2.6691 | 3.3250 | 3.8454 | 4.1612 | 4.3763 |
| CPT | | 2.8676 | 3.8877 | 4.9907 | 5.8900 | 6.6690 |
| Noor [17] | | 2.6440 | 3.3657 | 3.9359 | 4.2783 | 4.5091 |
| Author's | 6 | 2.62 | 3.40 | 4.02 | 4.40 | 4.66 |
| Owen [114] | | 2.6839 | 3.4085 | 3.9758 | 4.3233 | 4.5558 |
| CPT | | 2.8966 | 4.0215 | 5.2234 | 6.1963 | 7.0359 |
| Noor [17] | | 2.6583 | 3.4250 | 4.0337 | 4.4011 | 4.6498 |
| Author's | 10 | 2.64 | 3.44 | 4.08 | 4.46 | 4.72 |
| Owen [114] | | 2.6916 | 3.4527 | 4.0526 | 4.4140 | 4.6590 |
| CPT | | 2.9115 | 4.0888 | 5.3397 | 6.3489 | 7.2184 |

Continuation of table 4.1 (symmetric case)

| | | | | | | |
|---|---|---|---|---|---|---|
| Noor [17] | | 2.6474 | 3.2841 | 3.8241 | 4.1089 | 4.3006 |
| Author's | 3 | 2.64 | 3.39 | 3.93 | 4.25 | 4.47 |
| Owen [114] | | 2.6948 | 3.3917 | 3.8979 | 4.1941 | 4.3951 |
| CPT | | 2.9198 | 4.1264 | 5.4043 | 6.4336 | 7.3196 |
| Noor [17] | | 2.6587 | 3.4089 | 3.9792 | 4.3140 | 4.5374 |
| Author's | 5 | 2.64 | 3.45 | 4.06 | 4.42 | 4.67 |
| Owen [114] | | 2.6988 | 3.4534 | 4.0297 | 4.3704 | 4.5992 |
| CPT | | 2.9198 | 4.1264 | 5.4043 | 6.4336 | 7.3196 |
| Noor [17] | | 2.6640 | 3.4432 | 4.0547 | 4.4210 | 4.6679 |
| Author's | 9 | 2.64 | 3.47 | 4.10 | 4.48 | 4.74 |
| Owen [114] | | 2.6971 | 3.4708 | 4.0746 | 4.4360 | 4.6803 |
| CPT | | 2.9198 | 4.1264 | 5.4043 | 6.4336 | 7.3196 |

* Exact analysis

**EXAMPLE 4.2:** Fundamental natural frequencies are obtained for anti-symmetric angle-ply rectangular plates with all edges simply supported. All the lamina are to be of the same thickness and made of the same orthotropic material. Dimensionless material properties are same as that in ref. 18.

Material I :

$E_1/E_2 = 40$ ; $G_{12}/E_2 = 0.6$ ; $G_{13}/E_2 = G_{23}/E_2 = 0.5$ ; $\nu_{12}=0.25$

Material II:

$E_1/E_2 = 25$ ; $G_{12}/E_2 = 0.5$ ; $G_{13}/E_2 = G_{23}/E_2 = 0.2$ ; $\nu_{12}=0.25$

The effects of the lamination angle ($\theta$) and the number of layers on the dimensionless fundamental frequency for plates made of both the materials (I and II) are shown in Table 4.2.

Tables 4.3 and 4.4 show the effects of plate aspect ratio and length-to-thickness ratio on the dimensionless fundamental frequency for material I with lamination angle as $45^{o}$ and $30^{o}$ respectively.

**Table 4.2:** Effects of lamination angle ($\theta$) and number of layers on the dimensionless fundamental frequency $\bar{p}$ of a simply supported square plate ($\theta/-\theta/\theta/\ldots-\theta$, a/b=1.0, a/h=10).

| Material | $\theta$ | R | Number of layer | | | | | | | |
|---|---|---|---|---|---|---|---|---|---|---|
| | | | 2 | 4 | 6 | 8 | 10 | 12 | 14 | 16 |
| I | $30^{o}$ | A | 13.56 | 17.24 | 17.80 | 17.99 | 18.07 | 18.12 | 18.15 | 18.17 |
| | | R | 15.00 | 17.69 | 18.00 | 18.10 | 18.15 | 18.18 | 18.19 | 18.20 |
| | | B | 12.68 | 17.63 | 18.23 | 18.42 | 18.51 | - | - | 18.60 |
| $(\frac{E_1}{E_2}=40)$ | $45^{o}$ | A | 13.95 | 18.06 | 18.66 | 18.87 | 18.96 | 19.02 | 19.05 | 19.07 |
| | | R | 15.71 | 18.61 | 18.73 | 19.03 | 19.07 | 19.10 | 19.11 | 19.12 |
| | | B | 13.04 | 18.46 | 19.09 | 19.29 | 19.38 | - | - | 19.48 |
| II | $30^{o}$ | A | 10.57 | 12.46 | 12.77 | 12.88 | 12.93 | 12.96 | 12.98 | 12.99 |
| | | R | 11.35 | 12.74 | 12.90 | 12.95 | 12.97 | 12.99 | 12.99 | 13.00 |
| $(\frac{E_1}{E_2}=25)$ | $45^{o}$ | A | 10.93 | 12.99 | 13.33 | 13.45 | 13.51 | 13.54 | 13.56 | 13.57 |
| | | R | 11.75 | 13.30 | 13.47 | 13.52 | 13.55 | 13.56 | 13.57 | 13.58 |

R for source of reference where : A, Author's ; R, Reddy [18] ; and B, Bert and Chen [99]

**Table 4.3:** Effect of plate aspect ratio (a/b) and length-to-thickness ratio (a/h) on the dimensionless fundamental frequency, $\bar{p}$ of a simply supported rectangular plate made of material I ($45^{o}/-45^{o}/45^{o}/-45^{o}$).

| a/h | R | Aspect ratio | | | | | | | | | |
|---|---|---|---|---|---|---|---|---|---|---|---|
| | | 0.2 | 0.4 | 0.6 | 0.8 | 1.0 | 1.2 | 1.4 | 1.6 | 1.8 | 2.0 |
| 10 | A | 4.93 | 10.31 | 12.65 | 15.29 | 18.06 | 21.02 | 24.05 | 27.18 | 30.45 | 31.28 |
| | R | 8.72 | 10.54 | 12.97 | 15.71 | 18.61 | 21.57 | 24.60 | 27.74 | 30.98 | 34.25 |
| | B | 8.66 | 10.42 | 12.82 | 15.54 | 18.46 | 21.51 | 24.67 | 27.95 | - | 34.87 |
| 20 | A | 9.52 | 11.70 | 14.72 | 18.26 | 22.19 | 26.45 | 31.02 | 35.89 | 41.07 | 46.54 |
| | R | 9.48 | 11.77 | 14.90 | 18.56 | 22.58 | 26.86 | 31.40 | 36.25 | 41.37 | 46.79 |
| | B | 9.30 | 11.46 | 14.45 | 17.97 | 21.87 | 26.12 | 30.68 | 35.56 | - | 46.26 |
| 30 | A | 9.72 | 12.02 | 15.22 | 19.01 | 23.28 | 27.97 | 33.07 | 38.59 | 44.53 | 50.89 |
| | R | 9.67 | 12.07 | 15.39 | 19.30 | 23.68 | 28.38 | 33.46 | 38.94 | 43.83 | 51.13 |
| | B | 9.44 | 11.70 | 14.84 | 18.56 | 22.74 | 27.35 | 32.38 | 37.82 | - | 49.98 |
| 40 | A | 9.80 | 12.14 | 15.41 | 19.30 | 23.70 | 28.57 | 33.89 | 39.69 | 45.98 | 52.74 |
| | R | 9.76 | 12.21 | 15.85 | 19.60 | 24.12 | 29.00 | 34.40 | 40.07 | 46.31 | 53.01 |
| | B | 9.49 | 11.78 | 14.98 | 18.78 | 23.08 | 27.83 | 33.05 | 38.72 | - | 51.52 |
| 50 | A | 9.84 | 12.20 | 15.50 | 19.44 | 23.91 | 28.86 | 34.30 | 40.24 | 46.70 | 53.68 |
| | R | 9.82 | 12.28 | 15.69 | 19.76 | 24.34 | 29.32 | 34.74 | 40.65 | 47.07 | 53.99 |
| | B | 9.51 | 11.82 | 15.04 | 18.89 | 23.24 | 28.06 | 33.37 | 39.17 | - | 52.29 |

R for source of reference where : A, Author's ; R, Reddy [18] ; and B, Bert and Chen [99]

Fig. 4.1(a) shows the effect of lamination angle ($\theta$) and number of layers on dimensionless frequency of a simply supported square plate (material I). Effect of plate aspect ratios (a/b) and side to thickness ratio (a/h) on dimensionless frequency in given in Fig. 4.1(b).

**Table 4.4:** Effect of plate aspect ratio (a/b) and length-to-thickness ratio (a/h) on the dimensionless fundamental frequency, $\bar{p}$ of a simply supported rectangular plate made of material I ($30^{\circ}/-30^{\circ}/30^{\circ}/-30^{\circ}$).

| a/h | R | Aspect ratio | | | | | | | | | |
|---|---|---|---|---|---|---|---|---|---|---|---|
| | | 0.2 | 0.4 | 0.6 | 0.8 | 1.0 | 1.2 | 1.4 | 1.6 | 1.8 | 2.0 |
| 10 | A | 4.31 | 8.750 | 13.46 | 15.25 | 17.24 | 19.38 | 21.61 | 23.92 | 26.33 | 28.83 |
| | R | 11.11 | 12.17 | 13.73 | 15.62 | 17.69 | 19.88 | 26.28 | 24.46 | 26.84 | 29.29 |
| 20 | A | 12.70 | 13.98 | 15.90 | 18.28 | 20.02 | 24.01 | 27.23 | 30.65 | 34.25 | 38.03 |
| | R | 12.60 | 13.95 | 15.97 | 18.46 | 21.28 | 24.36 | 27.65 | 31.09 | 34.68 | 38.43 |
| 30 | A | 13.11 | 14.47 | 16.50 | 19.06 | 22.00 | 25.27 | 28.82 | 32.61 | 36.67 | 40.94 |
| | R | 12.97 | 14.40 | 16.54 | 19.20 | 22.25 | 26.62 | 29.24 | 33.09 | 37.13 | 41.39 |
| 40 | A | 13.27 | 14.65 | 16.74 | 19.36 | 22.39 | 25.76 | 29.44 | 33.40 | 37.64 | 42.14 |
| | R | 13.14 | 14.59 | 16.78 | 19.51 | 22.65 | 26.13 | 29.90 | 33.91 | 38.15 | 42.64 |
| 50 | A | 13.35 | 14.75 | 16.85 | 19.50 | 22.58 | 26.01 | 29.75 | 33.79 | 38.12 | 42.73 |
| | R | 13.23 | 14.70 | 16.91 | 19.67 | 22.85 | 26.39 | 30.23 | 34.33 | 38.68 | 43.28 |
| 60 | A | 13.40 | 14.80 | 16.92 | 19.59 | 22.68 | 26.14 | 29.93 | 34.01 | 38.40 | 43.07 |
| | R | 13.30 | 14.77 | 16.99 | 19.77 | 22.97 | 26.55 | 30.43 | 34.58 | 38.99 | 43.66 |

R for source of reference where : A, Author's ; R, Reddy [18] ;

**Example 4.3:** Fundamental frequencies for a square, simply supported sandwich plate is considered. The plate consists of eight layers ($0^{\circ}/45^{\circ}/90^{\circ}/\text{core}/90^{\circ}/45^{\circ}/30^{\circ}/0^{\circ}$). Material property is as given below:

**Face sheet:**

$E_1 = 1.308 \times 10^7$ N/cm$^2$ ; $E_2 = E_3 = 1.06 \times 10^6$ N/cm$^2$ ;

$G_{12} = G_{13} = 6.0 \times 10^5$ N/cm$^2$ ; $G_{23} = 3.9 \times 10^5$ N/cm$^2$ ;

$\rho = 1.58 \times 10^{-5}$ N s$^2$/cm$^4$ ; $\nu_{12} = \nu_{13} = 0.28$ ; $\nu_{23} = 0.34$

thickness of each top stiff layer = 0.025h

thickness of each bottom stiff layer = 0.08125h

Core:

$G_{23} = 1.772 \times 10^4$ N/cm$^2$ ; $G_{13} = 5.206 \times 10^4$ N/cm$^2$ ;

$\rho = 1.009 \times 10^{-6}$ N s$^2$/cm$^4$ ;

thickness of core = 0.6h

**Table 4.5:** Comparison of fundamental frequencies ($p/2\pi$) of a eight-layer square composite sandwich plate (a=b=100cm).

| Considering $G_{23}$ and $G_{13}$ of stiff layers | | | | Neglecting $G_{23}$ and $G_{13}$ of stiff layers | | | |
|---|---|---|---|---|---|---|---|
| a/h=10 | | a/h=100 | | a/h=10 | | a/h=100 | |
| A | K | A | K | A | K | A | K |
| 282 | 464 | 50 | 59 | 121 | 281 | 50 | 57 |

A : Author's ; K : Kant [19]

EXAMPLE 4.4: Convergence of the finite element solutions with mesh refinement and no. of sampling points are given in Table 4.6 and Fig. 4.1(c) respectively. Dimensionless fundamental frequencies are obtained for two layer square laminated plates with fibers oriented at $0^o$, $30^o$ and $45^o$ with the plate x-axis.

Material properties and plate geometry are same as that of example 4.2 (material I).

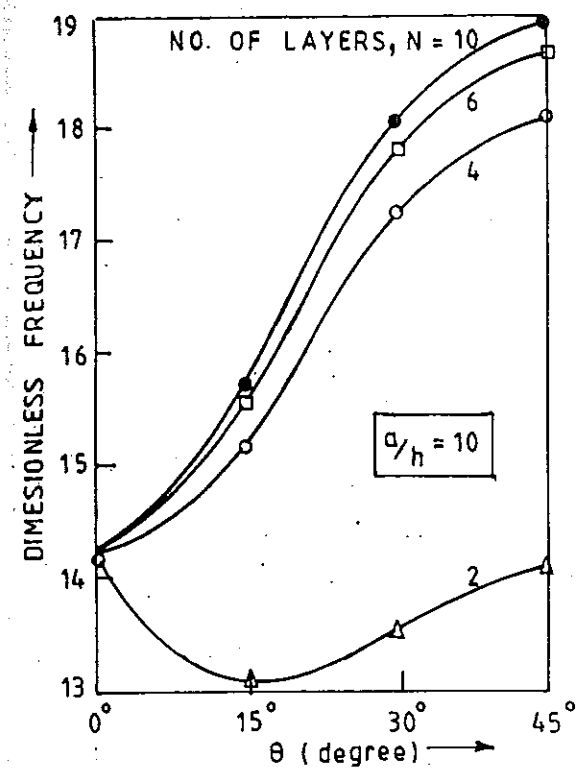


(a) EFFECT OF LAMINATION ANGLE (θ) AND NO. OF LAYERS

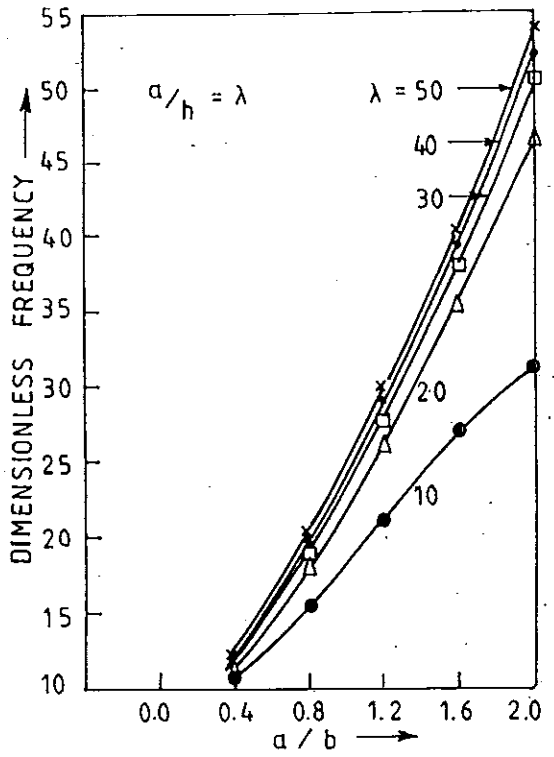


(b) EFFECT OF PLATE ASPECT RATIO ($a/b$) AND LENGTH / THICKNESS RATIO ($a/h$)

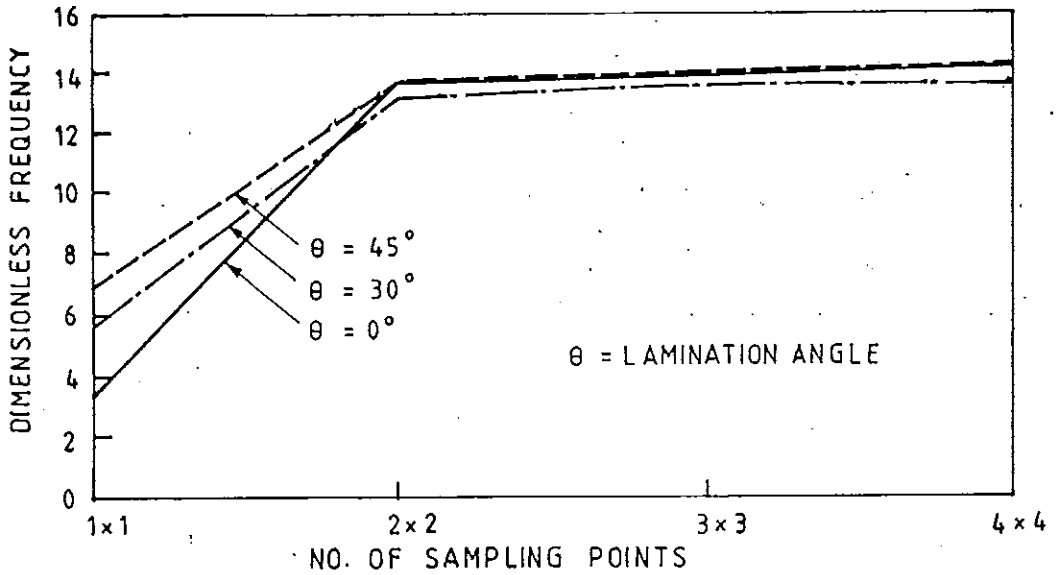


(c) CONVERGENCE WITH NO. OF SAMPLING POINTS

FIG. 4.1 EFFECT OF VARIOUS PARAMETERS ON DIMENSIONLESS FUNDMENTAL FREQUENCY, $\omega a^2 (\rho / E_2 h^2)^{1/2}$

**Table 4.6:** Effect of finite element mesh refinement on the dimensionless fundamental frequency, $\bar{p}$ of a simply supported square plate (a/h=10). In Table below, mesh signifies no. of elements in quarter of a plate.

| Material | Mesh | $\theta=0^{o}$ | $\theta=30^{o}$ | $\theta=45^{o}$ |
|---|---|---|---|---|
| I | 2X2 | 7.99 | 8.41 | 9.55 |
| | 3X3 | 12.49 | 11.14 | 12.08 |
| | 4X4 | 14.19 | 13.56 | 13.95 |
| Reddy[18] | | - | 15.00 | 15.71 |
| Bert [99] | | - | 12.68 | 13.04 |

## 4.6 Discussion

Fundamental frequencies for orthotropic plates with different lamination schemes are predicted by using the element developed in this thesis. The results are presented in Tables 4.1-4.6.

In Tables 4.2-4.4 and 4.6 dimensionless frequencies are presented as

$$\bar{p} = (pa^2/h)(\rho/E_2)^{\frac{1}{2}}$$

In table 4.1, fundamental frequencies for cross-ply laminates are compared with that of Noor[17], Owen [114] and CPT values. It reveals that the fundamental frequency is strongly dependent on the number of layer and stacking sequence. When Noor's three-dimensional elasticity values are compared with other results, it is evident that for most of the cases, present element predicts more accurate results than that by others. And error increases with the increase of degree of orthotropy. Noor demonstrated that the error in the fundamental frequency sharply increases as the number of

layers increases from 2 to 4 and then becomes insensitive to further increases in the number of layers. Fig. 4.1(a) agrees with Noor's demonstration. It is evident from the same table that CPT predicts higher frequencies than other theories where effect of transverse shears are accounted.

From Table 4.2, it is clear that for the case of angle-ply laminates, degree of orthotropy and no. of layers influence fundamental frequency in the similar manner as in the case of cross-ply laminate(Table 4.1).

The effect of shear-coupled flexural-extensional coupling decreases as the number of layers is increased, thus allowing dimensionless frequency factor to increase as shown in Fig. 4.1(a). It is also seen that the effect of increasing lamination angle, up to a value of $45^{\circ}$, is to increase the frequency (except for the two-layer case). However, it is noted that the effect of the number of layers is most pronounced at $\theta=45^{\circ}$ i.e. going from two to ten layers increases the frequency by 26 % at $\theta = 45^{\circ}$ but only by 6 % at $\theta = 5^{\circ}$. This is true for a/h = 10 and aspect ratio is 1 or more. But for lower aspect ratios, values corresponding to $\theta = 30^{\circ}$ is more than that for a plate with $\theta = 45^{\circ}$. This can be visualised by comparing the results presented in tables 4.3 and 4.4.

Free vibration analysis is conducted on sandwich plate in example 4.3. Thick and thin plates are studied. Only fundamental frequencies are compared with the results given by Kant [19]. Results compare well for thin plate but for thick plates present theory predicts much lower frequencies.

In Table 4.6, convergence of the finite element results with progressive mesh refinement is carried out. 4X4 elements in quarter plate yield reasonably accurate results.

Figure 4.1(b) presents dimensionless frequency as a function of a/b for various values of a/h. These plots will also be useful in extrapolating to aspect ratios beyond two.

Results, presented in tables compare well with the published values available in literature.

## 4.7 Conclusion

The simple finite element developed in chapter 3 is extended to free vibration analysis of laminated and sandwich plates. Free vibration equations of motions are obtained using Hamilton's principle. It is observed that the problem reduces to a set of algebraic equations which are symmetric in nature. Mass matrix of the plate element is consistently calculated. The governing differential equations are easily reduced to a standard eigenvalue problem yielding natural frequencies.

Based on the results discussed above, the following conclusions regarding free vibration analysis of laminated and sandwich plates can be reached:

(1) The effects of increasing lamination angle $\theta$ (up to $45^{\circ}$) is to increase the fundamental frequency, except for the case of two layers for which it decreases.

(2) Increasing the number of layers without changing the total thickness decreases the flexural-extensional coupling effect and thus increases the fundamental frequency. This effect of the number of layers is most pronounced at $\theta=45^{\circ}$.

(3) CPT over estimates frequencies as it ignores the effect of transverse shear.

(4) The effect of plate aspect ratio on the fundamental frequency is more pronounced in thicker plates (low a/h ratio) than it is for thin plates.

(5)Dimensionless frequency is maximum at $\theta=45^{o}$ for angle-ply laminates as long as a/h=10 and aspect ratio is one or more. But for higher a/h ratio and aspect ratio lower than one, the trend is opposite.

# CHAPTER 5

# EXPERIMENTAL INVESTIGATION

## 5.1 Introduction

A simple finite element, based on higher order shear deformation theory, is developed to predict the behaviour of laminated plates. Results predicted by the finite element method are compared with published results for static and free vibration cases in chapters 3 and 4 respectively. But before accepting the element, it is almost imperative to have an experimental evidence to support the theory. Only a few of the existing theoretical results have experimental backing with them.

Literature dealing with flat-plate vibration is extensive beginning with Chladin's [119] observations of modal patterns for completely free plates in 1802. It has grown continuously through years. This review is not intended to be exhaustive but rather to bring attention to a few of the significant developments in the area of clamped laminated plate analysis. Hazell and Mitchell [120] have partially bridged this gap by comparing their experimentally obtained results with those obtained through numerical techniques. Crawley [121] has obtained experimentally the

natural frequencies and mode shapes of a number of glass fiber/epoxy plates with various fiber volume ratios. Natural frequencies and mode shapes are compared with those calculated numerically using finite element method. Ashton and Waddoups [88], had obtained the natural frequencies and mode shapes of cantilevered plates using strain gage. Mode shapes were determined by sprinkling the plate with salt grains which migrate to the nodal lines when the plate was excited. They compared experimentally obtained natural frequencies with that predicted analytically. Bert and Mayberry [91] obtained approximate solutions using Rayleigh-Ritz method and the results were compared with the experimental results for symmetrically and unsymmetrically laminated plates.

Characterization of material properties of individual layers allows predictions of the behaviour of any laminate. In-plane lamina properties $E_1$, $E_2$, $\nu_{12}$ are obtained from uniaxial tensile tests. Off-axis configuration has been employed for the determination of inter-laminar shear modulus $G_{12}$. This procedure is an attractive alternative to performing direct torsion tests on composite tubes which are more difficult and expensive to fabricate.

It is known that the off-axis configuration can introduce errors in the measured values. The extent of error depends not only on the off-axis angle, specimen geometry, constraints, and degree of material anisotropy, but also different for diferent material parameters that are obtained from this type of test.

The effect of end constraints in an off-axis tensile specimen was first pointed out by Pagano and Halpin [122]. Their results were confirmed by a number of other researchers. Pagano and Kim [123] demonstrated that a hollow

circular cylinder is ideally suited to study the inter-laminar shear response of cloth-reinforced composites. End constraint phenomenon has a much more pronounced adverse effect on the determination of $G_{12}$ than on $E_\theta$ . This adverse effect is more prominent for the low off-axis angles ( i.e. $\theta < 30^\circ$ ) and increases with decreasing specimen aspect ratio. Pindera and Herakovich [124] have demonstrated that at $\theta = 45^\circ$ or more, effect of aspect ratio is almost nil.

Present study includes static and free vibration analysis of clamped plates. Under static analysis transverse deflections of plates under uniformly distributed load and point load are measured. Plates with fixed boundary conditions are studied as simply supported conditions are more difficult to simulate. Natural frequencies of both square (with and without central cut-out) and rectangular plate (aspect ratios 0.8 and 0.6) with all edges clamped are obtained using digital spectrum analyser. Two methods are used to excite the plate. Initially by impacting the plate by a standard instrumented hammer and later by using an electro-magnetic mini-shaker. Both the methods yielded identical results. Since the excitation caused by the hammer dies out quickly, this method is unsuitable when mode shapes are necessary. For this case the use of mini-shaker is found to be suitable. Vibration measurements are repeated a large number of times. The experimentation is continued for weeks together, with minor variations in the results.

To determine elastic moduli, tensile tests are performed using coupons conforming to ASTM standard D-638. For shear modulus $G_{12}$ , coupons at $\theta = 45^\circ$ are used. The following tests are carried out.

(1)Static analysis of clamped plates with different fiber volume ratios under uniformly distributed load

and point load.

(2)Free vibration frequencies and mode shapes for square and rectangular plates under clamped condition. The same test is extended to square plate with a central cut out.

(3)Determination of elastic moduli of the material of the plate at different strain rates.

(4)Determination of mass density of plate using mercury displacement method.

(5)To demonstrate that the element developed in the present thesis can predict acceptable results when compared with experimental results.

## 5.2 Fabrication of test specimen and set-up

### 5.2.1 Material used

**Fiber:** Epoxy compatible E-glass ($SiO_2$ 52, $Al_2O_3$ 14, CaO 21, MgO 2 ) is easily available in India.

**Matrix:** Cold curing is a widely used method of polymerization of epoxy as it requires no heating and pressure. The matrix is obtained by mixing hardener with araldite in the ratio 1:9 (by weight).

### 5.2.2 Casting of plate specimens

Following steps are adopted in casting the plates

(1)Woven glass fiber mat is cut to the required size of 540mm X 540mm.

(2)Teflon cloth (releasing surface) is laid on a plane surface.

(3)A thin coat of resin is spreaded on the cloth.

(4)First layer of the fiber mat is laid and resin

is spreaded over the layer so that every glass filament gets pregnated with the resin.

(5)Step 4 was repeated for each of the three layers of woven glass fiber mats.

(6)Pressure is applied using a roller after each layer is spreaded to squeeze out extra resin and air bubbles.

(7)On the top face some extra resin is put to get a glossy surface.

(8)Then it is left for curing for twenty-four hours.

For all future reference Plate 1 corresponds to the plate with fiber volume ratio of 59% and plate 2 with 56%.

### 5.2.3 Fabrication of experimental set-up

#### 5.2.3.1 For static test

up used to perform the static test involves four ISA (Indian standard angle) 50 X 50 X 5 sections (fig. 5.1). These angle sections are welded together with horizontal stiffners to form a box-frame. On this frame another square supporting frame with ISMB 175(Indian Standard Medium-weight Beam section of depth 175 mm.) is fabricated. Uniformly distributed loading is idealised in the experiment through sixteen point loading. A concentrated load applied through the hydraulic jack, gets distributed through two tiers of distributors as shown in Fig. 5.1 into sixteen equal parts. In order to simulate clamped boundary conditions the plate was clamped between the top flange of the ISMB 175 section and rigid steel plate on all sides as shown in Fig. 5.1. In order to avoid the damage of the plate by making bolt-holes, C-clamps were used for fixing the plate with the frame. Dial gages with magnetic base were placed below the plate at predetermined positions to measure transverse deflection at those locations.

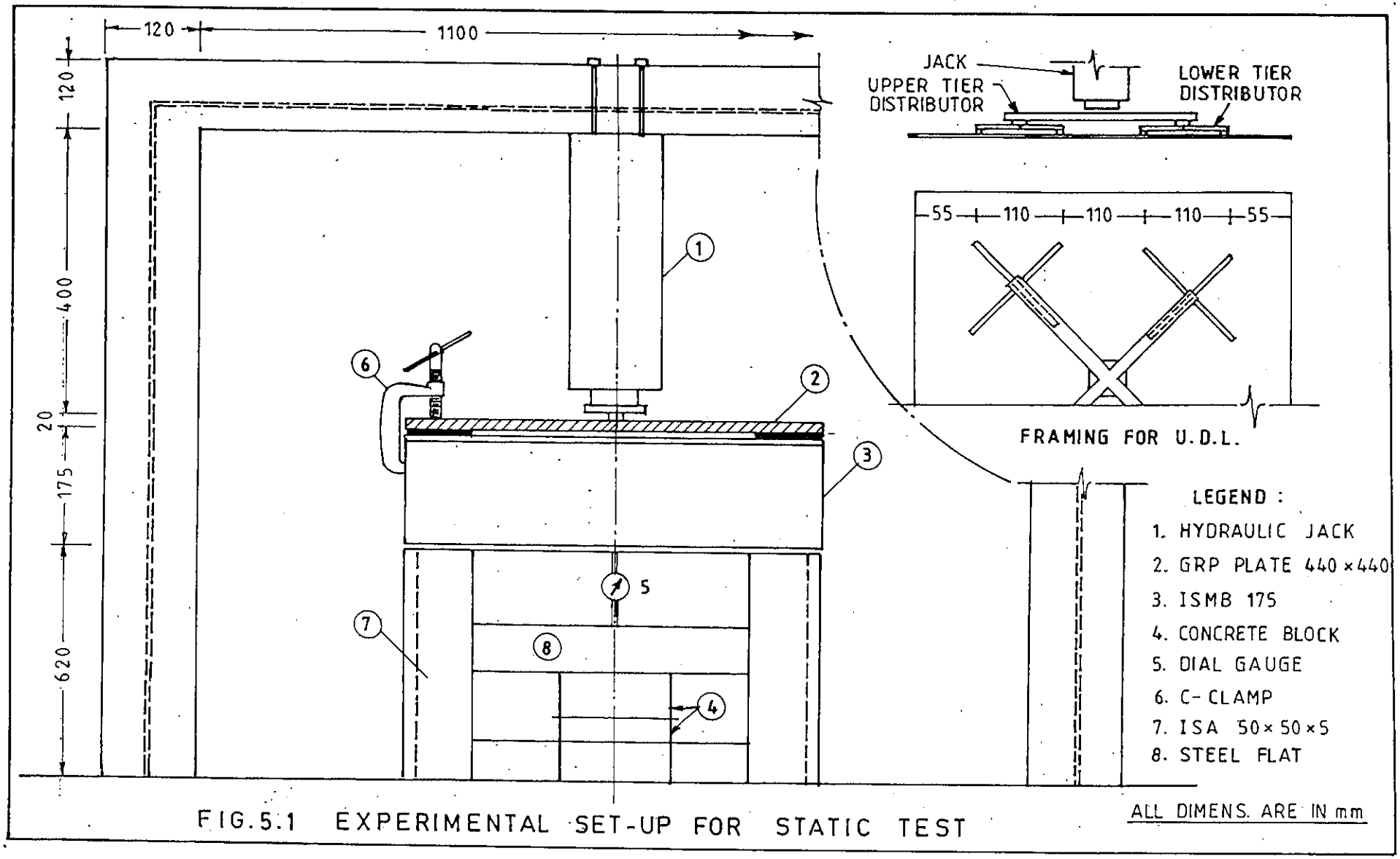


FIG.5.1 EXPERIMENTAL SET-UP FOR STATIC TEST

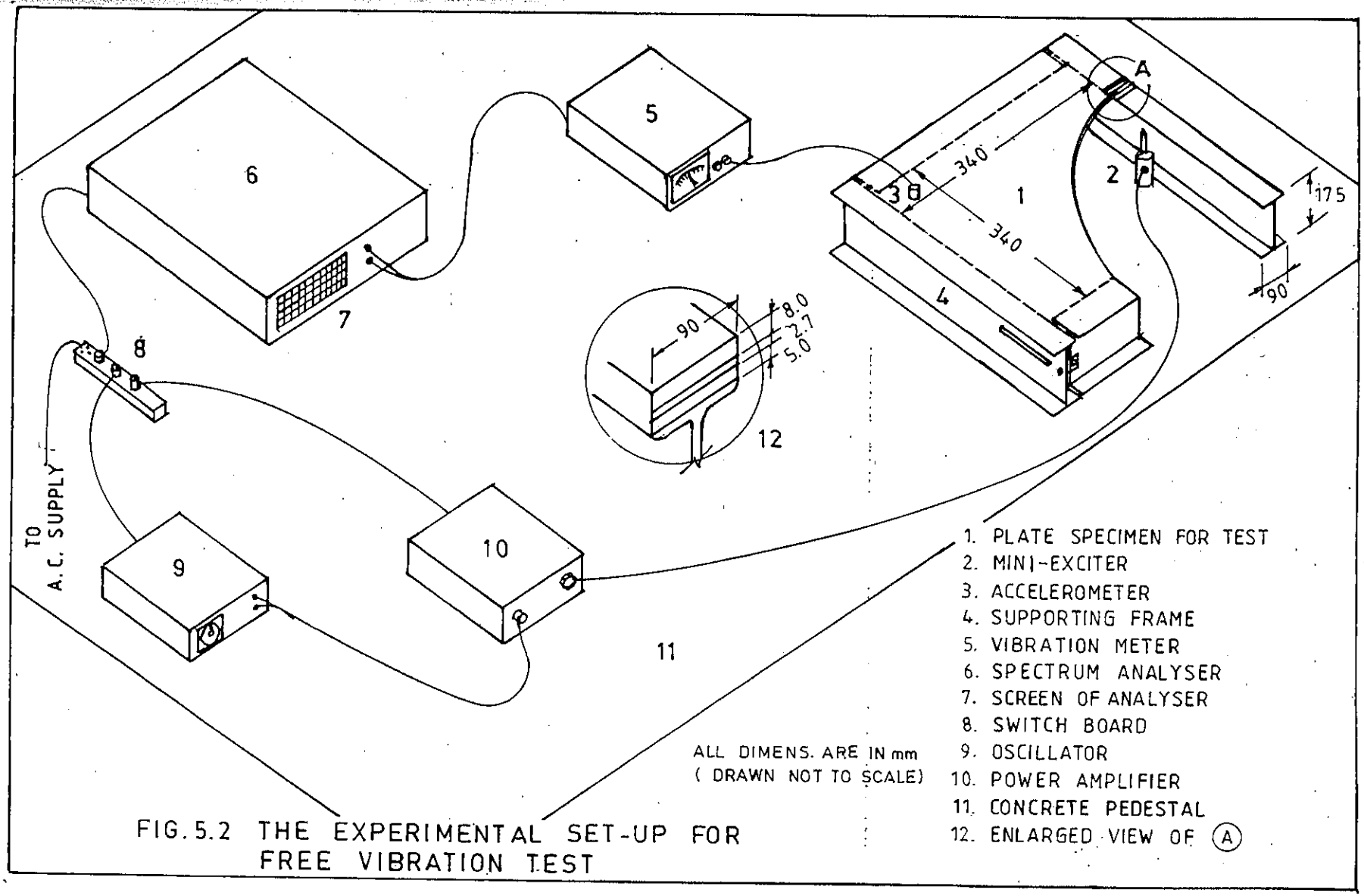


FIG. 5.2 THE EXPERIMENTAL SET-UP FOR FREE VIBRATION TEST

#### 5.2.3.2 For free vibration test

The same supporting frame fabricated using ISMB 175 is modified and used for free vibration analysis (Fig. 5.2). To absorb the vibration at the support, strips of leather are placed along the edges between the top flange of the supporting frame and the plate to be tested. On top of the plate steel plates are placed and clamped.

## 5.3 Experimental equipments

### 5.3.1 Static test

| | |
|---|---|
| Hydraulic Jack<br>Simplex, USA | 10 ton capacity<br>Hand pump operated with 6 inch travel |
| Dial Gage<br>Mitutoyo, Japan | 50 mm total travel<br>Least count of 0.01 mm |

### 5.3.2 Free vibration test

| | |
|---|---|
| Spectrum Analyser<br>(Hewlett Packard)<br>Model 3582 A | Frequency range: 0.02 Hz to 25 KHz<br>Amp. range 3 mV to 30 V<br>Maximum input display range 80 dB |
| Vibration Meter<br>(Bruel Kjaer)<br>Type 2511 | Frequency range: 0.30 Hz to 15 KHz.<br>Used in conjunction with a piezo-electric vibration pick up to measure acceleration, velocity and displacement. |
| Accelerometer<br>(Bruel Kjaer)<br>Type 4374 | Weight: 0.65 gm. excluding cable<br>Mounting: Adhesive |
| Exciter (Mini-shaker)<br>(Bruel Kjaer)<br>Type 4810 | Impedence: 3.5 ohm<br>Input power: 15 VA maximum. |

| | |
|---|---|
| Oscillator<br>(Philips)<br>Model pp 9060 | Frequency Range: 0 Hz to 1000 Hz<br>Sine and Square wave generator |
| Power Amplifyer<br>(Bruel Kjaer)<br>Type 2706 | Frequency range: 10 Hz to 20 KHz<br>Power output: 75 VA |

## 5.4 Tests and procedures

### 5.4.1 Static deflections

Following procedures are adopted in carrying out this test.

(1)The test plates are placed on the supporting frame and clamped using C-clamps.

(2)Dial gages are placed below the plate at the locations where deflections are to be measured.

(3)Two dial gages are fixed at the edges of the plate to check if the edges move in when the plate bends.

(4)Initial readings in the dial gages are noted when the lower end of the jack touches the plate.

(5)Loading is done very slowly and the increment is kept constant at 10 kgs.

(6)Dial gage readings are noted for every load increment.

(7)Loading is stopped at P=140 kg. and then unloaded to find that dial gages read approximately their initial values.

### 5.4.2 Fundamental frequency and mode shapes

Plate 2 is placed on the frame and the edges are clamped using C-clamps. Tests are conducted for square plate as well as for plates having aspect ratios of 0.8 and 0.6. The pick-up accelerometer is fixed to the plate with wax and is connected to the input of the vibration meter. The output of the vibration meter is fed to the spectrum analyzer. Amplitudes of the responses are observed on the screen of the spectrum analyser and the peak amplitude technique is used to locate the natural frequencies. The modal patterns of first four modes are obtained by measuring acceleration at some predetermined points and plotting them.

Adjusting the supporting frame, different aspect ratios of the plate can be obtained. Then a square opening is made in the centre of the plate and the same test is carried out to get the free vibration frequencies and mode shapes of the square plate with central cut-out.

### 5.4.3 Procedure

The instruments were switched on to reach a stable condition before the commencement of the experiment. The plate is excited by an electro-magnetic shaker. The spectrum analyser is adjusted for the frequency range of interest. Test involves following steps

(1)The plate is placed on the supporting frame and then clamped tight using C-Clamps as shown in photo.1.

(2)The mini exciter is placed under the plate in such a way that the tip of the exciter touches the lower face of the plate at a point near the support where nodal lines are present (photo. 2).

(3)Connection detail is as shown in Fig.5.2 and photo.3.

(4)Using the oscillator, driving frequency to the exciter is changed gradually and the response of the plate is seen in the spectrum analyser simultaneously. When the exciter frequency coincides with natural frequencies of the plate, resonance will occur and there will be a sharp rise in the plate response. The frequency correspond to first such rise is the fundamental frequency of the plate.

(5)Oscillator frequency is slowly increased to obtain other higher frequencies.

(6)To obtain the mode shape, response of the plate at various pre-marked points are obtained when the frequencies of excitation coincide with various natural frequencies of the plate and afterward on plotting these values.

(7)Next step is to make the central cut-out and the above steps are repeated (photo.4).

## 5.5 Precautions

### 5.5.1 Static test

At least $\frac{1}{10}$ th of the span should be inside the support to get a fixed support condition.

(1)Load should be applied very slowly to simulate static case. Rate of loading has a profound effect on the behaviour of the plate.

(2)Clamping should be proper. As support condition influences results to a great extent.

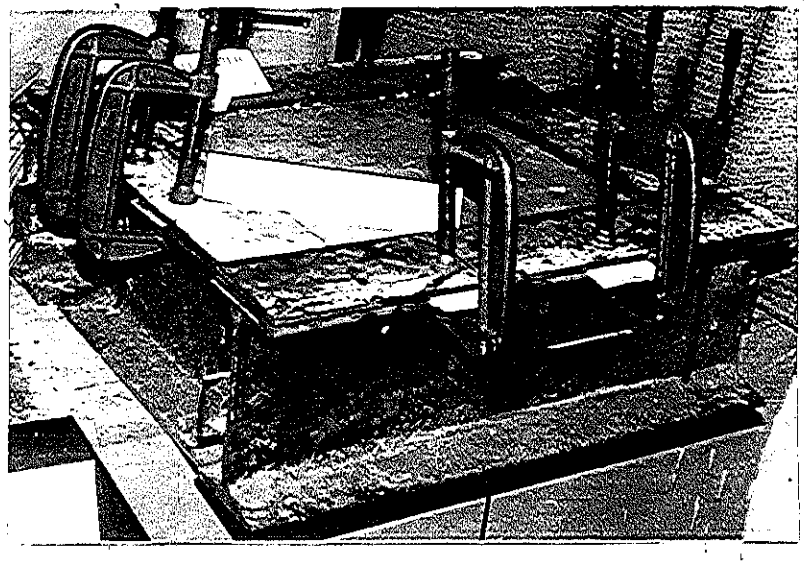

1(a)

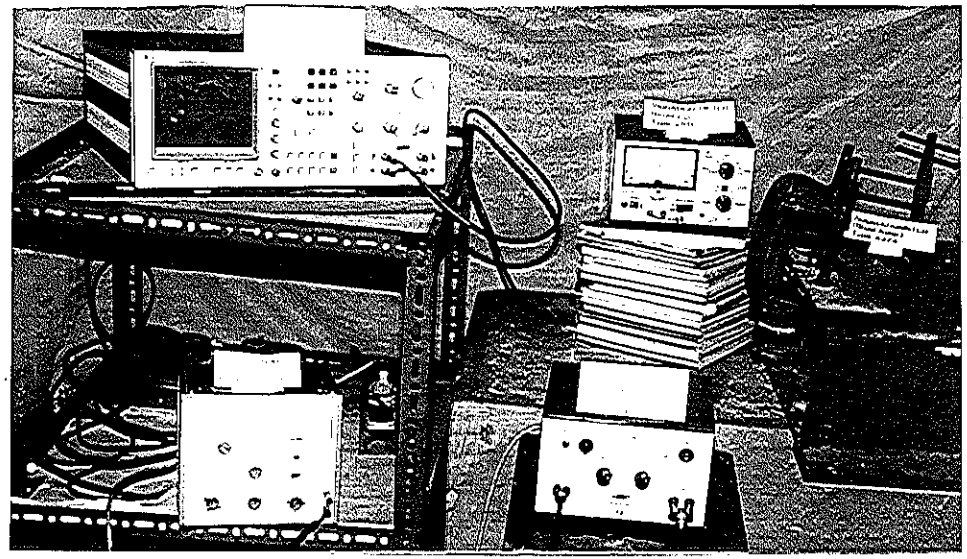

1(c)



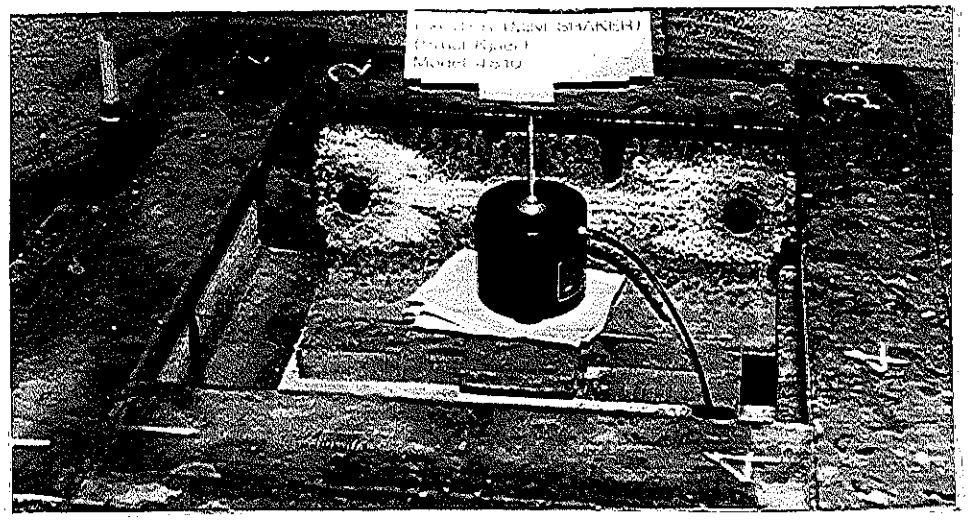

1(b)

1(a) Test plate on supporting bed along with clamping arrangement.

1(b) Placement of the exciter.

1(c) Testing instruments and their connection details

P L A T E 1

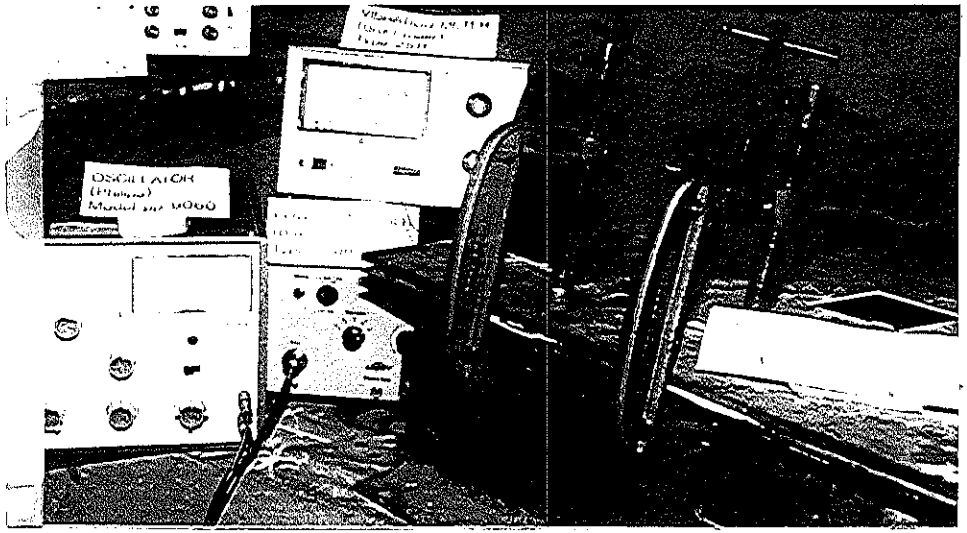


2(a)

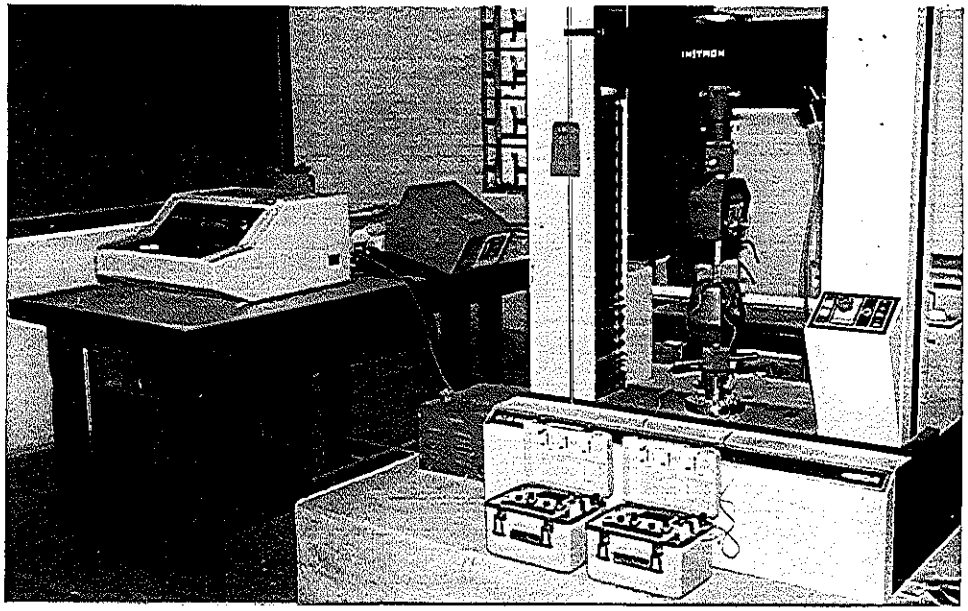


2(b)


2(c)

2(a) Square plate with square central cut-out on the testing bed.

2(b) Coupon with strain gages mounted in the INSTRON machine.

2(c) Hydraulic press to cast the jute -reinforced plastic composite.

P L A T E 2

### 5.5.2 Free vibration test

(1)Support should be heavy in comparison to the weight of plate. This will reduce the influence of plate vibration to support vibration.

(2)Accelerometer should be light.

(3)Exciter should be placed near the support where nodes are present.

(4)Tests are repeated for different aspect ratios starting with 1 and decreasing in steps through 0.8 and 0.6 and again 0.8 and ending at 1.

## 5.6 Observations and results

### 5.6.1 Static test

Table 5.1 gives deflection at three points of a square clamped plate (Dimension is 440mm X 440mm X 2.7mm and fiber volume ratio = 59%) under uniformly distributed load. Fig. 5.3(a) gives the corresponding load-deflection curves.

Table 5.1:Experimental and numerical results under U.D.L.

| Load (N) | U.D.L. $N/mm^2$ $X10^{-4}$ | Expt. values in mm at | | | Finite element values in mm at | | |
|---|---|---|---|---|---|---|---|
| | | 1 | 2 | 3 | 1 | 2 | 3 |
| 100 | 5.17 | 0.36 | 0.26 | 0.48 | 0.152 | 0.258 | 0.465 |
| 200 | 10.34 | 1.14 | 1.13 | 1.44 | 0.303 | 0.515 | 0.931 |
| 300 | 15.51 | 1.47 | 1.53 | 2.09 | 0.455 | 0.773 | 1.396 |
| 400 | 20.68 | 1.78 | 1.90 | 2.52 | 0.606 | 1.030 | 1.861 |
| 500 | 25.86 | 2.06 | 2.24 | 2.92 | 0.758 | 1.288 | 2.327 |
| 600 | 31.03 | 2.29 | 2.61 | 3.17 | 0.909 | 1.545 | 2.792 |
| 700 | 36.20 | 2.53 | 2.74 | 3.55 | 1.061 | 1.803 | 3.257 |
| 800 | 41.37 | 2.73 | 2.96 | 3.81 | 1.212 | 2.06 | 3.722 |
| 900 | 46.54 | 2.93 | 3.18 | 4.06 | 1.364 | 2.318 | 4.188 |
| 1000 | 51.71 | 3.08 | 3.33 | 4.14 | 1.515 | 2.575 | 4.65 |
| 1100 | 56.88 | 3.25 | 3.50 | 4.43 | 1.667 | 2.833 | 5.118 |
| 1200 | 62.05 | 3.39 | 3.64 | 4.60 | 1.818 | 3.090 | 5.584 |
| 1300 | 67.22 | 3.53 | 3.90 | 4.90 | 1.970 | 3.348 | 6.049 |
| 1400 | 72.39 | 3.82 | 4.11 | 5.13 | 2.12 | 3.610 | 6.51 |

Table 5.2 and Fig. 5.3(b) give mid-point deflection of two clamped-plates with fiber volume ratios as 56% and 59% under uniformly distributed load.

Table 5.2: Mid-point deflection for two clamped plates under U.D.L.

| Load (N) | U.D.L. $N/mm^2 \times 10^{-4}$ | Defl.(mm) with fiber volume ratios | |
|---|---|---|---|
| | | 56% | 59% |
| 100 | 5.17 | 0.744 | 0.480 |
| 200 | 10.34 | 1.700 | 1.440 |
| 300 | 15.51 | 2.364 | 2.090 |
| 400 | 20.68 | 2.829 | 2.520 |
| 500 | 25.86 | 3.180 | 2.920 |
| 600 | 31.03 | 3.437 | 3.170 |
| 700 | 36.20 | 3.885 | 3.550 |
| 800 | 41.37 | 4.133 | 3.810 |
| 900 | 46.54 | 4.390 | 4.060 |
| 1000 | 51.71 | 4.499 | 4.140 |
| 1100 | 56.88 | 4.836 | 4.430 |
| 1200 | 62.05 | 5.031 | 4.600 |

Table 5.3 and Fig. 5.3(c) give the mid-point deflection of a clamped-plate (vol. ratio = 59%) under point load at the middle of the plate.

Table 5.3: Experimental and numerical mid-point deflections under point load at the centre of the plate (fiber vol. ratio = 59%).

| Load (N) | Expt. value (mm.) | Finite element results (mm.) |
|---|---|---|
| 100 | 3.0 | 1.75 |
| 200 | 5.5 | 3.75 |
| 300 | 8.0 | 5.50 |
| 400 | 8.75 | 7.25 |
| 500 | 10.75 | 9.00 |
| 600 | 12.00 | 11.00 |
| 700 | 12.75 | 13.00 |
| 800 | 12.85 | 14.50 |
| 900 | 13.50 | 16.40 |
| 1000 | 15.25 | 18.25 |
| 1100 | 15.75 | 20.00 |
| 1200 | 15.875 | 21.75 |
| 1300 | 16.125 | 23.75 |
| 1400 | 17.00 | 25.50 |

### 5.6.2 Free vibration test

Fundamental frequencies and the corresponding mode shapes obtained from the experiment were given in Figs. 5.4-5.7.

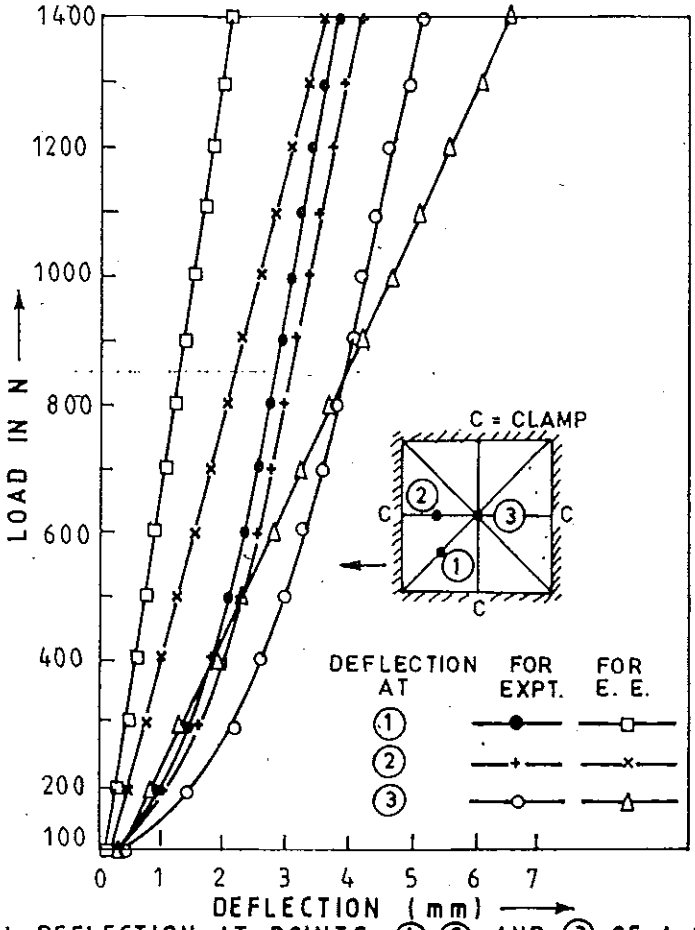


(a) DEFLECTION AT POINTS ①, ② AND ③ OF A CLAMPED SQUARE PLATE DUE TO UNIFORMLY DISTRIBUTED LOAD

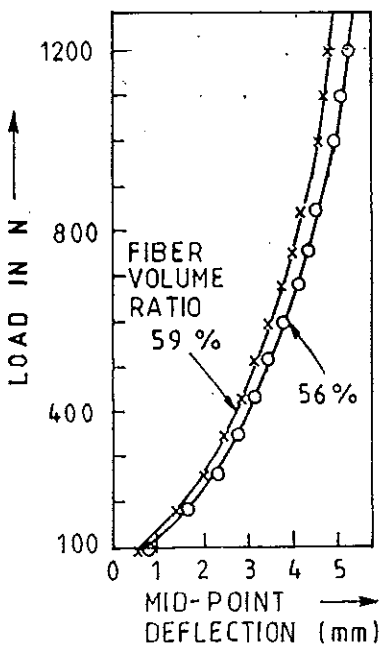


(b) MID-POINT DEFLECTION OF TWO PLATES WITH DIFFERENT FIBER VOLUME RATIO UNDER U. D. L.

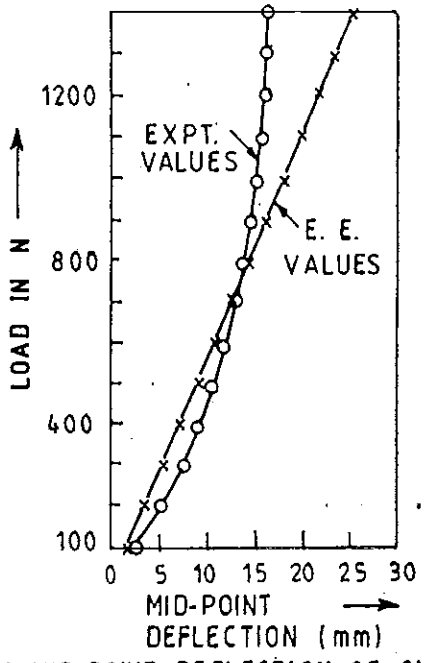


(c) MID-POINT DEFLECTION OF CLAMPED SQUARE PLATE DUE TO A POINT LOAD AT THE CENTRE

FIG. 5.3

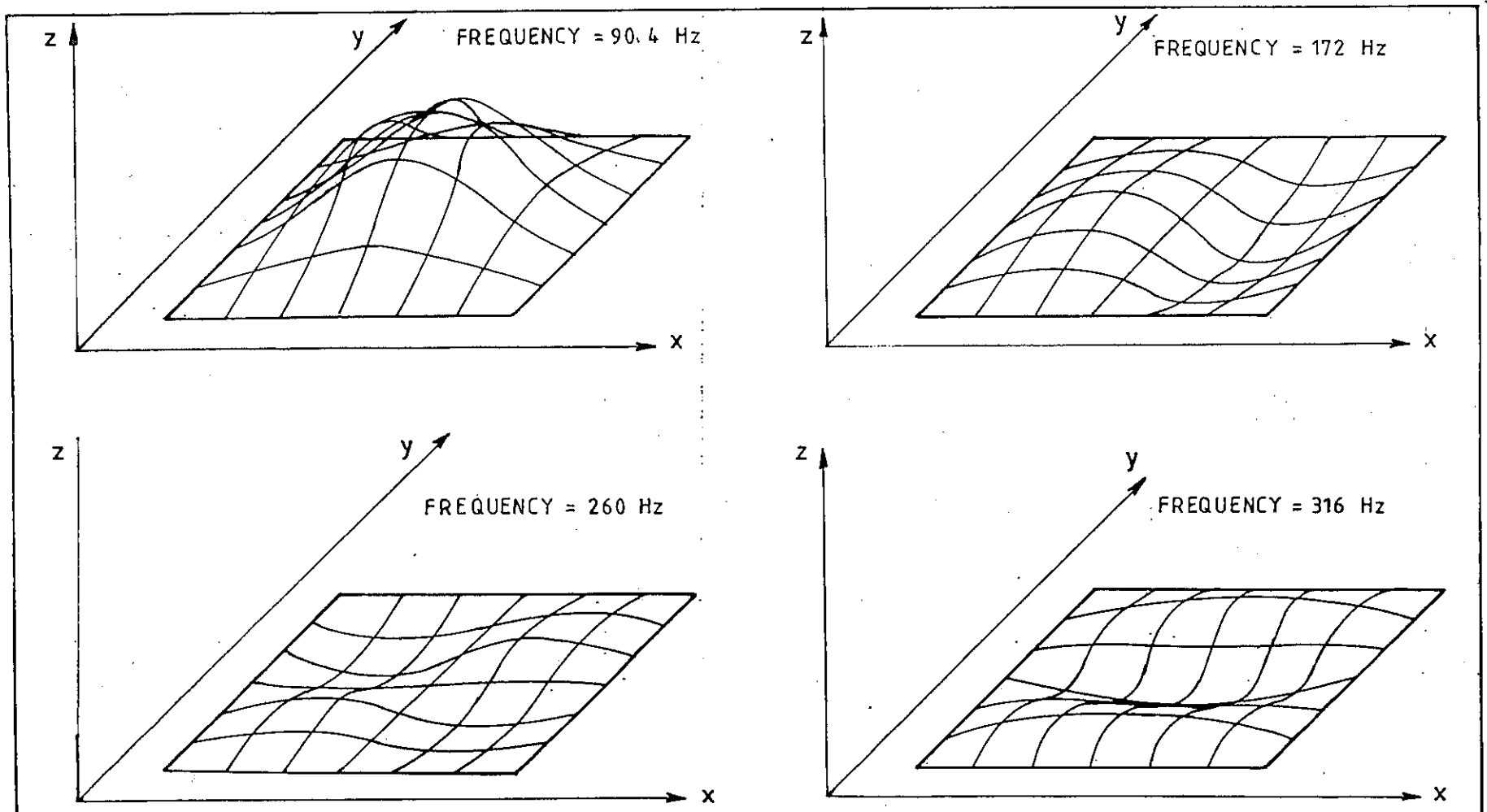


FIG.5.4 NATURAL FREQUENCIES AND CORRESPONDING MODE SHAPES FOR A SQUARE PLATE ( PLATE : 340 mm x 340 mm ; SUPPORT : ALL EDGES CLAMPED)

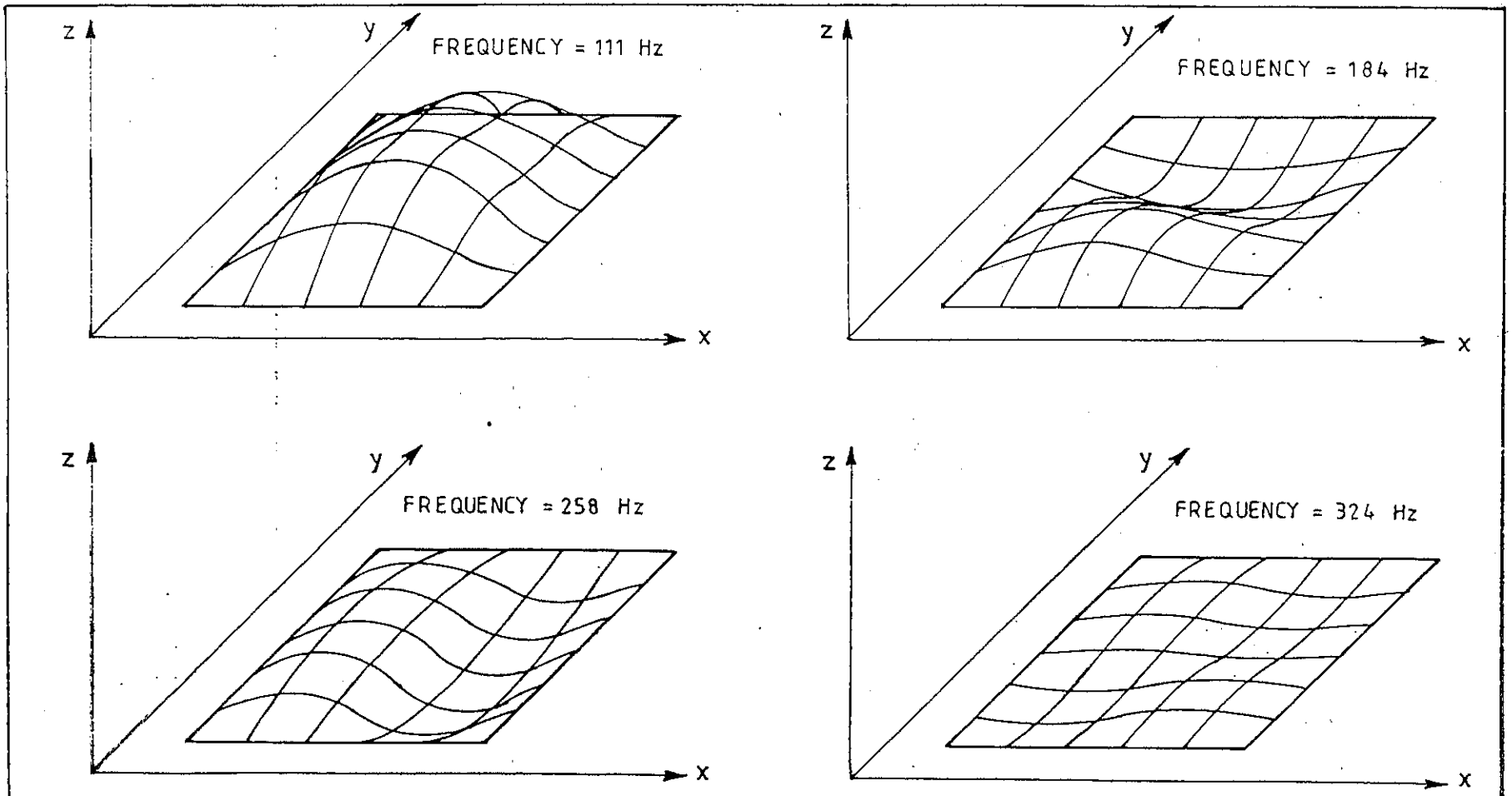


FIG.5.5 NATURAL FREQUENCIES AND CORRESPONDING MODE SHAPES FOR A PLATE WITH ASPECT RATIO = 0.8
( PLATE : 340mm x 270 mm , SUPPORT : ALL EDGES CLAMPED )

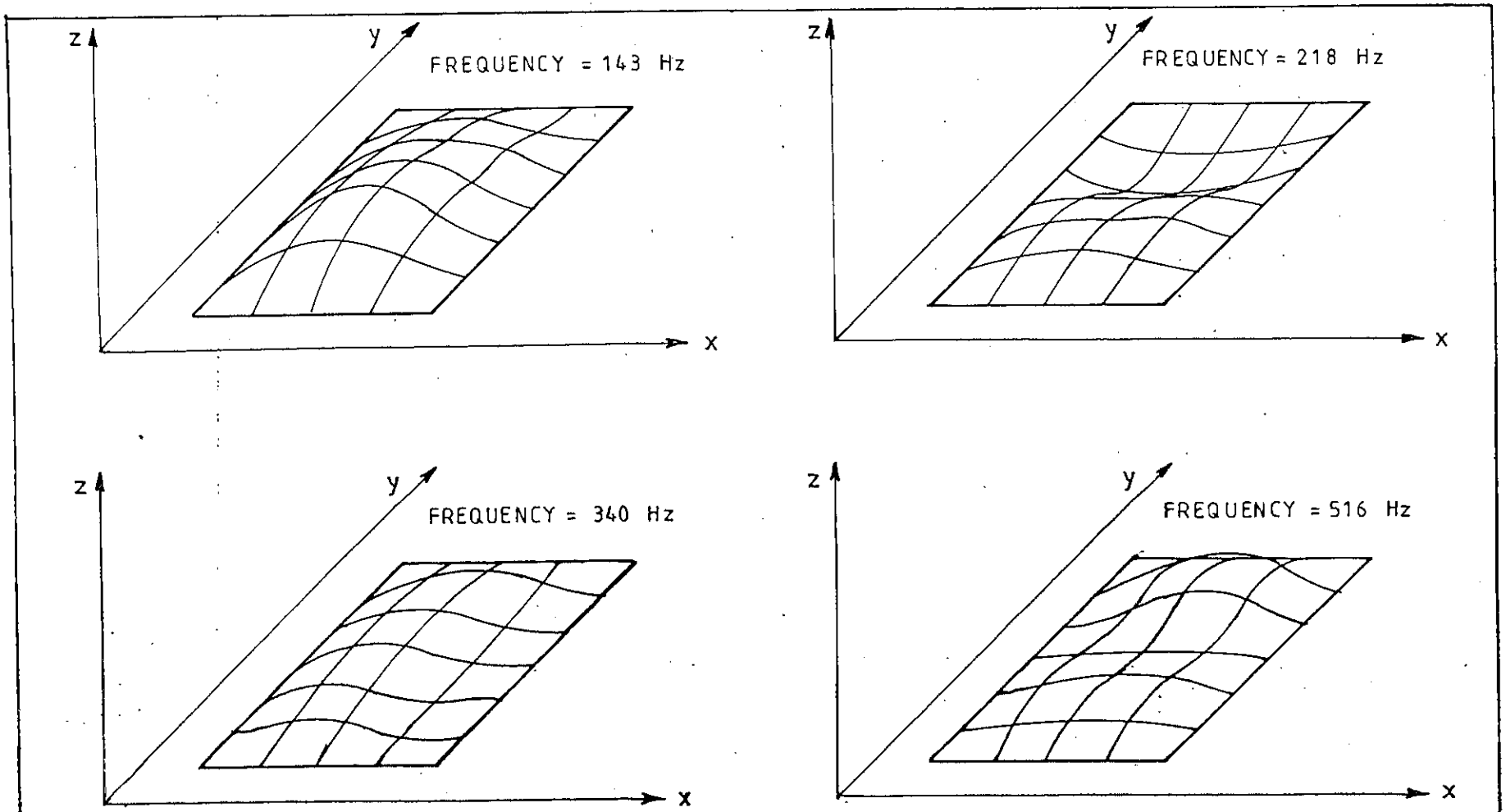


FIG. 5.6 NATURAL FREQUENCIES AND CORRESPONDING MODE SHAPES FOR A PLATE WITH ASPECT RATIO = 0.6
( PLATE : 340 mm x 204 mm ; SUPPORT : ALL EDGES CLAMPED )

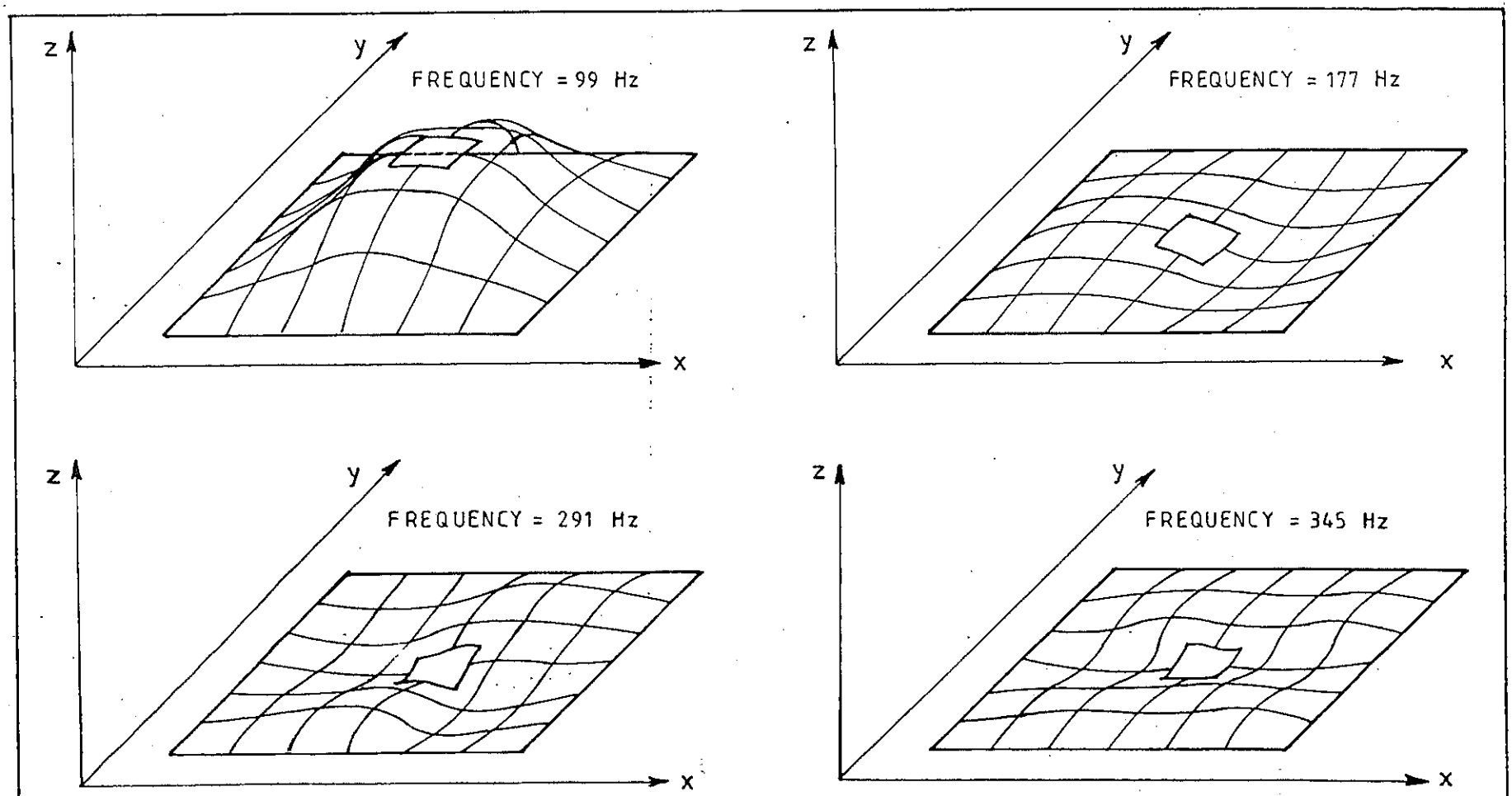


FIG. 5.7 NATURAL FREQUENCIES AND CORRESPONDING MODE SHAPES FOR A SQUARE PLATE WITH A SQUARE CUTOUT
(PLATE : 340 mm x 340 mm; CUTOUT : 85 mm x 85 mm; SUPPORT : ALL EDGES CLAMPED)

## 5.7. Determination of material constants

### 5.7.1. Elastic constants

The objective of finding elastic constants is to use these values as input data in the Finite Element program developed in connection with chapter 3 to compute plate response and to compare these values with the experimental results. Since wide variation among plates is possible, same plate was cut in the form of coupons after the test to determine material properties. Laminated plate behaved as an orthotropic laminae defined by four independent material constants. These constants are evaluated experimentally by performing unidirectional tensile tests on coupons cut in L (longitudinal) and T(transverse) and at $45^{\circ}$ to L direction. For each of these properties, around three replicate specimens are tested and mean value is adopted.

Coupons are machined carefully to minimise the residual stress after they are cut from panels at various configurations ($0^{\circ}$, $45^{\circ}$, $90^{\circ}$) as shown in Fig. 5.8.a. Specimen dimensions are shown in Fig. 5.8(a). A length of 40 mm at each ends of the specimen is provided for gripping. This yielded a test section with an aspect ratio of more than 10. Two strain gages are fixed with each specimen at the same location but at perpendicular to each other. Strains are obtained using strain indicators and are plotted against engineering stress in fig. 5.8(b). Finally, the experimentally determined material parameters have been employed to obtain predictions of plate behaviour.

5.7.2 Procedures

The specimen was first aligned in the grips and tightened in place. The specimen was then loaded monotonically to failure at a recommended rate of 0.02 cm/min. All the coupons are tested in an Instron machine with a fixed cross-head speed (photo 5). Strain gages with a resistance of 120 ohms and a gage length of 3.0 mm have been used. Fig. 5.8(b) gives the stress-strain curves. These curves were marked with a number and a letter. The number signifies the step number (given below) from which it is obtained and the letter L for longitudinal and T for transverse cases. Steps involved in obtaining the static material constants from Fig. 5.8(b) are

**Step 1:**

Coupon nos 1 and 2 (Fig.5.8.a) are tensioned uni-axially. Strains $\varepsilon_1$ and $\varepsilon_2$ are measured, then

$$\sigma_1 = \frac{P}{A} \; ; \quad E_1 = \frac{\sigma_1}{\varepsilon_1} \; ; \quad \nu_{12} = - \frac{\varepsilon_2}{\varepsilon_1} \qquad (5.1)$$

where P is the applied load and A is the cross-sectional area of the coupon in the middle section.

**Step 2:**

Similar uniaxial tensile test is done using coupon nos. 3 and 4 and as above

$$\sigma_2 = \frac{P}{A} \; ; \quad E_2 = \frac{\sigma_2}{\varepsilon_2} \; ; \text{ and } \quad \nu_{12} = - \frac{\varepsilon_1}{\varepsilon_2} \qquad (5.2)$$

Step 3:

Coupon nos. 5 and 6 are also tensioned identically using single strain gage. Longitudinal strain i.e. $\varepsilon_\Theta$ is measured. Thus,

$$E_\Theta = \left(\frac{P}{A}\right) / \varepsilon_\Theta \qquad (5.3)$$

and shear modulus $G_{12}$ obtained from equation 2.102 of reference [125]

$$G_{12} = \frac{1}{\left[\frac{4}{\bar{E}_\Theta} - \frac{1}{\bar{E}_1} - \frac{1}{\bar{E}_2} + \frac{2\nu_{12}}{\bar{E}_1}\right]} \qquad (5.3)$$

A similar set of material constants is obtained from uniaxial tensile tests on coupons cut from the plate 2 (i.e. fiber vol. ratio is 56%) as shown in Fig. 5.9(a). Coupons used were no. 1 and 3 for step 1; 7 and 9 for step 2 and 13 and 14 for step 3. Material properties are obtained from the curves are tabulated in Table 5.4. For data acquisition, Vishay strain indicators are used.

Table 5.4: Material properties of the plates

| Plate no. | Fiber volume ratio | $E_1$ in $N/mm^2$ | $E_2$ in $N/mm^2$ | $\mu_{12}$ | $G_{12}$ in $N/mm^2$ |
|---|---|---|---|---|---|
| 1 | 59% | 34290 | 24000 | 0.24 | 3710 |
| 2 | 56% | 29160 | 20000 | 0.26 | 3877 |

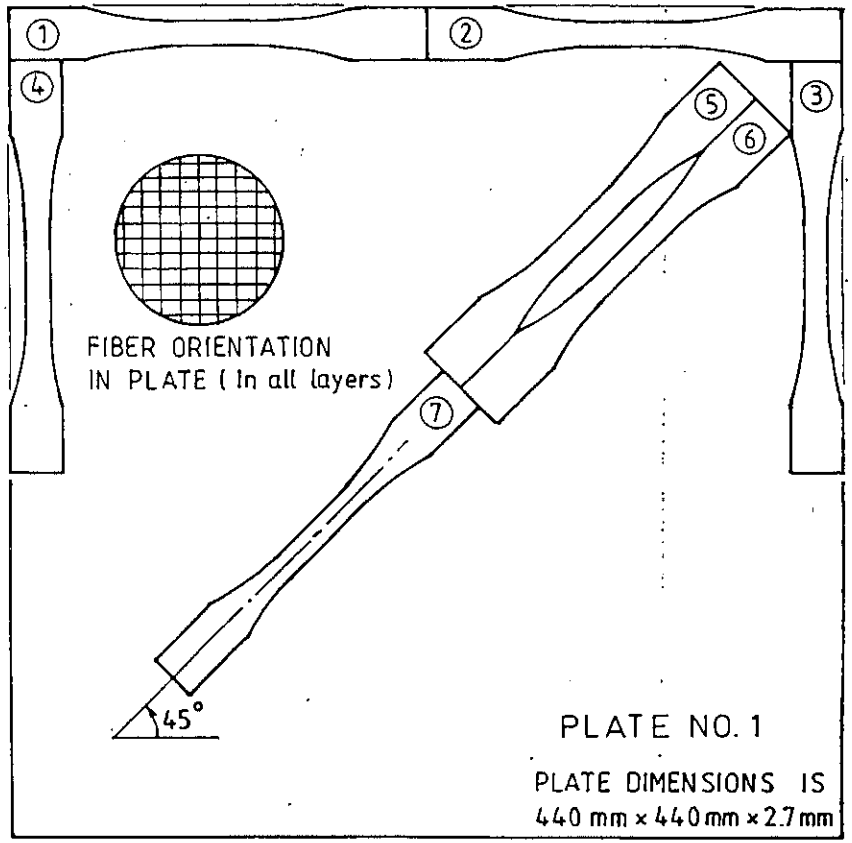


(a) COUPONS ARE CUTOUT FROM THE SAME PLATE AT DIFFERENT ORIENTATIONS

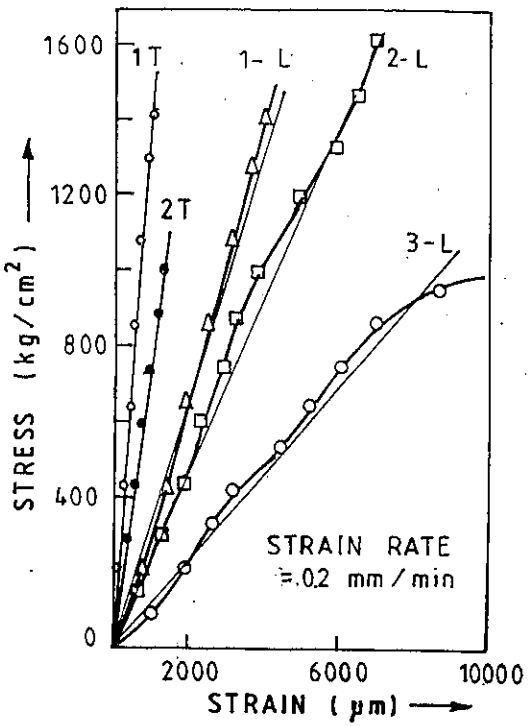


(b) STRESS STRAIN CURVES
( Fiber volume ratio = 59 % )

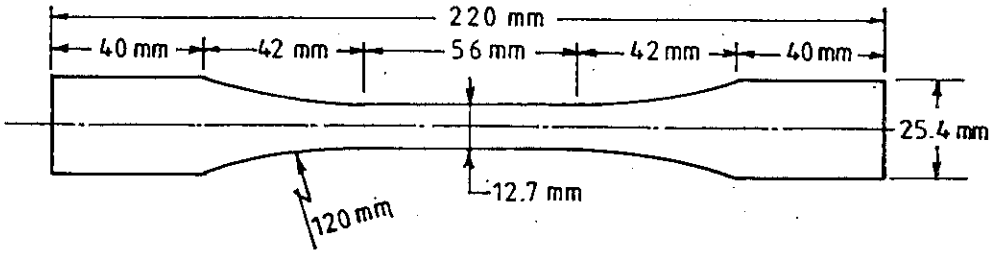


(c) GEOMETRY OF G.R.P. COUPON FOR TENSILE TEST

FIG. 5.8

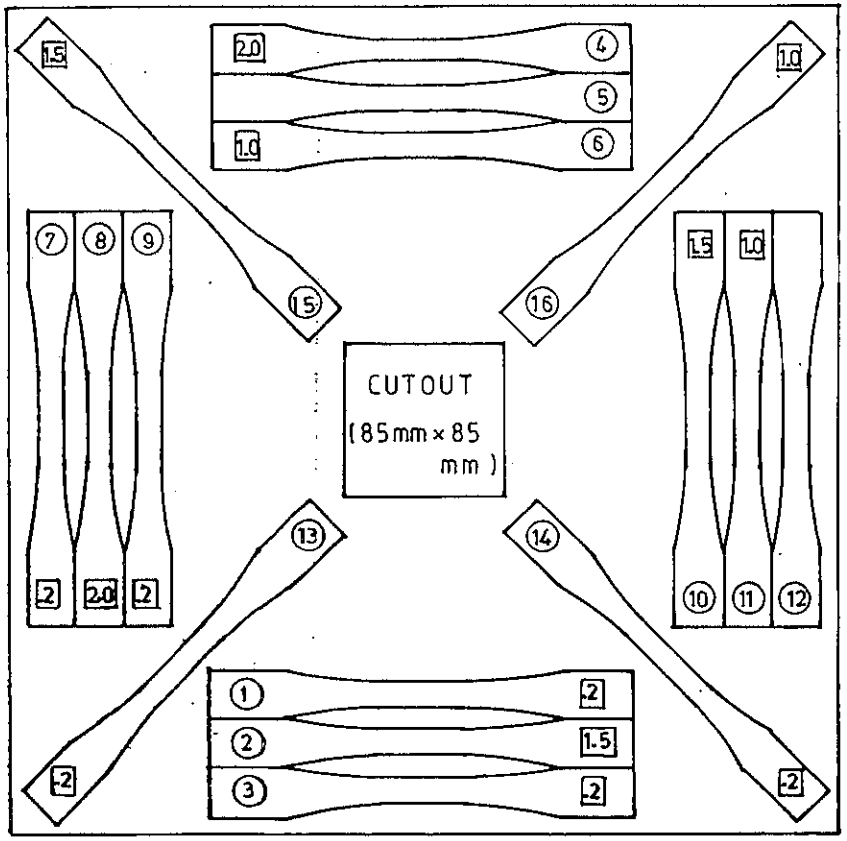


(a) COUPONS ARE CUTOUT FROM THE PLATE UNDER FREE VIBRATION TEST

○ COUPON IDENTIFICATION NUMBER

□ CROSS-HEAD SEPARATION RATE

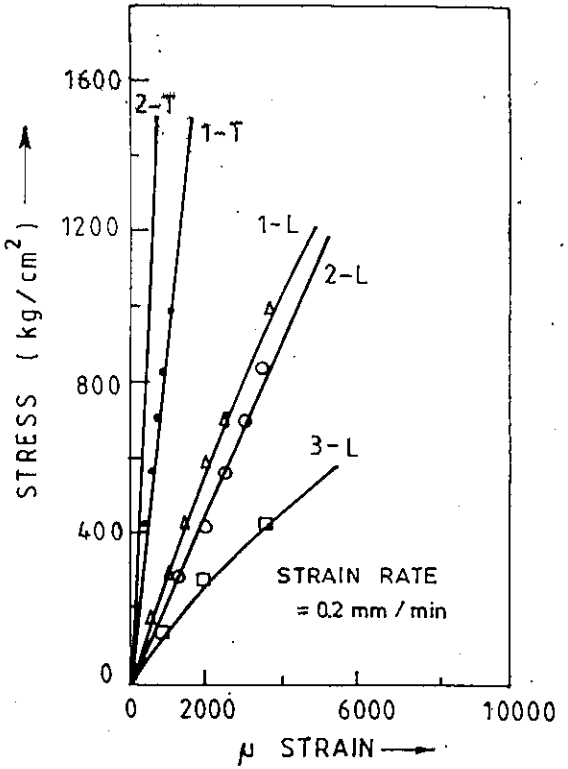


(b) STRESS-STRAIN CURVES
(Fiber volume ratio = 56 %)

FIG. 5.9

## 5.8. Mass density

Mass density is determined by mercury displacement method. The procedure adopted for this is

(1)Six specimen samples, three circular and three triangular are cut out from the plate.

(2)A small porceline pot is taken with mercury filled to the brim so that when the lid with three prons is placed on the pot leaves no air between the lid and the mercury surface.

(3)Samples are placed separately on the mercury surface and the lid is replaced every time. As a result, a volume of mercury equal to the volume of the specimen will be displaced and collected and measured using a measuring cylinder.

(4)Weight of each sample is taken accurately in a balance.

(5)Repeated steps (3) and (4) for all the samples.

(6)Ratio of values of step (4) to step (3) gives the mass density of the material.

### 5.8.1. Observation

Table 5.5 gives mass density of the Glass-reinforced-plastic plate (fiber vol. ratio= 56%)

Table 5.5: Mass density of Glass reinforced plastics

| Sample shape | No. | Volume (c.c.) | Weight (gm.) | Density (gm/cc) |
|---|---|---|---|---|
| Circular | 1 | 1.15 | 2.8 | 2.4389 |
| | 2 | 1.11 | 2.7 | |
| | 3 | 1.07 | 2.6 | |
| Triangular | 1 | 1.40 | 3.42 | |
| | 2 | 1.41 | 3.45 | |
| | 3 | 1.41 | 3.45 | |

## 5.9. Comparison

Material parameters as obtained in section. 5.7 (Table 5.4) are used in the finite element model developed in chapter 3 and 4 and the responses of the plates are computed. These numerical values are compared with the corresponding experimental values. Tables 5.1 and 5.3 give the comparison of static deflections and table 5.6 is for vibration frequencies.

Finite element analysis of the plate with cut-out is handled by substituting the thickness of the plate in the region of cut-out to be very small in compared to other portion.

Table 5.9 Experimental and numerical frequencies

| Expt. values | | | | Finite element | | | |
|---|---|---|---|---|---|---|---|
| Aspect ratios | | | | | | | |
| 1.0 | 0.8 | 0.6 | cut | 1.0 | 0.8 | 0.6 | cut |
| 90.4 | 111. | 143. | 99. | 125. | 154. | 219. | 131. |
| 172. | 184. | 218. | 177. | 270. | 318. | 395 | 295. |
| 260. | 258. | 340. | 291. | 289. | 406. | 652. | 322. |
| 316. | 324. | 516. | 345. | 450. | 575. | 711. | 451. |

## 5.10 Discussion

Experimental and numerical results for the static deflection and free vibration of plates with all four sides clamped are presented in this chapter

The experimentally observed results are compared with the computed results by the finite element analysis. Material properties are obtained for both the plates and are presented in Table 5.4.

Deflections at three specified locations of plate 1 subjected to U.D.L. are obtained both by experimentally and using finite element model. These values are presented in Table 5.1 and Fig. 5.3(a). Experimental results show that the material behaviour is non-linear.

Deflection of plates with two different fiber volume ratios are given in Table 5.2 and Fig. 5.3(b). As expected, the plate with higher fiber volume ratio has higher stiffness.

Experimental and numerical results obtained for plate (fiber vol. ratio = 59%) under a point load at mid-point are presented in Table 5.3 and Fig. 5.3(c). Comparing the values given in column 2nd of Table 5.3 and 4th column of Table 5.2, we see that under point load, deflection is more than that under U.D.L.

Fundamental frequency and the mode shape of plate 2 (fiber vol. ratio is 56%) for all edges clamped are obtained. These results are presented in Figs. 5.4-5.7. Results given in Table 5.6 show that experimental frequencies are lower than that predicted by the finite element modelling. This is true for all the cases of plate aspect ratios.

To compare the results obtained through experiments, numerical analysis of the same plate (plate 2) is carried out after evaluating its material parameters and mass density. Table 5.4 and 5.5 give the observations related to finding these quantities respectively. After the test, the plate was cut as shown in Fig. 5.9(a) in the form of rectangular elements. These are machined to form the coupons. Material constants obtained from the coupon test are presented in table 5.4. All these values correspond to uniaxial tensile loading at a deformation rate of 0.02 cm/min. of the cross

head. Using all these values and mass density as given in Table 5.5, plate behaviour can be predicted. These values are given in table 5.6.

From all the results above, following observation can be made

FRP (fiber reinforced plastics) materials are characteristically visco-elastic to some extent, thus demonstrated non-linear stress-strain behaviour. The dynamic performance of these materials is usually far different from their static performance. In the case of visco-elastic materials, the rate of loading assumes a pronounced influence on the response. Generally the strain is larger if the stress varies slowly. Under sinusoidal excitation, the strain is observed to lag behind the stress (Fig. 5.10).

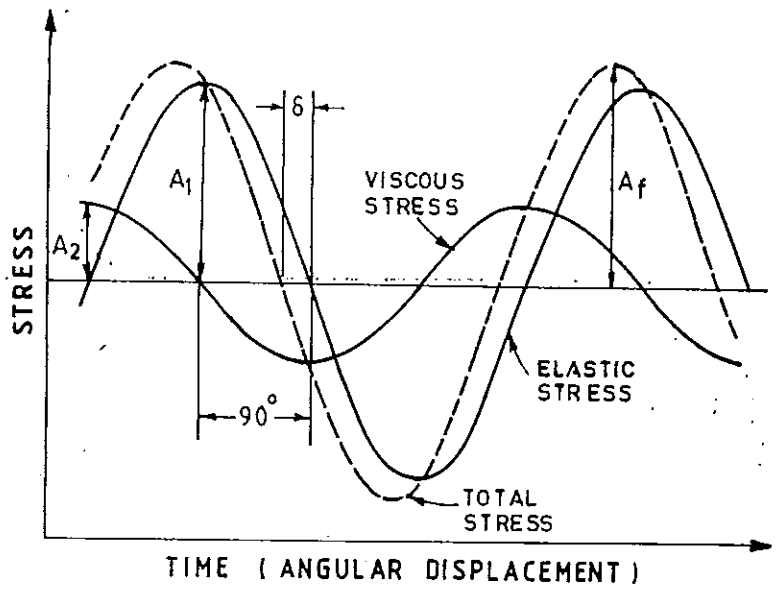


FIG. 5.10 SINUSOIDAL STRESS CYCLE: ELASTIC (IN PHASE) VISCOUS (OUT-OF-PHASE), AND RESULTANT TOTAL DISPLACED BY THE LOSS ANGLE, δ

The phase angle between them, denoted by $\delta$ is the loss angle. The stress may be separated into two components; one in-phase with the strain and one leading it by a quarter cycle. The magnitude of these components depend on the material and the frequency of excitation.

The complex modulus of a material is defined as

$$E^{*} = E' + iE''$$

where $E^{*}$ = Complex modulus ;
$E'$ = Storage modulus and
$E''$ = Loss modulus

For FRP materials both the component of the modulus depend very strongly on vibration frequency. For purposes of dynamic analysis, it is desirable to know the complex modull over a wide range of frequency. But in laboratory, it is difficult to obtain its accurate values at very high frequency. With the available instruments, it is possible to carry out test at specified strain rates (machine grips separation rate). The corresponding material properties are given in Table 5.7. These results indicate that values fluctuate with increasing strain rates. To get reliable data, many more coupon tests are necessary. With accurate instrumentation, material parameters can be obtained much more reliably and used in the finite element program to obtain a better prediction of the plate behaviour.

Table 5.7: Material properties of the plate at different strain rates or deformation rates.

**Table 5.7**

| Strain rate mm/min. | $E_1$ in $N/mm^2$ | $E_2$ in $N/mm^2$ | $\mu_{12}$ | $G_{12}$ in $N/mm^2$ |
|---|---|---|---|---|
| 0.2 | 29160 | 20000 | 0.26 | 3877.0 |
| 1.0 | 23600 | 19333 | .154 | 5133.0 |
| 1.5 | 18500 | 17000 | 0.18 | 4413.0 |
| 10.0 | 21500 | 18500 | .168 | - |

If clamping is not proper, natural frequency can be widely different from the correct result. On the other hand, if the fixity is not uniform, torsion will develop and the plate will show different natural frequencies.

In the present test, clamping was done using several C-clamps. So amount of fixity achieved can not be assessed. Tests were carried out on plate with aspect ratio 1.0 and going through 0.8 and 0.6 and back to 1.0 again. It was found that frequencies are almost the same in both the occasions. All the tests are carried out in the same day.

Only one plate is tested for free vibration case. As hand lay-up technique was used to fabricate the plate, wide variation in terms of homogenity, thickness, density is possible. So testing many plates require, material constants for each plate separately. That is why the same test is repeated several times to arrive at the accurate results.

## 5.11 Conclusion

Experimental investigations are carried out to study the behaviour of laminated plates under static loadings and free vibration. Only clamped boundary conditions are studied. Plates are fabricated using glass fiber (three layers of woven mat) in epoxy. Hand lay-up technique is used to cast the plates.

Plates are tested under static loadings (point load as well as u.d.l.). Deflections are measured at various points. These values are compared with numerical results. Plate behaviour is found to be non-linear nature.

Free vibration of both square and rectangular plates are carried out under clamped boundary condition. Natural frequencies obtained from the experiments are compared with numerical values. Numerical results are found to be higher than that obtained experimantally.

From the results it can be concluded that:

(1)The numerical model should account non-linearity in the material behaviour.

(2)Material parameters should be obtained over a wide range of frequency.

(3)Clamping should be proper and there must be a way to assess the amount of fixity.

# CHAPTER 6

# STATIC BUCKLING OF LAMINATED PLATES

## 6.1 Introduction

Since long, composite materials have been used extensively for tensile loaded structures but lately they found wide application for structures under compression such as wing surfaces, fuselage sections and missile skins. Thus, failure under buckling of these composite structures is a very common phenomenon.

In laminated composite structure, certain ply arrangements or combinations are elastically unsymmetrical about the mid surface so that under in-plane load, the plate will deflect in a bending mode and ultimately will fail under buckling. Initial imperfections can cause buckling of elastically symmetric plates, but it has been shown [126] that such imperfections do not significantly affect the "buckling load".

## 6.2 Survey of literature in the field

The accurate knowledge of critical buckling loads and mode shapes, as well as the subsequent post buckling behaviour, is essential for light weight structural design. Apparently, buckling analysis of orthotropic plates was first

carried out to deal with stiffened isotropic plates [127], and subsequently extensively used to study plywood panels. Equations governing the buckling of laminated composite plates are available in a number of text books [22,26,125,128,129], as well as in technical paper [130]. A brief review of literatures dealing with buckling of laminated plates is presented here. Reissner and Stavsky [23] used the reduced flexural stiffness to calculate the buckling load with classical theory. Ashton and Waddoups [88] utilized the Ritz's technique to find the buckling loads for rectangular plates with various boundary conditions. Whitney and Leissa [89] has extended the work of Reissner and Stavsky [23] by presenting solutions for the transverse vibration and buckling analysis of angle-ply composite plates.

Buckling of simply supported (SSSS) orthotropic plates under uni-axial and/or bi-axial loading was discussed in [131-134] and that under shear in [132-137]. A number of researchers had obtained experimental results. Dickinson [138] had derived a useful buckling formula to predict critical buckling stresses for biaxially loaded orthotropic plates. Buckling of clamped (CCCC) orthotropic plates was studied in [133-136,139-141]. Several other studies, both theoretical and experimental, were devoted to anti-symmetric laminated plates with various edge conditions.

Whitney and Leissa [89] observed that the effect of bending-extension coupling stiffnesses on the buckling load of an anti-symmetric laminate rapidly decreases to zero as the number of layers increases. Jones [93] showed the same coupling effect on buckling loads of a special class of unsymmetic cross-ply laminate decreases very slowly as the number of layers increases. Housner and Stein [136] used a finite difference energy method to make parametric studies

for angle-ply, graphite-epoxy plates having a large number of alternate ($\mp\ \theta$) plies and with either simply supported (SSSS) or Clamped (CCCC) edges. They concluded that

(1) The critical buckling stress is maximized for plies having $\mp\theta$ of approximately $45^{\circ}$.

(ii) A range of fiber orientations exists for which the buckling stress of the graphite - epoxy plates exceeds that of an equal weight, aluminium plate having the same planer dimension(a and b) and boundary conditions.

Fogg [135] obtained another extensive set of results for uniaxial compression and shear buckling of SSSS anisotropic plate. Srinivas et al [20] have presented a unified exact buckling analysis for thick lamiantes. Phan and Reddy [21] has used a higher order shear deformation theory to give stability analysis of laminated anisotropic composite plates. A comprehensive literature survey dealing with the buckling of composite plates is given by Leissa [142].

## 6.3 Formulation of the linear buckling problem

The potential energy of an elastic system consists of the potential energy of internal and external forces. The potential energy of internal forces is the strain energy U and the potential energy of external forces is the negetive work of the external forces $W_e$ thus

$$V = U - W_e \tag{6.1}$$

The total change in V due to any perturbation from equilibrium can be expanded in terms of infinitesimal variations as

$$\Delta V = \delta V + \delta^2 V + \text{higher order variations.} \qquad (6.2)$$

If, in addition, the external forces at equilibrium are independent of the displacements (perturbations), then $W_e$ is linear in displacements and its second variation is identically zero. Since the first variation $\delta V$ is also zero at equilibrium (principle of stationary potential energy), it is seen immediately that

$$\Delta V = \delta^2 U + \text{higher order variations} \qquad (6.3)$$

and the stability criterion can finally be written as

$$\text{Stable system: } V = \min \Rightarrow \Delta V > 0 \Rightarrow \delta^2 U > 0 \qquad (6.4)$$

Thus the second variation of the strain energy must be positive-definite for stability.

Since buckling involves large deflections, exact strain-displacement relations involving non-linear terms as given by

$$\varepsilon_{ij} = \frac{1}{2}\left[ \frac{\partial u_i}{\partial x_j} + \frac{\partial u_j}{\partial x_i} + \sum_{\alpha=1}^{3} \frac{\partial u_\alpha}{\partial x_i} \frac{\partial u_\alpha}{\partial x_j} \right] \qquad i,j = 1 \text{ to } 3 \qquad (6.5)$$

is to be used to derive the governing equation. The non-linear terms in the strain-displacement equations modify the element stiffness matrix [K], so that

$$[K] = [K_E] + [K_G] \qquad (6.6)$$

The elastic stiffness matrix $[K_E]$ is the same as that used in the linear analysis.

Geometric stiffness matrix $[K_G] = \lambda [K_G^*]$ (6.7)

where $[K_G^*]$ is the geometrical stiffness matrix for unit

value of the applied load.

Substituting Eq. 6.6 in Eq. 6.4, and after simplification one can get

$$([K_E] + \lambda [K_G^*]) \{d\} = \lambda \{P^*\} \tag{6.8}$$

where $\{P^*\}$ represents the relative magnitudes of the applied forces. Eq. 6.8 implies

$$\{d\} = ( [K_E] + \lambda [K_G^*] )^{-1} . \lambda\{P^*\} \tag{6.9}$$

From the formal definition of the matrix inverse as the adjoint matrix divided by the determinant of the co-efficients, it can be noted that the displacements $\{d\}$ tend to infinity when

$$\left| [K_E] + \lambda [K_G^*] \right| = 0 \tag{6.10}$$

Thus it is seen that the linear buckling problem is an eigenvalue problem similar to free vibration one, and the solution procedure is the same.

$[K_E]$ is already derived in chapter 3. $[K_G]$ will be derived using the non-linear terms of Eq. 6.5. as:

Strain energy due to stresses is given by

$$U_\sigma = \int_V [1/2(u,_x^2 + v,_x^2 + w,_x^2)\sigma_{xo} + \ldots\ldots\ldots$$

$$+ (u,_z u,_x + v,_z v,_x + w,_z w,_x)\tau_{zx}]dv \tag{6.11}$$

If we define $\{\delta'\}^T = [\, u,_x \; u,_y \; u,_z \; v,_x \; v,_y \; v,_z \; w,_x \; w,_y \; w,_z \,]^T$

(6.12)

Then Equ.6.11 can be written in the form

$$U_\sigma = 1/2 \int \{\delta'\}^T \begin{bmatrix} s' & o & o \\ o & s' & o \\ o & o & s' \end{bmatrix} \{\delta'\}\, dv \; ; \qquad (6.13)$$

where $$s' = \begin{bmatrix} \sigma_{xo} & \tau_{xyo} & \tau_{xzo} \\ \tau_{xyo} & \sigma_{yo} & \tau_{yzo} \\ \tau_{xzo} & \tau_{yzo} & \sigma_{zo} \end{bmatrix}$$

Assuming that only $\sigma_x, \sigma_y$ and $\tau_{xy}$ can cause buckling, Equ. 6.13 simplifies to

$$U_\sigma = 1/2 \int \{\delta\}^T [\sigma] \{\delta\} dv \text{ where} \qquad (6.14)$$

$$[\sigma] = \begin{bmatrix} s & o & o \\ o & s & o \\ o & o & s \end{bmatrix} \quad \text{and} \quad s = \begin{bmatrix} \sigma_x & \tau_{xy} \\ \tau_{xy} & \sigma_y \end{bmatrix}$$

$$\text{and } \{\delta\}^T = [\, u,_x \; u,_y \; v,_x \; v,_y \; w,_x \; w,_y \,] \qquad (6.15)$$

Differentiating the displacement functions given in Equ. 3.12 w.r.t. x, y and z, we get

$$u,_x = u_{o,x} + z\phi_{xo,x} + c_1\phi_{xo,x} + c_1 w,_{xx} \; ; \; u,_y = u_{o,y} + z\phi_{xo,y} + c_1\phi_{xo,y} + c_1 w,_{xy}$$

$$v,_x = v_{o,x} + z\phi_{yo,x} + c_1\phi_{yo,x} + c_1 w,_{yx} \; ; \; v,_y = v_{o,y} + z\phi_{yo,y} + c_1\phi_{yo,y} + c_1 w,_{yy}$$

$$w,_x = w_{o,x} \; ; \; w,_y = w_{o,y} \quad \text{where } c_1 = -(4z^3)/(3t^2) \qquad (6.16)$$

Thus

$$\{\delta\}=\begin{Bmatrix} u_{,x} \\ u_{,y} \\ v_{,x} \\ v_{,y} \\ w_{,x} \\ w_{,y} \end{Bmatrix}=\begin{bmatrix} u_{o,x}+z\phi_{xo,x}+c_1\phi_{xo,x}+c_1 w_{,xx} \\ u_{o,y}+z\phi_{xo,y}+c_1\phi_{xo,y}+c_1 w_{,xy} \\ v_{o,x}+z\phi_{yo,x}+c_1\phi_{yo,x}+c_1 w_{,yx} \\ v_{o,y}+z\phi_{yo,y}+c_1\phi_{yo,y}+c_1 w_{,yy} \\ w_{o,x} \\ w_{o,y} \end{bmatrix}=[A]\begin{Bmatrix} u_{o,x} \\ u_{o,y} \\ v_{o,x} \\ v_{o,y} \\ \phi_{xo,x} \\ \phi_{yo,x} \\ \phi_{xo,y} \\ \phi_{yo,y} \\ w_{,x} \\ w_{,y} \\ w_{,xx} \\ w_{,xy} \\ w_{,yy} \end{Bmatrix}=[A]\{d'\} \qquad (6.17)$$

where

$$[A]=\begin{bmatrix} 1 & o & o & o & z+c_1 & o & o & o & o & o & c_1 & o & o \\ o & 1 & o & o & o & o & z+c_1 & o & o & o & o & c_1 & o \\ o & o & 1 & o & o & z+c_1 & o & o & o & o & o & c_1 & o \\ o & o & o & 1 & o & o & o & z+c_1 & o & o & o & o & c_1 \\ o & o & o & o & o & o & o & o & 1 & o & o & o & o \\ o & o & o & o & o & o & o & o & o & 1 & o & o & o \end{bmatrix}$$

and

$$\{d'\}=\begin{Bmatrix} u_{o,x} \\ u_{o,y} \\ v_{o,x} \\ v_{o,y} \\ \phi_{xo,x} \\ \phi_{yo,x} \\ \phi_{xo,y} \\ \phi_{yo,y} \\ w_{,x} \\ w_{,y} \\ w_{,xx} \\ w_{,xy} \\ w_{,yy} \end{Bmatrix} = \begin{bmatrix} N_{1,x} & o & o & o & o & o & o & \cdots \\ N_{1,y} & o & o & o & o & o & o & \cdots \\ o & N_{1,x} & o & o & o & o & o & \cdots \\ o & N_{1,y} & o & o & o & o & o & \cdots \\ o & o & N_{1,x} & o & o & o & o & \cdots \\ o & o & o & N_{1,x} & o & o & o & \cdots \\ o & o & N_{1,y} & o & o & o & o & \cdots \\ o & o & o & N_{1,y} & o & o & o & \cdots \\ o & o & o & o & f_{1,x} & g_{1,x} & h_{1,x} & \cdots \\ o & o & o & o & f_{1,y} & g_{1,y} & h_{1,y} & \cdots \\ o & o & o & o & f_{1,xx} & g_{1,xx} & h_{1,xx} & \cdots \\ o & o & o & o & f_{1,xy} & g_{1,xy} & h_{1,xy} & \cdots \\ o & o & o & o & f_{1,yy} & g_{1,yy} & h_{1,yy} & \cdots \end{bmatrix} \begin{bmatrix} u_{o1} \\ v_{o1} \\ \phi_{xo1} \\ \phi_{yo1} \\ w_{o1} \\ w_{o,x1} \\ w_{o,y1} \\ \cdot \\ \cdot \\ \cdot \\ \cdot \\ w_{o,x4} \\ w_{o,y4} \end{bmatrix}$$

or $\{d'\}=[B]\{d\}$ (6.18)

i.e. $\{\delta\}=[A]\{d'\}=[A][B]\{d\}=[C]\{d\}$ (6.19)

Substituting Equ. 6.19 in Equ. 6.14, we get

$$U_\sigma = \frac{1}{2}\int_V \{\delta\}^T[\sigma]\{\delta\}dV = \frac{1}{2}\int_V \{d\}^T[C]^T[\sigma][C]\{d\}\ dV$$

$$= \frac{1}{2}\int_V \{d\}^T[B]^T[A]^T[\sigma][A][B]\ \{d\}\ dV$$

$$= \frac{1}{2}\int_A \{d\}^T[B]^T\left(\int_z [A]^T[\sigma][A]\ dz\right)[B]\{d\}\ dA$$

$$= \frac{1}{2}\int_A \{d\}^T\ [B]^T[D][B]\ \{d\}\ dA \Rightarrow [K_G] \equiv \int_A [B]^T[D][B]\ dA$$

where $[D] = \int_z [A]^T [\sigma] [A] \, dz$ (6.19)

The matrix [D] can be written in explicit form as

$[D] =$

$$\begin{bmatrix}
K_{G11} & K_{G12} & 0 & 0 & K_{G15} & 0 & K_{G17} & 0 & 0 & 0 & K_{G111} & K_{G112} & 0 \\
 & K_{G22} & 0 & 0 & K_{G25} & 0 & K_{G27} & 0 & 0 & 0 & K_{G211} & K_{G212} & 0 \\
 & & K_{G33} & K_{G34} & 0 & K_{G36} & 0 & K_{G38} & 0 & 0 & 0 & K_{G312} & K_{G313} \\
 & & & K_{G44} & 0 & K_{G46} & 0 & K_{G48} & 0 & 0 & 0 & K_{G412} & K_{G413} \\
 & & & & K_{G55} & 0 & K_{G57} & 0 & 0 & 0 & K_{G511} & K_{G512} & 0 \\
 & & & & & K_{G66} & 0 & K_{G68} & 0 & 0 & 0 & K_{G612} & K_{G613} \\
 & & & & & & K_{G77} & 0 & 0 & 0 & K_{G711} & K_{G712} & 0 \\
 & & & & & & & K_{G88} & 0 & 0 & 0 & K_{G812} & K_{G813} \\
 & & & & & & & & K_{G99} & K_{G910} & 0 & 0 & 0 \\
 & & & & & & & & & K_{G1010} & 0 & 0 & 0 \\
 & & & & & & & & & & K_{G1111} & K_{G1112} & 0 \\
 & & & & \text{Symmetric} & & & & & & & K_{G1212} & K_{G1213} \\
 & & & & & & & & & & & & K_{G1313}
\end{bmatrix}$$

where

$K_{G11}=N_x$ ; $K_{G12}=N_{xy}$ ; $K_{G15}=M_x+cP_x$ ; $K_{G17}=M_{xy}+cP_{xy}$ ; $K_{G111}=cP_x$ ; $K_{G112}=cP_{xy}$ ;

$K_{G22}=N_y$; $K_{G25}=M_{xy}+cP_{xy}$; $K_{G27}=M_y+cP_y$; $K_{G211}=cP_{xy}$; $K_{G212}=cP_y$

$K_{G33}= N_x$ ; $K_{G34}= N_{xy}$ ; $K_{G36}= M_x+cP_x$ ; $K_{G38}= M_{xy}+cP_{xy}$ ; $K_{G312}=cP_x$; $K_{G313}=cP_{xy}$

$K_{G44}= N_y$ ; $K_{G46}= M_{xy}+cP_{xy}$ ; $K_{G48}= M_y+cP_y$ ; $K_{G412}=cP_{xy}$ ; $K_{G413}=cP_y$ ;

$K_{G55}=S_x+c^2T_x+2cR_x$; $K_{G57}=S_{xy}+c^2T_{xy}+2cR_{xy}$; $K_{G511}=cR_x+c^2T_x$; $K_{G512}=cR_{xy}+c^2T_{xy}$;

$K_{G66}=S_x+c^2T_x+2cR_x$; $K_{G68}=S_{xy}+c^2T_{xy}+2cR_{xy}$; $K_{G612}=cR_x+c^2T_x$; $K_{G613}= cR_{xy}+c^2T_{xy}$;

$K_{G77} = S_y + c^2 T_y + 2cR_y$ ; $K_{G711} = cR_{xy} + c^2 T_{xy}$ ; $K_{G712} = cR_y + c^2 T_y$ ;

$K_{G88} = S_y + c^2 T_y + 2cR_y$ ; $K_{G812} = cR_{xy} + c^2 T_{xy}$ ; $K_{G813} = cR_y + c^2 T_y$ ;

$K_{G99} = N_x$ ; $K_{G910} = N_{xy}$ ;

$K_{G1010} = N_y$ ;

$K_{G1111} = c^2 T_x$ ; $K_{G1112} = c^2 T_{xy}$ ;

$K_{G1212} = c^2 (T_x + T_y)$ ; $K_{G1213} = c^2 T_{xy}$ ;

$K_{G1313} = c^2 T_y$.

$$c = -\frac{4}{3t^2} ;$$

The other symbols have the following meanings

$$(N_x, M_x, S_x, P_x, R_x, T_x) = \int_z \sigma_x (1, z, z^2, z^3, z^4 \text{ and } z^6) dz$$

$$(N_y, M_y, S_y, P_y, R_y, T_y) = \int_z \sigma_y (1, z, z^2, z^3, z^4 \text{ and } z^6) dz$$

$$(N_{xy}, M_{xy}, S_{xy}, P_{xy}, R_{xy}, T_{xy}) = \int_z \tau_{xy} (1, z, z^2, z^3, z^4 \text{ and } z^6) dz$$

## 6.4 Numerical examples

The object of this section is to use geometrical stiffness of rectangular element developed in this chapter for the stability analysis of orthotropic and laminated plates with simply supported boundary conditions and under in-plane loads.

**EXAMPLE 6.1:** A simply supported square orthotropic plate under uniform normal stress $N_x$ as shown in Fig. 1.8(a) on edges x = 0 and x = a. values of asymptotic $k_x$ for various h/b ratios are given in Table 6.1.

A good agreement is observed with the results obtained by exact theory. All these values are obtained from Table 9 of ref. [20].

---

Orthotropic plate material properties are given in Fig. 1.8(a). The ratio of h/b is varied from 0.05 to 0.2.

**Table 6.1:** Asymptotic $k_x$ for buckling of homogenous orthotropic square plates under uniform normal stress $p_x$ on edges x=0 and a.

**Table 6.1**

| h/b | Present | Exact | Mindlin | Thin plate | % error from exact |
|---|---|---|---|---|---|
| .05 | 2.9662 | 2.966 | 2.965 | 3.039 | .006 |
| .10 | 2.7695 | 2.770 | 2.768 | 3.039 | .016 |
| .20 | 2.260 | 2.210 | 2.204 | 3.039 | 2.26 |

$$p_x = \frac{N_x}{h} \quad \text{and} \quad k_x = (P_{x_{cri}}/E)(12/\pi^2)(b/h)^2$$

**EXAMPLE** 6.2: Rectangular plate under similar loading condition as given above is considered. Variation of buckling stress parameter $k_x$ with h/b and a/b is given in Table 6.2 and Fig. 6(a).

Table 6.2

| a/b | h/b | | |
|---|---|---|---|
| | 0.05 | 0.10 | 0.20 |
| 0.5 | 5.21 | 4.39 | 2.72 |
| 1.2 | 2.884 | 2.750 | 2.336 |
| 1.4 | 2.979 | 2.8647 | 2.496 |
| 1.6 | 3.176 | 3.0697 | 2.664 |
| 1.8 | 3.450 | 3.3459 | 2.541 |
| 2.0 | 3.787 | 3.5174 | 2.445 |
| 2.2 | 3.709 | 3.2844 | 2.375 |
| 2.4 | 3.478 | 3.1133 | 2.326 |
| 2.6 | 3.315 | 2.9906 | 2.296 |
| 2.8 | 3.200 | 2.9042 | 2.282 |
| 3.0 | 3.127 | 2.8486 | 2.281 |
| 3.2 | 3.085 | 2.8164 | 2.294 |
| 3.4 | 3.069 | 2.8068 | 2.316 |
| 3.6 | 3.077 | 2.8124 | 2.348 |
| 3.8 | 3.097 | 2.8349 | 2.390 |
| 4.0 | 3.134 | 2.8699 | 2.440 |

**EXAMPLE** 6.3: A three-ply laminate with identical top and bottom plies (Fig. 1.8(b)) is considered under similar loading as given in example 6.1. Elastic moduli of top and bottom layers are same as above. Middle layer material properties are related to top or bottom layer material property by

$$\beta = \frac{E_{x_1}}{E_{x_2}} = \frac{E_{x_3}}{E_{x_2}} \; ; \; \mu = \frac{P_{x_i}}{E_{x_i}} \quad (i=1,2,3) \; ; \; k_x = 12\mu\left(\frac{b}{h}\right)^2/\pi^2$$

$$\frac{h_1}{h} = 0.1 \; ; \; \frac{h_2}{h} = 0.8 \text{ and } \frac{h}{b} = 0.1$$

In Table 6.3, the asymptotic value of $k_x$ is given for three ply laminates. Elastic moduli for all plies are as given in the above example. Top and bottom plies are identical. Corresponding plot is given in Fig. 6(b).

**Table 6.3**

| $\beta$ | Author's | Exact value | Thin plate | % Error from Exect |
|---|---|---|---|---|
| 1 | 2.7695 | 2.770 | 3.039 | 0.018 |
| 2 | 3.3365 | 3.330 | 3.768 | 0.190 |
| 5 | 4.0922 | 4.046 | 4.984 | 1.140 |
| 10 | 4.3477 | 4.200 | 5.852 | 3.520 |
| 15 | 4.3036 | 4.037 | 6.263 | 6.600 |

**EXAMPLE 6.4:** Buckling of an anti-symmetric cross-ply square plates subjected to in-plane uniaxial compressive loads (Fig 1.8(c)). Material properties are same as of material II of example 4.2. The buckling loads as a function of modular ratio of anti-symmetric cross-ply plates are presented in Table 6.4 and the corresponding plot is in Fig. 6(c).

**Table 6.4**

| $\frac{E_1}{E_2}$ | CPT | HSDT [21] | 3-D Elasticity [143] | Author's | % error from 3-D value[143] |
|---|---|---|---|---|---|
| 3 | 5.7538 | 5.1143 | 5.2944 | 5.220 | 1.41 |
| 10 | 11.492 | 9.7740 | 9.7621 | 9.125 | 6.53 |
| 20 | 19.712 | 15.298 | 15.0191 | 14.004 | 6.76 |
| 30 | 27.936 | 19.957 | 19.3040 | 18.245 | 5.49 |
| 40 | 36.160 | 23.340 | 22.8807 | 21.976 | 3.95 |

where ($\lambda_b = N_{xo}.\ a^2/E_2h^3$)

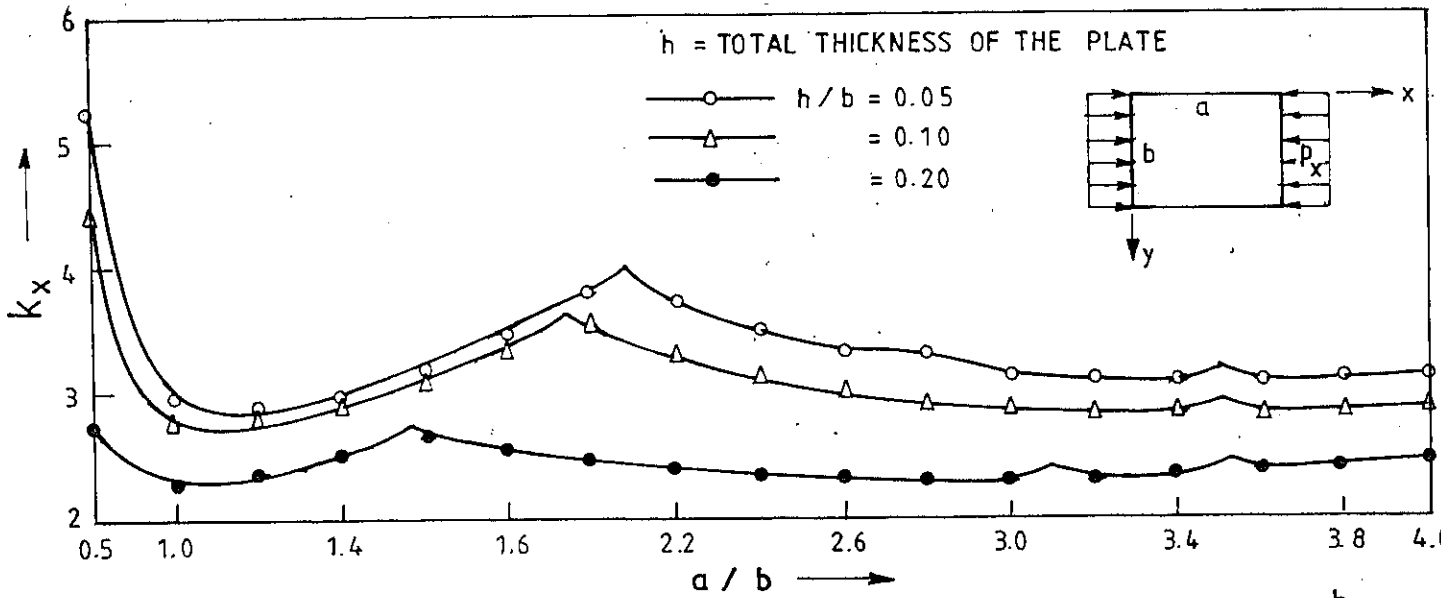


FIG. 6(a) VARIATION OF BUCKLING STRESS PARAMETER $k_x$ WITH $h/b$ AND $a/b$ FOR PLATE LOADED ON $x = 0, a$

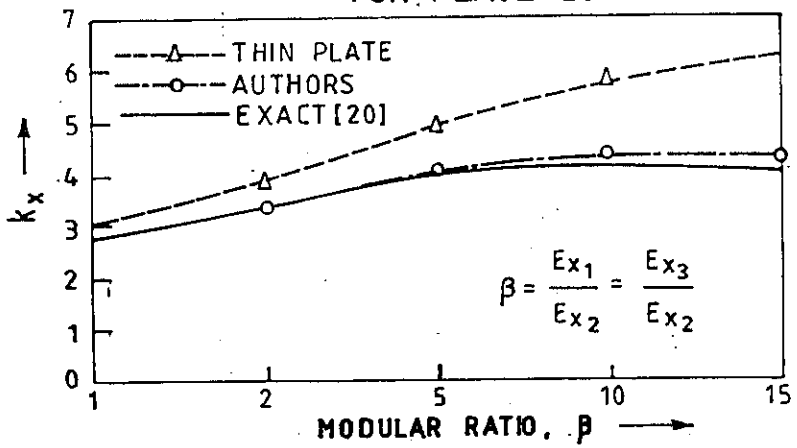


FIG. 6(b) EFFECT OF MODULAR RATIO

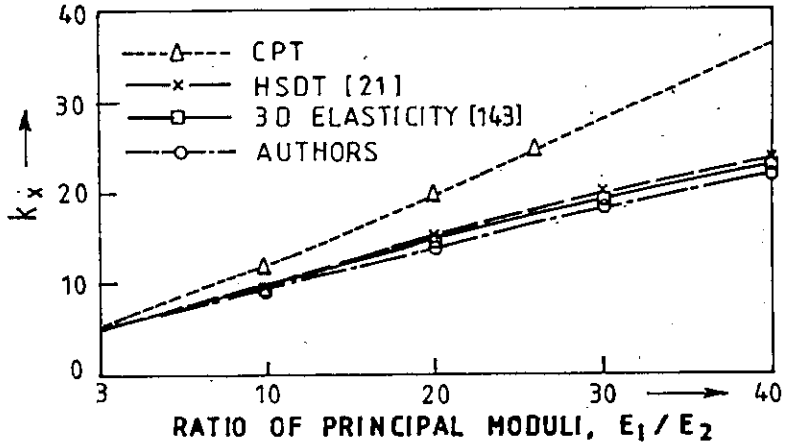


FIG. 6(c) EFFECT OF MATERIAL ANISOTROPY (0°/90°/90°/0°), SQUARE PLATE, ($a/h$=10)

## 6.5 Discussion

A comparison of the buckling loads obtained using present element and the available literature valuesfor the examples given herein indicates that a good agreement, even with a relatively coarse discretization of the plate is achievable using the present element.

In Table 6.1 and 6.2, the asymptotic values of the buckling stress parameter $k_x$ are given for homogenous orthotropic plates with h/b= 0.05, 0.1 and 0.2. In Table 6.3, the same is given for three-ply laminates. In Fig. 6(a), a system of curves are obtained. For long plate $k_x$ remains constant and does not change with a/b ratio. It can be seen that the factor $k_x$ is equal to 2.4, 2.8 and 3.0 for h/b = 0.2, 0.1 and 0.05 respectively for a number of a/b ratios. From these data the following observations on buckling of orthotropic plates and laminates may be made.

(i)Thin plate theory that ignores the effect of transverse shear deformation, predicts higher buckling loads than that by shear deformation theories.

(ii)Mindlin theory as well as the theory presented in this thesis yield accurate buckling stresses even for thick homogenous plates.

(iii)Modular ratio of plies has significant effect on the error in buckling stress due to the assumption of thin plate theory. It is also observed that the errors increase as moduli of outer plies are increased.

Critical buckling load of a four layer $[0^\circ/90^\circ/90^\circ/0^\circ]$ cross-ply plate is compared with the three-dimensional linear elasticity solutions. As in the case of static deflection and

free vibration, shear deformation effect is more significant for material with high degree of anisotropy. The buckling stress parameter, $k_x$, as a function of degree of orthotropy of anti-symmetric cross-ply and angle-ply plates are plotted in Fig. 6(c). It is confirmed by other investigators, that the coupling effect on the buckling loads is more pronounced with the increasing degree of anisotropy.

## 6.6 Conclusion

The finite element developed in this thesis is extended to the study of orthotropic and laminated plates. Geometrical stiffness matrix of the plate element is obtained in presence of $\sigma_x$, $\sigma_y$ and $\tau_{xy}$ only. Effect of a number of parameter on critical buckling load is determined. From the results presented in Tables 6.1 to 6.4, following conclusions can be made:

(1)CPT over estimates buckling stress as this theory ignores transverse shear effect.

(2)Mindlin's theory as well as the present theory predicts very accurate results.

(3)Buckling stress parameter decreases with the increase of thickness-to-length ratios.

(4)With the increase of modular ratio, critical buckling load increases for both symmetric and anti-symmetric laminates.

# CHAPTER 7

# MATERIAL DEVELOPMENT

## 7.1 Introduction

Plates tested in chapter 5 are fabricated using glass fibers embeded in a matrix of epoxy. Epoxy is a good adhesive but very expensive. So, the search is on for alternate matrix and fiber to obtain an efficient composite based on following criteria:

(1) materials should be available locally and easily;

(2) materials should be less expensive.

Thus the development of a new material was considered to be a part of this research program.

In general, fibers can be classified as follows:

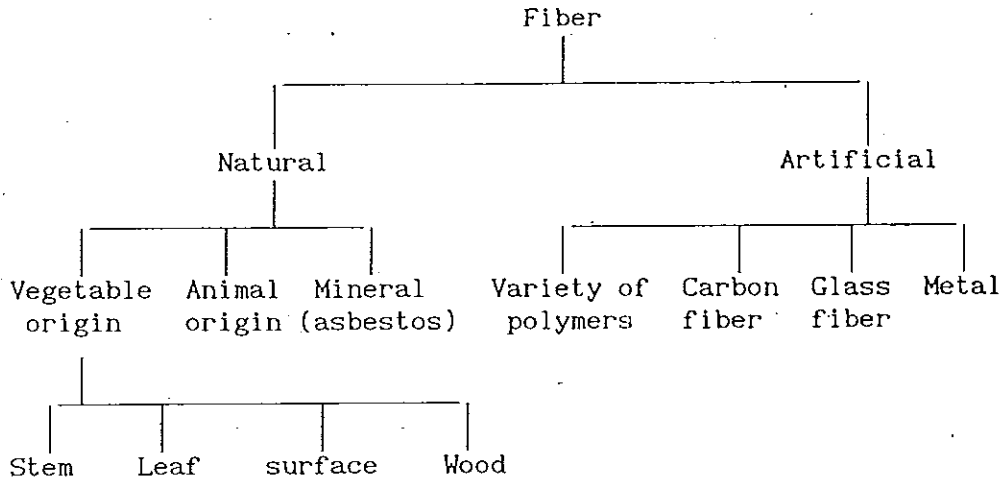


Typical mechanical properties of some common natural and artificial fibers are given below:

| Natural | | Artificial | |
|---|---|---|---|
| Fibers | Ultimate tensile strength (GPa) | Fibers | Ultimate tensile strength (GPa) |
| Sisal | 0.278 | E-glass | 3.50 |
| Flax | 0.340 | S-glass | 4.90 |
| Jute | 0.217 | Z-glass | 1.65 |
| Elephant grass | 0.180 | Asbestos | 2.80 |
| Water seed | 0.70 | Boron | 2.10 |
| Bamboo strip | 0.350 | Carbon | 2.80 |

Traditionally, thermoset polymers have been used as a matrix material for fiber reinforced composites. Plastics are organic materials with very high molecular weights, constructed from simpler repeating units under suitable conditions of temperature and catalytic action. Because of their amorphous nature, most plastics are characterised by low elastic moduli. They all have low specific gravities and high co-efficients of thermal expansion. There are two kinds of plastics:

(1) thermoplastics;

(2) thermosetting plastics.

Thermoplastics consist of linear polymer molecules which are not interconnected. Because of their unconnected chain structure, thermoplastics may be repeatedly softened and hardened by heating and cooling respectively; with each repeated cycle, however, the material tends to become more brittle. Because of this characteristics, these materials are not generally used as matrix for composite construction.

Thermosetting plastics initially occur in liquid or semi-liquid form and then harden irreversibly. This chemical reaction is known as polymerisation. On completion of this reaction, the material can not be softened or made plastic again without change of molecular structure. Though unreinforced thermosetting plastics are not suitable for structural elements but when reinforced with fibers, they form composites which possess adequate load-bearing capacity.

Most of the common plastics used in construction can be grouped as

thermoplastic - PVC; Acrylic; Polystyrenes;
thermosetting plastic - Polyester; Epoxy; Polyrethane; Phenolics.

Epoxides are very costly and have a long cure time. Polyesters and vinyl esters suffer from high volumetric shrinkage. Being relatively cheap, phenol-formaldyhyde isused as the matrix in the present study along with jute as the fiber. A brief description of this fiber is given below.

## 7.2 Jute fiber

The process involved in obtaining jute fiber is given in third paragraph of section 1.4.

For the preparations of this composite, jute in the form of woven fabric has been used.

On the average, jute contains the following constituents:

**Chemical composition of jute fiber**

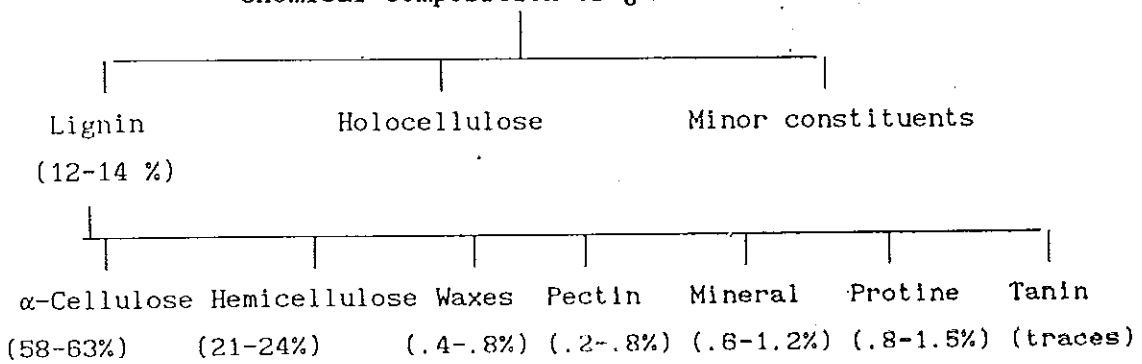

Physical composition of Jute fiber

Length/breadth ≅ 110 ; Filament gravity fineness (Tex) ≅ 1.25-4.0

Extension at break (%) = 1.5 ; Density = 1.445 gm/cc ;

Moisture regain (%) at 65% relative humidity = 12.0

Swelling of Jute in water : 23% in diameter and 40% in cross-section.

## 7.3 Matrix

The most important thermosetting resins suitable for commerical application, are formaldehyde which is a condensation product with phenol(phenolic resins) or with urea or melamine (amino resins).

Phenolic resins have been used commercially longer than any other synthetic polymer except cellulose nitrate. A number of industrial applications are based on the excellent adhesive properties and bonding strength of the phenolics. Phenol-formaldehyde (Pf) is widely used as resin in the manufacture of plastics laminates. Some of the important characteristics are listed below :

(1) The reinforced Pf, especially laminates and resin-wood products are strong and being light, possess high specific strength.

(2) Pf is thermosetting and organic polymer. The former allows applications extending over a considerable temperature range, whilst the latter fixes the upper limit. Mineral fibers improve the heat resistance of phenolic composities.

(3) Pf has good electrical insulating properties. These plastics are very suitable for use in the field of electrical insulation, particularly for standard fittings and components.

(4) Chemical inertness of Pf results in its applications in the construction of Chemical plants where contact with acids, organic solvents and to a lesser extent mild alkalies, is contemplated. It does not corrode and is not attacked by fungi. Thus, especially when combined with suitable fillers, phenolic resins have good chemical and thermal resistance, dielectric strength and dimensional stability. Products made with these resins are inherently low inflamable, creep resistant and low moisture absorbants.

## 7.4 Procedures

Following procedures are adopted in casting the plates

(1) Jute fabric is cut to the required size according to the size of the mould available in laboratory (14cm X 14cm).

(2) Phenol formaldehyde solution (60% solid content) is poured in a tray. Six layers of jute fabrics are soaked into the solution one over another.

(3) Jute fabric is allowed to soak in the solution for fifteen minutes.

(4) The phenol formaldehyde resin impregnated jute fabric is placed in another tray and a roller is used on it to squeeze out excess phenol formaldehyde resin.

(5) Phenol formaldehyde impregnated jute fabric is oven dried at $80^{o}C$ for 30 minutes.

(6) After drying, the phenol formaldehyde impregnated jute fabric is enclosed in two aluminium foils and transfered to the mould which is then placed in the hydraulic press (photo 2.c.).

(7) Pressure of 1.5 tonnes per square inch applied intermittently (apply and release for 6 times), each time for 10-12 seconds. The pressure is kept at 1.5 $t/in^{2}$ and the temperature is raised to $150^{o}C$ and kept for 40 minutes.

(8) At the end of 40 minutes, supply of heat is stopped and the plattens are cooled by passing a jet of cold water through them without releasing the pressure.

(9) The pressure is then released and the mould is removed from the hydraulic press when it becomes sufficiently cold.

(10) The plate is then pulled out from the mould.

## 7.5 Observations and results

### 7.5.1 Cost analysis

For this purpose three plates are casted using steel mould (7.5cm X 2.5cm)

Amount of material and the cost involved per plate are:

Weight of fiber = 3.0938 gm/layer

Weight of matrix = 2.6150 gm/layer

Cost of jute fabric = Rs. 15.00/$m^{2}$

Cost of matrix = Rs. 60.00/kg.

∴ Cost of jute/plate = (15 X 7.5 X 2.5 X 6)/10000
= Rs. 0.1688 per plate

Cost of matrix = (2.615 X 60)/1000
= Rs. 0.1569 per plate

∴ Total cost = Rs.0.3257

Area of the plate = 18.75 $cm^2$

∴ Cost of 1 $m^2$ plate = Rs. 174.00

This cost does not include the cost of using the hydraulic press.

Cost of glass reinforced plastics is estimated to be Rs. 795 /$m^2$.

### 7.5.2 Mass density

Mass density of the jute reinforced plastic material is determined using mercury displacement method. Observations are given in Table 7.1 below.

**Table 7.1**

| Sample no. | Weight (gm) | Volume (cc) | Density (gm/cc) |
|---|---|---|---|
| 1 | 2.36 | 2.2 | 1.07 |
| 2 | 2.73 | 2.4 | 1.14 |
| 3 | 2.42 | 2.2 | 1.10 |

Average density = 1.1 gm/cc.

### 7.5.3: Material properties

Two coupons are cut from the plate and tested under uni-axial tension. The geometry of the coupons is given in Fig. 7.1.b. Average stress-strain curve is plotted in Fig. 7.1.a. Poisson's ratio variation with loading is given in Fig. 7.1.c.

From the stress-strain curve, initial modulus of elasticity can be seen to be 37.8 $N/mm^2$. Ultimate strength is 14.30 $N/mm^2$.

## 7.6 Discussion

Characterization of fiber reinforced composites require the development of a broad range of information that is largely a function of the end application. Many of these properties are strong functions of temperature and moisture content. Therefore, each of these properties must be characterized for temperature and moisture content over the range of interest.

The new material conceived in this chapter, should be tested to obtain all possible information. But in this present thesis, only a part of it is considered and the results are given in Table 7.1 and Fig. 7.1.

Mass density of jute reinforced plastics (JRP) is 1.1 gm/cc, which is less than 1/2 that of glass reinforced plastics (GRP) as given in Table 5.5. Strength of JRP is around 1/10 th that of GRP. Cost ratio is around 1/5 th that of GRP.

Shape and geometry of the coupons used to obtain material properties of JRP are so taken that length/width ratio of the middle portion is maximum. This will reduce the end constraint effect as discussed in chapter 5. It is found that fractures of both the coupons have taken place in the middle portion under uniaxial tension. The maximum length of the coupon that can be obtained in the laboratory is 14 cm.

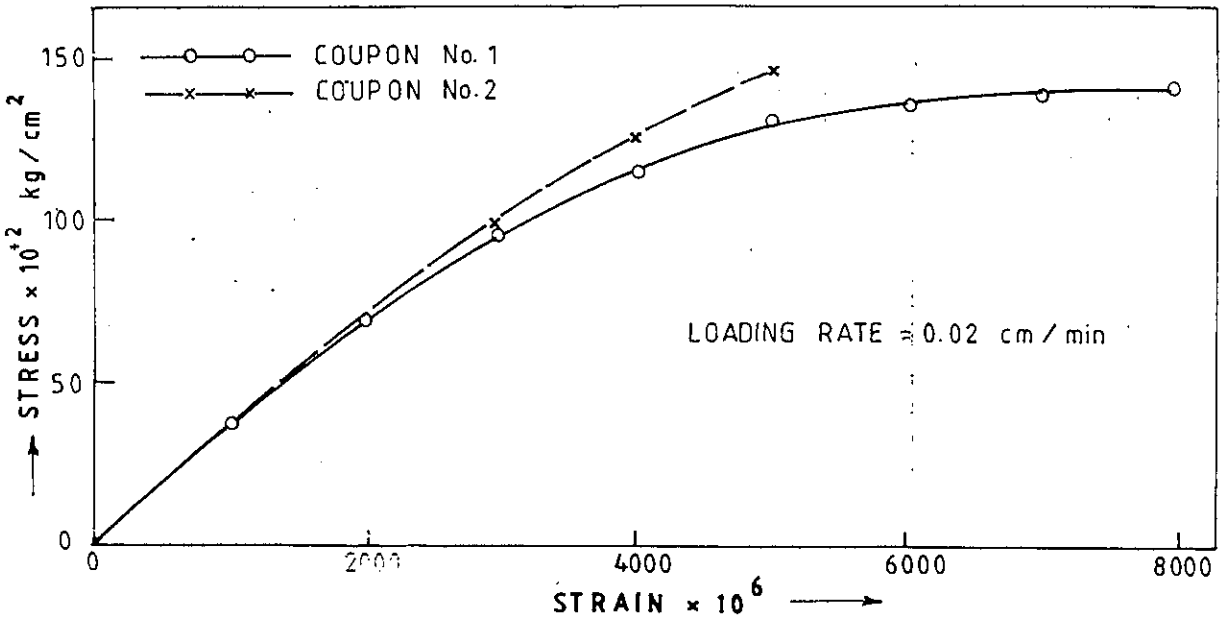


FIG. 7(a) STRESS STRAIN CURVE ( Jute reinforced plastics )

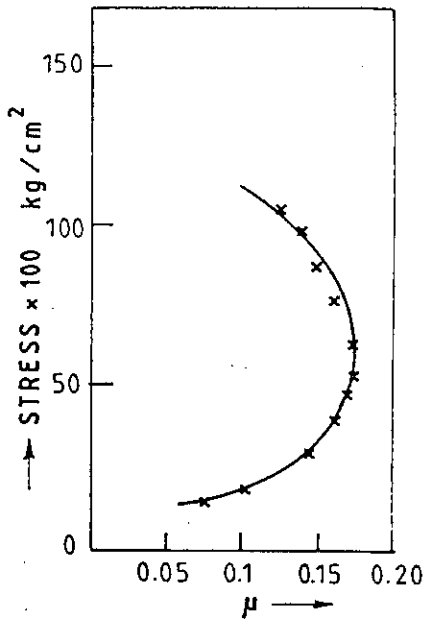


FIG.7(c) VARIATION OF POISSON'S RATIO WITH STRESS

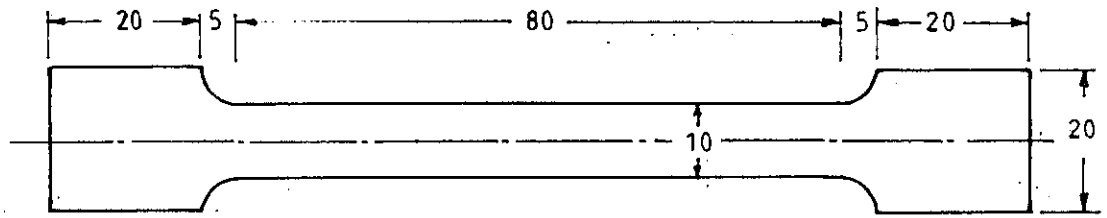


Thickness = 4.30 mm
dimens. in mm

FIG.7(b) JUTE REINFORCED PLASTIC COUPON

The stress-strain curve shows that the modulus of elasticity of the composite is quite low. The behaviour of this material is found to be non-linear for most part of the loading history. It is observed from the Fig. 7.1(c) that Poisson's ratio is low at low stress level and increases with the increase of stress to a certain limit and then the ratio falls.

## 7.7 Conclusion

A new composite is conceived which may eventually substitute some of the existing composites viz. plywood, timber and many other expensive FRPs. Natural fiber like jute is present in abundance in this region. Jute fiber in the form of woven mat is embedded in a matrix of phenol formaldehyde, a cheap resin, to fabricate the composite. Only few tests are conducted. Results are encouraging specially for the fact that this composite is very light. In regards to its stiffness and strength, it is possible to use better variety of jute fiber to arrive at higher stiffness and strength values.

# CHAPTER 8

# SUMMARY, CONCLUSION AND SCOPE FOR FUTURE RESEARCH

## 8.1 Summary

A simple four noded rectangular element is developed to analyse the behaviour of laminated and sandwich plates under a variety of loading conditions. The major findings of this work includes:

(1)Classical Plate Theory (CPT) ignores transverse shear effect, which results in lower deflection values, higher frequencies as well as higher buckling stress than by the theory adopted in present work;

(2)in static analysis, it is noticed that in-plane normal and shear stresses are predicted more accurately than transverse shear stresses;

(3) it is found that with the increase of number of layers in the plate, coupling effect reduces and frequency value increases;

(4)Bert [99] has presented in his investigation that with the increase of lamination angle in a plate, frequency increases and reaches maximum value for $\theta=45^{o}$ for N>2, a/h=10 and a/b=1. It is noticed in the present investigations that with the increase of lamination angle in plates having a/b < 1 and a/h > 10, the fundamental frequency at $\theta=30^{o}$ exceeds the value at $\theta=45^{o}$.

(5)Computed frequencies are found to be higher than corresponding experimental values.

On the basis of this study, the following conclusions may be drawn:

## 8.2 Conclusion

Present finite element predicts the behaviour of laminated and sandwich plates for stiffness, free vibration frequency and buckling stress values satisfactorily.

Composite that is developed in chapter 7 has good potentials but before its recommendation, full characterisation is necessary.

## 8.3 Scope for future research

The investigation carried out here is confined to small deflection behaviour (except the stability analysis) of laminated plates under any system of transverse loading. Solutions have been obtained by finite element techniques using Cyber 840 system. Experiments on glass reinforced plastic plates confirm the applicability of this theory.

During the experimental investigation of plates, it is noticed that the plates undergo considerable deflection. At this stage, the basic assumptions of small deflection theory

does not hold good. The study of large deflection behaviour of laminated plates should be an important field of study.

Although laminated plates are easy to construct, their analysis, in general, is very complex. Specially in the case of thick plates interlayer slip is very pronounced. A description of a basic theory accounting interlayer slip should be an important field of future research.

From the actual testing of composite material in the laboratory, it is found that the material behaves in a non-linear manner throughout the loading history. This demands for an analytical model that can account non-linearity of material behaviour.

Polymers are mostly viscous in character. So, the whole formulation is to be modified using other appropriate constitutive laws to predict the actual behaviour of the composite.

Literature dealing with the response of composite structures due to impact loading is comparatively meagre and experimental investigations are rather scarce. So, a concentrated effort is to be initiated to understand the impact damage of composites through rigorous analyses and meaningful experimentation.

Deformation and stress analysis of laminated plates subjected to hygrothermal effects has been the subject of current research interest. Temperature change can also cause buckling. A systematic study should be conducted to characterise composites over a wide range of temperature and humidity.

# BIBLIOGRAPHY


[1] Whitney, J.M.,"The Effect of Transverse Shear Deformation on Bending of Laminated Plates", J. Comp. Mat.,Vol.3 (July 1969), pp. 534-547

[2] Noor, A.K. and Burton, W.S.,"Assesment of Shear Deformation Theories for Multilayered Composite Plates", Appl. Mech. Rev., Vol.42, No. 1, Jan 1989, pp. 1-12.

[3] Reissner, E.,"Note on the Effect of Transverse Shear Deformation in Laminated Anisotropic Plates, Comput. Methods Appl. Mech. Engin., 20(3), 1979, pp. 203-209.

[4] Whitney, J.M, and Pagano, J.J., "Shear Deformation in Heterogeneous Anisotropic Plates", J. Appl. Mech. 37(4), 1970, pp. 1031-1036.

[5] Whitney, J M, "Stress Analysis of Thick Laminated Composite and Sandwich Plates", J. Compos. Mat. 6(Oct),1972, pp. 426-440.

[6] Yang, P.C, Norris, C.H. and Stavsky, Y., "Elastic Wave Propagation in Heterogeneous Plates", Int. J. Solids Struct, 2, 1966, pp. 665-684.

[7] Dennard, E.H., "The New Approach to Shell Theory: Circular Cylinders", J. Appl. Mech., 20(1), 1953, pp. 33-40.

[8] Mindlin, R.D.,"High Frequency Vibrations of Crystal Plates" Quart. Appl. Math. 19, 1961, pp. 51-61.

[9] Friedrichs,K.O.,and Dressler, R.F., "A Boundary Layer Theory for Elastic Plates", Commun. Pure. Appl. Math., 14, 1961, pp. 1-33.

[10] Johnson, M.W., and Widers, O.E.,"An Asymptotic Theory for the Vibration of Non-Homogeneous Plates", Acta Mech. 12, 1971, pp. 131-142.

[11] Reissner, E.,"On the Theory of Transverse Bending of Elastic Plates", Int. J. Solids Struct., 12, 1976, pp. 545-554.

[12] Kilchevskll, N.A.,"Basic Analytical Mechanics of Shells" English transl. in NASA TT-F-292, 1963.

[13] Pryor, C.W. and Barker, R.M.,"A Finite Element Analysis Including Transverse Shear Effects for Applications to Laminated Plates", AIAA J.,I, 1971, pp. 912-917.

[14] Reddy,J.N.,"A Simple Higher Order Theory for Laminated Composite Plates", J.of Appl. Mech., Dec 1984, Vol.51, pp. 745-752.

[15] Di Sciuva, M.,"Development of An Anisotropic Multi-layered Shear Deformable Rectangular Plate Element", Comp. and Struc., 21, 1985 ,pp. 779-786.

[16] Zienkiewicz,O.C. and Cheung,Y.K.,"The Finite Element Method for the Analysis of Elastic, Isotropic and Orthotropic Slabs", Proc. Inst. of Civil Engrs., 28, 1964, pp. 471-488.

[17] Noor, A. K.,"Free Vibration of Multi-layered Composite Plates", AIAA J., Vol.11, No.7, 1973, pp. 1038-1039.

[18] Reddy, J. N.,"Free Vibration of Anti-Symmetric Angle-ply Laminated Plates Including Transverse Shear Deformation by the Finite Element Method", J. of Sound and Vibration, (1979), 66(4), pp. 565-576.

[19] Kant. T and Mallikarjuna,"Vibration of Unsymmetrically Laminated Plates Analyzed by Using a Higher Order Theory with A $C^{o}$ Finite Element Formulation", J. of Sound and Vibration, (1989), 134(1), pp. 1-16.

[20] Srinivas,S. and Rao,A.K.,"Bending, Vibration and Buckling of Simply Supported Thick Orthotropic Rectangular Plates and Laminates", Int. J. Solids Structures, 1970, Vol.6, pp. 1463-1481.

[21] Phan,N.D. and Reddy,J.N.,"Analysis of Laminated Composite Plates Using a Higher-Order Shear Deformation Theory", Int. J. for Num. meth. in Engg., Vol.21, 1985, pp. 2201-2219.

[22] Lekhnitskii, S.G. "Anisotropic plates", translated from the Russian by S.W.Tsai and T.Cheron, Gordon and Breach, NewYork, 1968.

[23] Reissner. E., and Stavsky, Y., "Bending and Stretching of Certain Types of Heterogenous Aelotropic Elastic Plates", J. of Appl. Mech., Vol.28, No.3, Trans. ASME, Vol.83, Series E, Sept., 1961, pp 402-408.

[24] Stavsky. Y., "Bending and Stretching of Laminated Aelotropic Plates", Proceedings of American Society of Civil Engg.(J. of Engg. Mech. Div.); Vol.87, EM6, Dec. 1961, pp 31-56.

[25] Stavsky. Y., "On the Theory of Heterogenous Anisotropic Plates", Doctor's thesis, M.I.T., Cambridge, Mass,1959.

[26] Ambartsumyan, S.A., **Theory of Anisotropic Plates,** translated from Russian by Cherno,T. and ed. Ashton, J.E., Technomic, 1969.

[27] Reissner.E, "On the Theory of Bending of Elastic Plates," J.Math. Phy, 23, 1944, pp 184-191.

[28] Reissner.E, "The Effect of Transverse Shear Deformations on the Bending of Elastic Plates," J.Appl.Mech.,Trans ASME, Vol 12(1), 1945, pp. A-69 to A-77.

[29] Reissner, E.,"On Bending of Elastic Plates",Q. Appl. Math., 5, pp. 55-68, 1947.

[30] Basset,A.B.,"On the Extension and Flexure of Cylindrical and Spherical Thin Elastic Shells",Phil. Trans. Royal Soc.,(London), Ser. A, 181 (6), pp. 433-480 (1890).

[31] Hildebrand, F.B., Reissner, E. and Thomas, G.B.,"Note on the Foundations of the Theory of Small Displacements of Orthotropic Shells", NACA Tech. Note No. 1833 (Mar 1949).

[32] Hencky, A.,"Uber Die Berucksichtigung Der Schubverzerrung in Ebenen Platten", Ing. Arch., 16, 1947.

[33] Mindlin, R.D., "Influence of Rotarary Inertia and Shear on Flexural Motions of Isotropic Elastic Plates", J. of App. Mech.,Vol.18, No.1. Trans. ASME, Vol. 73, Mar.1951 pp 31-38.

[34] Chow,T.S., "On the Propagation of Flexural Waves in An Orthotropic Laminated Plates and its Response on An Impulsive Load," J.comp.Mat., Vol 5, 1971, pp 306-319.

[35] Whitney, J.M.,"Shear Correction Factors for Orthotropic Laminates Under Static Load," J.App.Mech.,40(1), 1973, pp.302-304.

[36] Bert, C.W., "Simplified Analysis of Static Shear Factors For Beams of Non-homogenous Cross-Section, - J. Comp. Mat.,7(Oct.),1973,pp. 525-529.

[37] Pagano, N.J.,"Exact Solutions for Composite Laminates in Cylindrical Bending", J. Comp. Mat., Vol.3, (July), 1969.

[38] Srinivas,S.,Rao, C.V.Joga and Rao, A.K.,"An Exact Analysis for Vibrations of Simply Supported Homogenous and Lamianted Thick Rectangular Plates",J. Sound & Vib.,12(2), 1970, 187-199.

[39] Pagano, N.J. and Hatfield, S.J., "Elastic Behaviour of Multilayered Bidirectional Composites",AIAA, J. ,10(7), 1972, 931-933.

[40] Reissner, E.,"On a Variational Theorem in Elasticity", J. Math. Phys.,29(2), 1950, 90-95.

[41] Panc, V.,"Theories of Elastic Plates", tranl. from czech.,Noordhoff, Leyden, Netherlands, 1975.

[42] Naghdi,P.M. "On the Theory of Thin Elastic Shells, "Quart. of Appl. Math., Vol.14, 1957, pp. 369-380.

[43] Essenburg,F.,"On the Significance of the Inclusion of the Effect of Transverse Normal Strain in Problems Involving Beams With Surface Constraints," J. of App. Mech., Vol.42, No.1, trans. ASME, Vol.97 series E, Mar. 1975, pp 127-132.

[44] Whitney, J.M. and Sun, C.T.,"A Refined Theory for Laminated Anisotropic Cylindrical Shells," J. of Appl.Mech., Vol.41, No.2, Trans. ASME, Vol 96, Series E. June 1974, pp 471-476.

[45] Nelson, R.B. and Lorch, D.R., "A Refined Theory of Laminated Orthotropic Plates," J. of app. Mech., vol. 41, No.1, Trans.ASME, Vol.96, Series E., March 1974, pp 177-183.

[46] Reissner, E., "On Transverse Bending of Plates Including the Effects of Transverse Shear Deformation", Int. J. of solids and structures, 11, 569-573, 1975.

[47] Lo.K.H., Christensen R.M. and Wu. E.M., " A High Order Theory of Plate Deformation - Part I, Homogenous Plates, ASME, J. of App. Mech., 44, 663-669, 1977.

[48] Lo.K.H., Christensen R.M. and Wu. E.M., "A High Order Theory of Plate Deformation - Part II; Laminated plates, ASME, J. of App. Mech. 44, 669-676, 1977.

[49] Lo.K.H., Christensen R.M. and Wu.E.M., "Stress Solution Determination for High Order Plate Theory", Int. J. of Solid & Structure, 655-662, 1978.

[50] Levinson,M.,"An Accurate Simple Theory of The Statics And Dynamics of Elastic Plates," Mech.Res.Commun., 7, 343-350,1981.

[51] Murthy, M.V.V.,"Improved Transverse Shear Deformation Theory for Laminates An Isotropic Plates,NASA Technical paper, 1903, 1981.

[52] Reissner, E. "Reflections on The Theory of Elastic Plates", Appl. Mech. Rev., Vol.38, No. 11, pp. 1453-64, 1985.

[53] Hrabok,M.M. and Hrudey,T.M., "A Review and Catalogue of Plate Bending Finite Elements" Comps. & Structures, Vol.19, No.,3, pp 479-495, 1984.

[54] Clough, R.W. and Tocher, J.L., "Finite Element Stiffness Matrices for the Analysis of Plate Bending, Proc. 1st conf. on Matrix meth. in structural Mech., Ohio, pp.515-545(Oct.1965).

[55] Adini, A. and Clough, R.W., "Analysis of Plate Bending by The Finite Element Method. Report submitted to the National Science Foundation (Grant G7337)Wash., D.C., 1960.

[56] Melosh, R.J., "A Stiffness Matrix for the Analysis of Thin Plates in Bending, J.Aero. Science 28(1), 34-42, 1961.

[57] Tocher, J.L., "Analysis of Plate Bending Using Triangular Elements. Thesis presented in partial fulfilment of the requirements for the degree of Doctor of Philosophy, Dept. of C.E., Uni. of California, Barkeley 1962.

[58] Morley, L.S.D., "The Triangular Equilibrium Element in The Solution of Plate Bending Problems. The Aeronautical Quart. 19, 149-169 1968.

[59] Elias, Z.M., "Duality in Finite Element Methods, J. Engg. Mech.Div., ASCE 94 (EM4), pp 931-946 1968.

[60] Severn, R.T. and Taylor, P.R., "The Finite Element Method of Flexure when Stress Distributionsare assumed", Proc. Inst. of Civil Engg., Vol. 34, pp. 153-170, June 1966.

[61] Herrmann, L.R., "A Bending Analysis for Plates, proc. 1st conf.on matrix method in structural mechanics, Ohio, pp.577-602 Oct.1965.

[62] Barker, R.M., Lin, F.T. and Dana, J.R. "Three Dimensional Finite Element Analysis of Laminated Composites," Natl, symp. Computerised Structural Anal, Des., George Washington Univ., 1972.

[63] Mau,S.T., Tong,P. and Pian,T.H.H. "Finite Element Solutions for Laminated Thick Plates," J. Comp. Matls., 6, pp 304-311, 1972.

[64] Mau,S.T., Pian, T.H.H. and Tong,P. " Vibration Analysis of Laminated Plates and shells by a Hybrid stress Elelment," AIAA J., 11, pp 1450-1452(1973).

[65] Noors,A.K. and Mathers,M.D. "Finite Element Analysis of Anisotropic Plates", Intl. J.Numer. Methods Engr., 11, pp. 289-307 (1977).

[66] Mawenya, A.S. and Davies,J.D. " Finite Element Bending Analysis of Multilayer Plates", Intl. J. Numer. Methods. Engr., 8, pp 215-225, 1974.

[67] Panda, S.C. and Natarajan,R. " Finite Element Analysis of Laminated Composite Plates", Intl. J. Numer. Methods Engr., 14, pp 69-79,(1979).

[68] Ahmad,S.,Irons,B.M. and Zienkiewicz,O.C., " Analysis of Thick and Thin Shell Structures by Curved Finite Elements," Intl. J. Numer. Methods Engr., 2, pp 419-451 (1970).

[69] Spilker,R.L., Chou,S.C. and Orringer,O., "Alternate Hybrid Stress Elements for Analysis of Multilayer Composite Plates", J.Composite Mats., 11, pp 51-70, 1977.

[70] Reddy,J.N.,"A Penalty Plate Bending Element for the Analysis of Laminated Anisotropic Composite Plates", Intl. J. Numer. Methods Engr., 15, pp 1187-1206 (1980).

[71] Reddy, J.N. and Bert,C.W. "Analysis of Plates Constructed of Fiber-Reinforced Bimodulus Materials", Mechanics of Bimodulus Materials,(Bert. C,W. Ed), AMD, Vol. 33, ASME, pp 29-37, 1979.

[72] Reddy,J.N. and Chao,W.C. "Finite Element Analysis of Laminated Bimodulus Composite Material Plates", Computers Struc, 12, pp 245-251, 1980.

[73] Pryor,C.W. " Finite Element Analysis of Laminated Isotropic Plates Including Transverse Shear Deformation", Ph.d.,Thesis, Virginia Polytechnique Institute, USA 1970.

[74] Rao, K.P.,"A Rectangular Laminated Anisotropic Shallow Thin Shell Finite Element",ISD-report, no. 217, Stuttgart, 1977.

[75] Moser,K.,Lehar,H. and Schmid,A. ,"About the Analysis of Lamianted Composite Structures", Finite Element in Engng. applications, 1987, 395-416, INTES GmbH, Stuttgart.

[76] Ghosh, A.K. and Dey, S.S.,"A Simple Finite Element for the Analysis of Lamianted Plates",Accepted for publication in Computers and Structures.

[77] Reddy, J.N.,"Finite Element Modeling of Layered, Anisotropic Composite Plates and Shells: A Review of Recent Research ,Shock & Vib., Vol.13, 7-12,1981.

[78] Hinton, E.and Campbell, J.S.,"Local and Global Smoothing of Discontinuous Finite Element Functions Using a least square method", Int. J. Num. Meth. Engng., Vol. 8, pp 461-480, 1974.

[79] Pagano, N.J.,"Exact Solutions for Rectangular Bi-directional Composites and Sandwich Plates", J. Comp. Mats., 4, pp 20-34, 1970.

[80] Pagano, N.J.,"Influence of Shear Coupling in Cylindrical Bending of Anisotropic Plates", J. Comp. Mats., 4, pp 330-343, 1970.

[81] Rayleigh, Lord, Theory of Sound , 1st, 2nd Ed.,Macmillan and Co.,London,1945.

[82] Timoshenko, S.,Vibration Problems in Engineering, 2nd Ed.,Van Nostrand (1937).

[83] Young,D.,"Vibration of Rectangular Plates by The Ritz Method," J. Appl. Mech., 17, pp. 448-453 (1950).

[84] Hearmon,R.F.S.,"The Frequency of Vibration of Rectangular Isotropic Plates," J. Appl. Mech., 19, pp. 402-403, (1952).

[85] Warburton, G.B.,"The Vibration of Rectangular Plates," Proc. Instt. Mech. Eng.,Ser.A, 168, pp. 371-384 (1954).

[86] Pister, K.S., "Flexural Vibration of Thin Laminated Plate"; Journal of the Accoustical society of America, Vol 31, pp. 233-234, 1959.

[87] Stavsky, Y., "Thermoelastic Vibrations of Heterogenous Membranes and Inextensible Plates", AIAA,J., Vol.1, pp. 722-723, 1963.

[88] Ashton, J.E. and Waddoups, M.E., "Analysis of Anisotropic Plates", J. of Comp. Mat.,Vol.3, pp. 148-165, 1969.

[89] Whitney,J.M. and Leissa,A.W. "Analysis of Heterogenous Anisotropic Plates",J.Appl. Mech.,Trans. ASME, 36(2), June, pp. 261-266,1969.

[90] Ashton,J.E. and Anderson,J.D.,"Dynamic Response of Anisotropic Plates",General Dynamics Corp.,Fort Worth Div., Contract No. AF 33(615)-5257, Report FZM-5088 (Mar 29, 1968).

[91] Bert,C.W. and Mayberry,B.L."Free vibration of Unsymmetricaly Laminated Anisotropic Plates With Clamped Edges",J. Comp. Mat., Vol.3, pp. 282-293. Apr. 1969.

[92] Ambartsumyan "Theory of Anisotropic Shells, Moscow, 1961, English.translation, NASA TT F-118, (May,1964).

[93] Jones,R.M., "Buckling and Vibration of Rectangular Unsymmetrically Laminated Cross-ply Plates",AIAA J., pp. 1626-1632, Dec. 1973.

[94] Jones,R.M., Morgan, H.S. and Whitney,J.M.,"Buckling and Vibration of Anti-Symmetrically Laminated Angle-ply Rectangular Plates", J.Appl. Mech., pp.1143-1144, Dec. 1973.

[95] Sun, C.T. and Whitney,J.M., "Theories for the Dynamic Response of Laminated Plates", AIAA, J., 11, pp. 178, 1973.

[96] Fortier, R.C. and Rossettos, J.N. "On the Vibration of Shear Deformable Curved Anisotropic Composite Plates J.Appl.Mech., 40, pp. 299, 1973.

[97] Sinha, P.K. and Rath, A.K., "Vibration and Buckling of Cross-ply Laminated Circular Cylindrical Panels. Aeronaut. Quart. 26, pp. 211, 1975.

[98] Dong,S.B.,"Studies Relating to the Structural Dynamic Behaviour of Laminated Plates and Shells", UCLA-Eng-7236, Uni. of Calif., LA, May. 1972.

[99] Bert, C.W. and Chen,T.L.C., "Effect of Shear Deformation on Vibration of Antisymmetric Angle-ply Laminated Rectangular Plates", Int. J. Solids Structures, Vol.14, pp. 465-473, 1978.

[100] Reddy,J.N. and Chao,W.C.," "Non-Linear bending of thick rectangular, laminated composite plates", Int. J.on Non-Linear Mech., 16, pp.291-301, 1981.

[101] Reddy, J.N. and Chao,W.C.,'Large Deflection and Large Amplitude free Vibration of Laminated Composite Material Plates", Comp. and Struc.,13(2), pp.341-347, (1981).

[102] Reddy, J.N." "On the Solutions to Forced Motions of Rectangular Composite Plates" J. of App. Mech., 49, pp. 403-408,1982.

[103] Reddy, J.N. and Chao,W.C.," Non linear Oscillations of Laminated Anisotropic Rectangular Plates" J.of App. Mech., 49, pp. 396-402,1982.

[104] Reddy, J.N.,""Geometrically Nonlinear Transient Analysis of Laminated Composite Plates", AIAA J., 21, 621-629, 1983.

[105] Chandra Sekhra, S.,"Free Vibration Analysis of Layered Plates and Composites by a Mixed Method : State Space Approach, Ph.D. thesis, Georgia Institute of Tech, Atlanta,GA, 1982.

[106] Vlasov,V. Z. and Leontev,U.N.,"Beams, Plates and Shells on Elastic Foundation, NASA TTF-357, 1966.

[107] Chandra Shekara, S. and Santosh, U.,"Natural Frequencies of Cross-ply Laminates by State Space Approach", J. of Sound & Vibration, 136(3), pp. 413-424, 1990.

[108] Chandra Shekara,S. and Chander, R.,"Vibration of Layered Composites by a Mixed Method of Elasticity. Trans, ASME, 1989.

[109] Iyenger, N.G., and Umaretiya,J.R.," Transverse Vibration of Hybrid Laminated Plates", J. of Sound and Vibration, Vol. 104, pp. 425-435, 1986.

[110] Ochoa,O.O., Engblom. J.J. and Tucker,R. "Fundamental Frequency of Composite Plates", J. of Sound and Vibration, Vol.101,pp.141-148, 1985.

[111] Hinton, E., "A Note on A Thick Finite Strip Method for the Free Vibration of Laminated Plates". Int. J. Earthquake Engr. Struct. dynam., 4, pp 511-514, 1976.

[112] Puteta, N.S. and Reddy, J.N.,"Stability and Vibration Analysis of Laminated Plates by Using A Mixed Element Based on a Refined Plate Theory, J.Sound & Vibr. 104, pp. 285-300, 1986.

[113] Reddy,J.N. and Phan, N.D.,"Stability and Vibration of Isotropic and Laminated Plates According to a Higher Order Shear Deformation Theory", J. Sound and Vib., 98, pp. 157-170, 1985.

[114] Owen, D.R.J. and Li,Z.H.,"A Refined Analysis of Laminated Plates by Finite Element Displacement Methods - II. Vibration and Stability., Comp. & Struc., Vol.26, No.6, pp. 915-923, 1987.

[115] Mallikarjuna and Kant,T.,"Dynamics of Laminated Composite Plates with Higher Order Theory and Finite Element Discretisation",J. Sound and Vibration, 126(3), pp. 463-475, 1988.

[116] Archer, J.S.,"Consistent Mass Matrix for Distributed Mass System", J. of the Struc. div., Proceed. of ASCE, Aug. 1963.

[117] Hinton,E., Rock, T. and Zienkiewiicz,O.C. "A Note on Mass lumping and Related Processes in the Finite Element Method", Earthquake Engg. and Struc. Dyna., 4, 245-249, 1976.

[118] Rock,T. and Hinton,E. "A Finite Element Method for the Free Vibration of Plates Allowing for Transverse Shear Deformation", Comp.& Struc., Vol.6, pp 37-44, 1976.

[119] Chladin, E.F.F., "Die Akustik"(1802)" Neue Bietrage Zur Akustik(1817).

[120] Hazell, C.R. and Mitchell.A.K.,"Experimental Eigenvalues and Mode shapes for flat clamped Plates", " Experimental Mechanics, pp 209-216.

[121] Crawley,E.F.,"The Natural Modes of Graphite/Epoxy cantilever Plates and Shells", J. Comp. Materials, vol.13, July 1979, pp. 195-205.

[122] Pagano,N.J.and Halpin,J.C. " Influence of End Constraint in the Testing of Anisotropic Bodies", J. Comp. Materials 2(1); 18-31, 1968.

[123] Pagano, N.J. and Kim, R.Y., "Interlaminar Shear Strength of Cloth-reinforced Composites", Expt. Mech.,117, 1987.

[124] Pindera, M.J. and C.T.Herakovich, "Shear Characterization of Unidirectional Composites with the Off-axis Tension Test",Experimental Mechanics, March 1986, pp 103-111.

[125] Jones, R.M.,Mechanics of Composite Material, McGraw-Hill book Co.

[126] Gerard. G., "Minimum weight Analysis of Orthotropic Plates under Compressive Loading", Journal of the Aerospace Sciences, Vol.27, No.64, Jan 1960, pp 21-26.

[127] Gerard.G. and Becker,H., Handbook of structural stability. Part VII. - Strength of thin-wing construction, Technical note, NACA TN D-162,1959.

[128] Ashton, J.E. and Whitney, J.M.,"Theory of laminated plates", Technomic Publishing, Stamford CT, 1970.

[129] Chia, C.Y.,Nonlinear analysis of plates, McGraw-Hill, New York 1980.

[130] Dong, S.B, Pister, K S. and Taylor, R L , On the Theory of Laminated Anisotropic Shells and Plates, J. Aeronaut Sci., 29, 1962, pp. 969-975.

[131] Hoff, N.J., Boley,B.A. and Coan, J.M.,"The Development of a Technique for Testing Stiff Panels in Edgewise Compression",Proc. Soc. Exp. Stress Anal.,5(2),pp.14-24, 1948.

[132] Chamis, C. C., "Buckling of Anisotropic Composite Plates", J Struct. Div., 95 (ST 10), 1969, pp. 2119-2139.

[133] Chamis, C. C., "Buckling of Anisotropic Composite Plates", Closure and Errata, J. Struct. Div., 97, 1971, pp. 960-962.

[134] Brunelle,. E.J., and Oyibo, G.A., Generic Buckling Curves for Specially Orthotropic Rectangular Plates, AIAA J., 21, Aug. 1983, pp. 1150-1156.

[135] Fogg, L., "Stability Analysis of Laminated Materials, State of the Art Design and Analysis of Advanced Composite Materials", Lockheed California Company, Sessions I and II, 1981.

[136] Housner, J. M. and Stein, M., "Numerical Analysis and Parameter of the Buckling of Composite Orthotropic Compression and Shear Panels", NASA TN D-7996, Oct.1975.

[137] Stein, M., and Housner, J.M.,"Application of a Trigonometric finite Difference Procedure to Numerical Analysis of Compressive and shear Buckling of Orthotropic Panels", Comput Struct 9(1) 1978 pp 17-25.

[138] Dickinson, S.M., "The Buckling and Frequency of Flexural Vibration of Rectanggular Isotropic and Orthotropic Plates Using Rayleigh's Method", J. Sound Vib., 61(1), 1978, pp. 1-8.

[139] Wittrick, W. H.,"Correlation Between Some Stability Problems for Orthotropic and Isotropic Plates Under Bi-axial and Uni-axial Direct Stress, Aeronaut. quart., 4 (part I), 1952, pp. 83-92.

[140] Ashton J. E. and Love, T. S., "Experimental Study of the Stability of Composite Plates", Composite Mat., 3, 1969, pp. 230-242.

[141] Chia, C. Y. and Prabhakara, M.K. "Nonlinear Analysis of Orthotropic Plates", J. Mech. Eng. Sci., 17(3), 1975, pp. 133-138.

[142] Leissa, A.W.,"A Review of Laminated Composite Plate Buckling,"Appl. Mech. Rev.,Vol.40,No.5,pp. 1987.

[143] Noor,A.K.,"Stability of Multi-layered Composite Plates",Fibre Sci. Technol.,8(2), pp. 81-89, 1975.

```
C     .....................................................................
C     .                                                                   .
C     .                                                                   .
C     .                                                                   .
C     .                    P R O G R A M   L A M I N A T E                .
C     .                                                                   .
C     .                                                                   .
C     .                                                                   .
C     .....................................................................
C     .  FINITE ELEMENT ANALYSIS OF CROSS-PLY LAMINATED PLATE UNDER       .
C     .                  VARIOUS LOADING CONDITIONS                       .
C     .....................................................................
C     .                                                                   .
C     .                    DESCRIPTION OF THE VARIABLES                   .
C     .                                                                   .
C     .       NUMNP= TOTAL NUMBER OF NODAL POINTS IN THE PLATE ;          .
C     .       NE   = NUMBER OF ELEMENTS ;                                 .
C     .       NEDOF= NUMBER OF ELEMENT DEGREE OF FREEDOM ;                .
C     .       NEQ  =  NUMBER  OF  EQUATIONS;                              .
C     .       ND   = TOTAL NO. OF ELEMENT D.O.F.                          .
C     .       NWK  = ARRAY STORES ADDRESSES OF DIAGONAL ELEMENTS          .
C     .       NINT = NO. OF GAUSS SAMPLING POINTS;                        .
C     .       TH   = THICKNESS OF THE PLATE;                              .
C     .       XX(I,J) = CO-OR. OF THE FOUR NODES OF THE ELEMENT           .
C     .                 CONSIDERED;                                       .
C     .       X(N)    = X CO-OR. OF N-NODES;                              .
C     .       Y(N)    = Y CO-OR. OF N-NODES;                              .
C     .       P(N)    = ANGLE OF LAMINATION OF N LAYERS;                  .
C     .       HGT(N)  = Z/T VALUES OF THE INTERFACES OF LAYERS, WHERE     .
C     .                 T IS THE TOTAL THICKNESS OF THE LAMINATE;         .
C     .       XG(I,J) = CO-OR. OF GAUSS SAMPLING POINTS;                  .
C     .       WGT(I,J)= CORRESPONDING WEIGHTS;                            .
C     .       IID(I,J)= IDENTIFICATION ARRAY;                             .
C     .       LM(I,J) = ARRAY STORES ASSEMBLAGE D.O.F. OF ALL ELEMENTS.   .
C     .       MAXA(N) = ADDRESSES OF THE DIAGONAL ELEMENTS;               .
C     .       SK(N)   = 1-D ARRAY CONTAINING STIFFNESS CO-EFF. OF         .
C     .                 ALL ELEMENTS;                                     .
```

```
C     .      S(I,J)  = ELEMENT STIFFNESS MATRIX;                    .
C     .      D(I,J)  = CONSTITUTIVE MATRIX                          .
C     .      BB(I,J) = STRAIN-DISPLACEMENT MATRIX;                  .
C     .      R(N)    = 1-D LOAD VECTOR OF ALL ELEMENTS;             .
C     .      ELD(N)  = 1-D LOAD VECTOR OF AN ELEMENT;               .
C     .      F(I),G(I) AND H(I)s ARE SHAPE FUNCTIONS AS GIVEN IN    .
C     .                          EQUATION 3.                        .
C     .      CARTD(I,J)= CARTESIAN DERIVATIVE OF SHAPE FUNCTION;    .
C     .      DERIV(I,J)= DERIVATIVE OF SHAPE FUNCTION W.R.T. r & s; .
C     ..........................................................
C     .                    MATERIAL PARAMETERS                    .
C.    ..........................................................
C     .      EX1 = YOUNG'S MODULUS IN X DIRECTION;                  .
C     .      EY1 = YOUNG'S MODULUS IN Y DIRECTION;                  .
C     . .    G12 = SHEAR MODULUS(XY-PLANE);                         .
C     .      G13 = SHEAR MODULUS(XZ-PLANE);                         .
C     .      G23 = SHEAR MODULUS(YZ-PLANE);                         .
C     .      V12 = POISSON'S RATIO(ν12);                            .
C     ..........................................................
C     ..........................................................
      PROGRAM LAMINATE
      COMMON/DIM/XX(2,4),X(100),Y(100),NODN(100,4)
      COMMON/ELT/NUMNP,NE,NEDOF,IID(7,100),LM(28,100),MAXA(1000)
     +,NWK,SK(10000),S(28,28),R(150),ELD(28),NEQ,MHT(1000),NEQ1,ND
      COMMON/GAUS/XG(4,4),WGT(4,4),NINT,TH
      COMMON/STIF/EY1,EY2,G12,G13,G23,V12,V21,P(3),HGT(4)
      COMMON/MAT/CARTD(2,4),DERIV(2,4),QO(5,5),Q90(5,5)
     #,SHAPE(4),BTDB(28,28),F(4),GX(4),HY(4),D(13,13)
      COMMON/TRY/BB(13,28),B2(5,13),B(5,28),DB(13,28),
     #BTD(28,5),BT(28,13),FX(4),FXX(4),FXY(4),FYY(4),FY(4),GY(4),
     #GXX(4),GYY(4),GXY(4),HX(4),HXX(4),HYY(4),HXY(4),G(4),H(4)
      OPEN(UNIT=1,FILE='$USER.LAMIN')
      OPEN(UNIT=2,FILE='$USER.LAMOUT')
```

```
C     .....
C     .                    READING PROBLEM DATA                    .
C     .....
      READ(1,*)NUMNP,NE,NNDOF,NEDOF
      READ(1,*)NINT,TH
      READ(1,*)((XG(I,J),J=1,4),I=1,4)
      READ(1,*)((WGT(I,J),J=1,4),I=1,4)
      READ(1,*)(P(K),K=1,3)
      READ(1,*)(HGT(K),K=1,4)
      READ(1,*)EY1,EY2,G12,G13,G23,V12,V21
      DO 10 N=1,NE
10    READ(1,*)(NODN(N,I),I=1,4)
      DO 11 I=1,150
11    R(I)=0.0
      CALL GENERAT
      CALL PLATE(TH)
      CLOSE(UNIT=1)
      CLOSE(UNIT=2)
      STOP
      END
      SUBROUTINE GENERAT
      IMPLICIT REAL*8(A-H,O-Z)
      COMMON/ELT/NUMNP,NE,NEDOF,IID(7,100),LM(28,100),MAXA(1000)
     +,NWK,SK(10000),S(28,28),R(150),ELD(28),NEQ,MHT(1000),NEQ1;ND
      COMMON/DIM/XX(2,4),X(100),Y(100),NODN(100,4)
C     .....
C     .          READ AND GENERATE NODAL POINT DATA          .
C     .    BOUNDARY CONDITION CODES (0 = FREE, 1 = FIXED      .
C     .....
20    READ(1,*)NOLD,(IID(I,NOLD),I=1,7),X(NOLD),Y(NOLD),KNOLD
      READ(1,*)N,(IID(I,N),I=1,7),X(N),Y(N),KN
      NUM=(N-NOLD)/KNOLD
      NUMN=NUM-1
      XNUM=NUM
      DX=(X(N)-X(NOLD))/XNUM
      DY=(Y(N)-Y(NOLD))/XNUM
```

```
      K=NOLD
      DO 22 J=1,NUMN
      KK=K
      K=K+KNOLD
      X(K)=X(KK)+DX
      Y(K)=Y(KK)+DY
      DO 22 I=1,7
      IID(I,K)=IID(I,KK)
22    CONTINUE
      IF(N.NE.NUMNP)GOTO 20
C     .....................................................
C     . FROM INPUT FILE ALL D.O.Fs. ARE READ FIXED. HERE THEY WILL .
C     .                          UPDATED                  .
C     .....................................................
      IID(1,1)=0
      IID(2,1)=0
      IID(1,2)=0
      IID(2,2)=0
      IID(3,2)=0
      IID(6,2)=0
      IID(1,3)=0
      IID(2,3)=0
      IID(3,3)=0
      IID(6,3)=0
      IID(1,4)=0
      IID(2,4)=0
      IID(3,4)=0
      IID(6,4)=0
      IID(1,5)=0
      IID(3,5)=0
      IID(6,5)=0
      IID(1,6)=0
      IID(2,6)=0
      IID(4,6)=0
      IID(7,6)=0
      DO 24 I=1,7
```

```
      IID(I,7)=0
      IID(I,8)=0
      IID(I,9)=0
      IID(I,12)=0
      IID(I,13)=0
      IID(I,14)=0
      IID(I,17)=0
      IID(I,18)=0
   24 IID(I,19)=0
      IID(1,10)=0
      IID(3,10)=0
      IID(5,10)=0
      IID(6,10)=0
      IID(1,11)=0
      IID(2,11)=0
      IID(4,11)=0
      IID(7,11)=0
      IID(1,15)=0
      IID(3,15)=0
      IID(5,15)=0
      IID(6,15)=0
      IID(1,16)=0
      IID(2,16)=0
      IID(4,16)=0
      IID(7,16)=0
      IID(1,20)=0
      IID(3,20)=0
      IID(5,20)=0
      IID(6,20)=0
      IID(2,21)=0
      IID(4,21)=0
      IID(2,22)=0
      IID(4,22)=0
      IID(5,22)=0
      IID(7,22)=0
      IID(7,21)=0
```

```
      IID(2,23)=0
      IID(4,23)=0
      IID(5,23)=0
      IID(7,23)=0
      IID(2,24)=0
      IID(4,24)=0
      IID(5,24)=0
      IID(7,24)=0
      IID(5,25)=0
      NEQ=0
      DO 29 N=1,NUMNP
      DO 29 I=1,7
      IF(IID(I,N))28,30,28
30    NEQ=NEQ+1
      IID(I,N)=NEQ
      GOTO 29
28    IID(I,N)=0
29    CONTINUE
      NEQ1=NEQ+1
      RETURN
      END
      SUBROUTINE PLATE(TH)
      COMMON/DIM/XX(2,4),X(100),Y(100),NODN(100,4)
      COMMON/STIF/EY1,EY2,G12,G13,G23,V12,V21,P(3),HGT(4)
      COMMON/ELT/NUMNP,NE,NEDOF,IID(7,100),LM(28,100),MAXA(1000)
     +,NWK,SK(10000),S(28,28),R(150),ELD(28),NEQ,MHT(1000),NEQ1,ND
      COMMON/MAT/CARTD(2,4),DERIV(2,4),Q0(5,5),Q90(5,5)
     #,SHAPE(4),BTDB(28,28),F(4),GX(4),HY(4),D(13,13)
      COMMON/TRY/BB(13,28),B2(5,13),B(5,28),DB(13,28),
     #BTD(28,5),BT(28,13),FX(4),FXX(4),FXY(4),FYY(4),FY(4),GY(4),
     #GXX(4),GYY(4),GXY(4),HX(4),HXX(4),HYY(4),HXY(4),G(4),H(4)
C     .....................................................
C     . LOOPS OVER ALL ELEMENTS TO GENERATE THE CONNECTIVITY MATRIX .
C     .....................................................
      DO 40 I=1,28
      DO 40 J=1,NE
```

```
40      LM(I,J)=0
        DO 42 N=1,NE
        I1=NODN(N,1)
        I2=NODN(N,2)
        I3=NODN(N,3)
        I4=NODN(N,4)
        DO 42 MM=1,7
        LM(MM,N)=IID(MM,I1)
        LM(MM+7,N)=IID(MM,I2)
        LM(MM+14,N)=IID(MM,I3)
42      LM(MM+21,N)=IID(MM,I4)
        CALL COLHT
        CALL ADDRES
        DO 45 I=1,NWK
45      SK(I)=0.0
C       ..................................................................
C       .  LOOPS OVER ALL ELEMENTS TO OBTAIN ELEMENT STIFFNESS MATRIX .
C       .  LOAD VECTOR AND THEY WILL BE ASSEMBLED TO GLOBAL VECTORS   .
C       ..................................................................
        DO 43 N=1,NE
        I1=NODN(N,1)
        I2=NODN(N,2)
        I3=NODN(N,3)
        I4=NODN(N,4)
        XX(1,1)=X(I1)
        XX(1,2)=X(I2)
        XX(1,3)=X(I3)
        XX(1,4)=X(I4)
        XX(2,1)=Y(I1)
        XX(2,2)=Y(I2)
        XX(2,3)=Y(I3)
        XX(2,4)=Y(I4)
        CALL LAMSTIF(N)
        CALL ASEMBLY(N)
43      CONTINUE
        CALL SOLUTION
```

```
      CALL STRESS(TH)
      RETURN
      END
      SUBROUTINE COLHT
C     .....
C     .    SUBROUTINE TO CALCULATE THE ACTIVE COLUMN HEIGHTS      .
C     .....
      COMMON/ELT/NUMNP,NE,NEDOF,IID(7,100),LM(28,100),MAXA(1000)
     +,NWK,SK(10000),S(28,28),R(150),ELD(28),NEQ,MHT(1000),NEQ1,ND
      DO 50 I=1,NEQ
50    MHT(I)=0
      ND=NEDOF
      DO 55 N=1,NE
      LS=10000
      DO 53 I=1,ND
      IF(LM(I,N))51,53,51
 51   IF(LM(I,N)-LS)52,53,53
 52   LS=LM(I,N)
 53   CONTINUE
      DO 54 I=1,ND
      II=LM(I,N)
      IF(II.EQ.0)GOTO 54
      ME=II-LS
      IF(ME.GT.MHT(II))MHT(II)=ME
 54   CONTINUE
 55   CONTINUE
      RETURN
      END
      SUBROUTINE ADDRES
C     .....
C     .  CALCULATES THE ADDRESSES OF DIAGONAL ELEMENTS IN BANDED    .
C     .       MATRIX WHOSE COLUMN HEIGHTS ARE ALREADY KNOWN         .
C     .....
      COMMON/ELT/NUMNP,NE,NEDOF,IID(7,100),LM(28,100),MAXA(1000)
     +,NWK,SK(10000),S(28,28),R(150),ELD(28),NEQ,MHT(1000),NEQ1,ND
      NN=NEQ1
```

```
      DO 60 I=1,NN
60    MAXA(I)=0
      MAXA(1)=1
      MAXA(2)=2
      MK=0
      IF(NEQ.EQ.1)GOTO 80
      DO 70 I=2,NEQ
      IF(MHT(I).GT.MK)MK=MHT(I)
70    MAXA(I+1)=MAXA(I)+MHT(I)+1
80    MK=MK+1
      NWK=MAXA(NEQ+1)-MAXA(1)
      RETURN
      END
      SUBROUTINE ASEMBLY(N)
C     ..................................................................
C     .  ASSEMBLE UPPER TRIANGULAR ELEMENT MATRIX INTO COMPACTED       .
C     .                    GLOBAL STIFFNESS MATRIX                     .
C     ..................................................................
      IMPLICIT REAL*8(A-H,O-Z)
      COMMON/ELT/NUMNP,NE,NEDOF,IID(7,100),LM(28,100),MAXA(1000)
     +,NWK,SK(10000),S(28,28),R(150),ELD(28),NEQ,MHT(1000),NEQ1,ND
      DO 70 I=1,ND
      II=LM(I,N)
      IF(II)70,70,30
30    DO 60 J=1,ND
      JJ=LM(J,N)
      IF(JJ)60,60,40
40    MI=MAXA(JJ)
      IJ=JJ-II
      IF(IJ)60,50,50
50    KK=MI+IJ
      SK(KK)=SK(KK)+S(I,J)
60    CONTINUE
70    CONTINUE
      DO 33 IJ=1,28
      K=LM(IJ,N)
```

```
      IF(K.EQ.0)GO TO 33
      R(K)=R(K)+ELD(IJ)
   33 CONTINUE
  100 RETURN
      END
      SUBROUTINE SOLUTION
C     ..................................................................
C     .  SOLVE FINITE ELEMENT STATIC EQUILIBRIUM EQUATIONS IN CORE     .
C     .     USING COMPACTED STORAGE AND COLUMN REDUCTION SCHEME        .
C     ..................................................................
      IMPLICIT REAL*8(A-H,O-Z)
      COMMON/ELT/NUMNP,NE,NEDOF,IID(7,100),LM(28,100),MAXA(1000)
     +,NWK,SK(10000),S(28,28),R(150),ELD(28),NEQ,MHT(1000),NEQ1,ND
      DIMENSION A(10000),V(150)
C     ..................................................................
C     .      Perform L*D*L  factorization of stiffness matrix          .
C     ..................................................................
      DO 31 I=1,NEQ
      PP=MAXA(I)
      P=SK(PP)
      IF(P.EQ.0.0)GO TO 35
      GOTO 31
   35 WRITE(*,*)'ZERO ELEMENT IN THE DIAGONAL'
      WRITE(*,300)I,PP,P
  300 FORMAT(2I5,5X,E20.8)
   31 CONTINUE
      DO 99 I=1,NWK
   99 A(I)=SK(I)
      DO 32 I=1,NEQ
   32 V(I)=R(I)
      NN=NEQ
   40 DO 140 N=1,NEQ
      KN=MAXA(N)
      KL=KN+1
      KU=MAXA(N+1)-1
      KH=KU-KL
```

```
      IF(KH)110,90,50
50    K=N-KH
      IC=0
      KLT=KU
      DO 80 J=1,KH
      IC=IC+1
      KLT=KLT-1
      KI=MAXA(K)
      ND=MAXA(K+1)-KI-1
      IF(ND)80,80,60
60    KK=MINO(IC,ND)
      C=0.
      DO 70 L=1,KK
70    C=C+A(KI+L)*A(KLT+L)
      A(KLT)=A(KLT)-C
80    K=K+1
90    K=N
      B=0.
      DO 100 KK=KL,KU
      K=K-1
      KI=MAXA(K)
      C=A(KK)/A(KI)
      B=B+C*A(KK)
100   A(KK)=C
      A(KN)=A(KN)-B
110   IF(A(KN))120,120,140
120   WRITE(2,*)'N,A(KN)'
      WRITE(2,*)N,A(KN)
      STOP
140   CONTINUE
C     ..................................................................
C     .  WRITE(2,*)'Reduce the right hand side of the load vector'   .
C     ..................................................................
150   DO 180 N=1,NN
      KL=MAXA(N)+1
      KU=MAXA(N+1)-1
```

```
      IF(KU-KL)180,160,160
160   K=N
      C=0.
      DO 170 KK=KL,KU
      K=K-1
170   C=C+A(KK)*V(K)
      V(N)=V(N)-C
180   CONTINUE
      DO 200 N=1,NN
      K=MAXA(N)
200   V(N)=V(N)/A(K)
      IF(NN.EQ.1)STOP
      N=NN
      DO 230 L=2,NN
      KL=MAXA(N)+1
      KU=MAXA(N+1)-1
      IF(KU-KL)230,210,210
210   K=N
      DO 220 KK=KL,KU
      K=K-1
220   V(K)=V(K)-A(KK)*V(N)
230   N=N-1
C     ..................................................................
C     .                    WRITES  DISPLACEMENT'                       .
C     ..................................................................
      DO 240 N1=1,NEQ
240   R(N1)=V(N1)
      WRITE(2,*)(R(NEQ))
C8    FORMAT(8(E15.7,2X))
      RETURN
      END
      FUNCTION MINO(IC,ND)
      MA=IC-ND
      IF(MA.GT.0)GOTO 250
      MINO=IC
      GOTO 260
```

```
250   MINO=ND
260   RETURN
      END
      SUBROUTINE LAMSTIF(N)
C     .....................................................
C     .      ROUTINE THAT CALCULATES ELEMENT STIFFNESS MATRIX      .
C     .....................................................
      IMPLICIT REAL*8(A-H,O-Z)
      COMMON/ELT/NUMNP,NE,NEDOF,IID(7,100),LM(28,100),MAXA(1000)
     +,NWK,SK(10000),S(28,28),R(150),ELD(28),NEQ,MHT(1000),NEQ1,ND
      COMMON/STIF/EY1,EY2,G12,G13,G23,V12,V21,P(3),HGT(4)
      COMMON/GAUS/XG(4,4),WGT(4,4),NINT,TH
      COMMON/DIM/XX(2,4),X(100),Y(100),NODN(100,4)
      COMMON/MAT/CARTD(2,4),DERIV(2,4),Q0(5,5),Q90(5,5)
     #,SHAPE(4),BTDB(28,28),F(4),GX(4),HY(4),D(13,13)
      COMMON/TRY/BB(13,28),B2(5,13),B(5,28),DB(13,28),
     #BTD(28,5),BT(28,13),FX(4),FXX(4),FXY(4),FYY(4),FY(4),GY(4),
     #GXX(4),GYY(4),GXY(4),HX(4),HXX(4),HYY(4),HXY(4),G(4),H(4)
      CALL CONSTI
      DO 10 I=1,28
      DO 10 J=1,28
10    S(I,J)=0.0
      DO 15 I=1,28
15    ELD(I)=0.0
C     .....................................................
C     .          LOOPS OVER ALL THE GAUSS SAMPLING POINTS          .
C     .....................................................
      DO 20 LX=1,NINT
      RI=XG(NINT,LX)
      DO 20 LY=1,NINT
      SI=XG(NINT,LY)
      DJACB=0.0
      WX=WGT(NINT,LX)
      WY=WGT(NINT,LY)
      CALL SFR(RI,SI,DJACB)
      CALL BMAT(TH,RI,SI)
```

```
C       CALL UDL16(RI,SI,DJACB,WX,WY)
        CALL LOAD(RI,SI,DJACB,WX,WY)
        WT=WX*WY*DJACB
        DO 30 I=1,28
        DO 30 J=1,28
30      S(I,J)=S(I,J)+WT*BTDB(I,J)
20      CONTINUE
160     RETURN
        END
        SUBROUTINE SFR(S,T,DJACB)
C       ..................................................................
C       . ROUTINE TO CALCULATE THE JACOBIAN OF AN ELEMENT AND CART-      .
C       .          ESIAN DERIVATIVES OF SHAPE FUNCTIONS                  .
C       ..................................................................
        COMMON/DIM/XX(2,4),X(100),Y(100),NODN(100,4)
        COMMON/MAT/CARTD(2,4),DERIV(2,4),QO(5,5),Q90(5,5)
       #,SHAPE(4),BTDB(28,28),F(4),GX(4),HY(4),D(13,13)
        DIMENSION XJ(2,2),XJI(2,2)
        SP=1.0+S
        TP=1.0+T
        SN=1.0-S
        TN=1.0-T
        SHAPE(1)=0.25*SN*TN
        SHAPE(2)=0.25*SP*TN
        SHAPE(3)=0.25*SP*TP
        SHAPE(4)=0.25*SN*TP
        DERIV(1,1)=-0.25*TN
        DERIV(1,2)=0.25*TN
        DERIV(1,3)=0.25*TP
        DERIV(1,4)=-0.25*TP
        DERIV(2,1)=-0.25*SN
        DERIV(2,2)=-0.25*SP
        DERIV(2,3)=0.25*SP
        DERIV(2,4)=0.25*SN
        DO 110 I=1,2
        DO 110 J=1,2
```

```
      DUM=0.0
      DO 105 K=1,4
105   DUM=DUM+DERIV(I,K)*XX(J,K)
110   XJ(I,J)=DUM
      DJACB=XJ(1,1)*XJ(2,2)-XJ(2,1)*XJ(1,2)
      DUM=1.0/DJACB
      XJI(1,1)=XJ(2,2)*DUM
      XJI(1,2)=XJ(2,1)*DUM
      XJI(2,1)=XJ(1,2)*DUM
      XJI(2,2)=XJ(1,1)*DUM
C     WRITE(2,*)'XJI'
C     WRITE(2,*)((XJI(I,J),J=1,2),I=1,2)
      DO 130 IDIME=1,2
      DO 130 INODE=1,4
      CARTD(IDIME,INODE)=0.0
      DO 130 JDIME=1,2
      CARTD(IDIME,INODE)=CARTD(IDIME,INODE)+
     #XJI(IDIME,JDIME)*DERIV(JDIME,INODE)
130   CONTINUE
      RETURN
      END
      SUBROUTINE CONSTI
C     .....................................................
C     . CALCULATES THE STIFFNESS MATRIX OF A LAMINA AND STORES IN .
C     . Q0 AND Q90 FOR LAMINATION ANGLE 0^O AND 90^O RESPECTIVELY .
C     .....................................................
      DOUBLE PRECISION SP,QB(5,5),PI
      COMMON/STIF/EY1,EY2,G12,G13,G23,V12,V21,P(3),HGT(4)
      COMMON/MAT/CARTD(2,4),DERIV(2,4),Q0(5,5),Q90(5,5)
     #,SHAPE(4),BTDB(28,28),F(4),GX(4),HY(4),D(13,13)
      DIMENSION A(5,5),B(5,5),C(5,5),CC(3,5,5),
     #D1(5,5),E(5,5),G(5,5)
      Q11=EY1/(1.0-V12*V21)
      Q12=V12*EY2/(1.0-V12*V21)
      Q22=EY2/(1.0-V12*V21)
      Q33=G12
```

```
      Q44=G13
      Q55=G23
      DO 210 I=1,5
      DO 210 J=1,5
      QB(I,J)=0.0
      A(I,J)=0.0
      B(I,J)=0.0
      C(I,J)=0.0
      D1(I,J)=0.0
      E(I,J)=0.0
      G(I,J)=0.0
      Q0(I,J)=0.0
210   Q90(I,J)=0.0
      DO 220 IP=1,3
      THETA=P(IP)
      PI=4.DO*DATAN(1.DO)
      SP=THETA*PI/180.0
      QB(1,1)=Q11*DCOS(SP)**4.0+2.0*(Q12+2.0*Q33)
     #*DCOS(SP)**2.0*DSIN(SP)**2.0+Q22*DSIN(SP)**4.0
      QB(1,2)=(Q11+Q22-4.0*Q33)*DCOS(SP)**2.0*DSIN(SP)**2.0
     #+Q12*(DCOS(SP)**4.0+DSIN(SP)**4.0)
      QB(2,2)=Q11*(DSIN(SP)**4.0)+2.0*(Q12+2.0*Q33)*(DCOS(SP)**2.0)
     #*(DSIN(SP)**2.0)+Q22*(DCOS(SP)**4.0)
      QB(3,3)=(Q11+Q22-2.0*Q12-2.0*Q33)*(DCOS(SP)**2.0)*(DSIN(SP)
     #**2.0)+Q33*((DCOS(SP)**4.0)+(DSIN(SP)**4.0))
      QB(1,3)=(Q11-2.0*Q33-Q12)*(DCOS(SP)**3.0)*DSIN(SP)+
     #(Q12-Q22+2.0*Q33)*DCOS(SP)*(DSIN(SP)**3.0)
      QB(2,3)=(Q11-2.0*Q33-Q12)*DCOS(SP)*(DSIN(SP)**3.0)+
     #(Q12-Q22+2.0*Q33)*(DCOS(SP)**3.0)*DSIN(SP)
      QB(4,4)=Q44*(DCOS(SP)**2.0)+Q55*(DSIN(SP)**2.0)
      QB(4,5)=(Q55-Q44)*DCOS(SP)*DSIN(SP)
      QB(5,5)=Q44*(DSIN(SP)**2.0)+Q55*(DCOS(SP)**2.0)
      DO 230 I=1,5
      DO 230 J=1,5
230   QB(J,I)=QB(I,J)
      IF(THETA.EQ.0.0)GOTO 235
```

```
      IF(THETA.EQ.90.0)GOTO 240
235   DO 250 I=1,5
      DO 250 J=1,5
250   Q0(I,J)=QB(I,J)
      GOTO 260
240   DO 255 I=1,5
      DO 255 J=1,5
255   Q90(I,J)=QB(I,J)
260   CONTINUE
      DO 275 I=1,5
      DO 275 J=1,5
      A(I,J)=A(I,J)+QB(I,J)*(HGT(IP+1)-HGT(IP))
      B(I,J)=B(I,J)+QB(I,J)*((HGT(IP+1)**2.0-HGT(IP)**2.0)/2.0)
      C(I,J)=C(I,J)+QB(I,J)*((HGT(IP+1)**3.0-HGT(IP)**3.0)/3.0)
      D1(I,J)=D1(I,J)+QB(I,J)*((HGT(IP+1)**4.0-HGT(IP)**4.0)/4.0)
      E(I,J)=E(I,J)+QB(I,J)*((HGT(IP+1)**5.0-HGT(IP)**5.0)/5.0)
      G(I,J)=G(I,J)+QB(I,J)*((HGT(IP+1)**7.0-HGT(IP)**7.0)/7.0)
275   CONTINUE
220   CONTINUE
      DO 280 I=1,13
      DO 280 J=1,13
280   D(I,J)=0.0
      DO 290 I=1,3
      DO 290 J=1,3
      D(I,J)=A(I,J)
      D(I,J+5)=B(I,J)
      D(I,J+10)=D1(I,J)
      D(I+5,J+5)=C(I,J)
      D(I+5,J+10)=E(I,J)
290   D(I+10,J+10)=G(I,J)
      DO 300 I=4,5
      DO 300 J=4,5
      D(I,J)=A(I,J)
      D(I,J+5)=C(I,J)
300   D(I+5,J+5)=E(I,J)
      DO 310 I=1,13
```

```
      DO 310 J=1,13
310   D(J,I)=D(I,J)
      RETURN
      END
      SUBROUTINE BMAT(TH,R,S)
C     ..................................................................
C     .   ROUTINE TO FIND THE STRAIN-DISPLACEMENT MATRIX AT THE       .
C     .                  SAMPLING POINTS                               .
C     ..................................................................
      COMMON/MAT/CARTD(2,4),DERIV(2,4),Q0(5,5),Q90(5,5)
     #,SHAPE(4),BTDB(28,28),F(4),GX(4),HY(4),D(13,13)
      COMMON/DIM/XX(2,4),X(100),Y(100),NODN(100,4)
      COMMON/TRY/BB(13,28),B2(5,13),B(5,28),DB(13,28),
     #BTD(28,5),BT(28,13),FX(4),FXX(4),FXY(4),FYY(4),FY(4),GY(4),
     #GXX(4),GYY(4),GXY(4),HX(4),HXX(4),HYY(4),HXY(4),G(4),H(4)
      DIMENSION RR(4),SS(4)
      DO 309 I=1,13
      DO 309 J=1,28
309   BB(I,J)=0.0
      DO 320 I=1,28
      DO 320 J=1,28
320   BTDB(I,J)=0.0
      DO 330 I=1,28
      DO 330 J=1,13
      DB(J,I)=0.0
330   BT(I,J)=0.0
      C3=-4.0/(3.0*TH**2)
      C2=-4.0/(TH**2)
      AA=XX(1,2)-XX(1,1)
      B1=XX(2,3)-XX(2,2)
      RR(1)=-1.0
      RR(2)=1.0
      RR(3)=1.0
      RR(4)=-1.0
      SS(1)=-1.0
      SS(2)=-1.0
```

```
 SS(3)=1.0
 SS(4)=1.0
 DO 335 I=1,4
 F(I)=0.125*(1.0+R*RR(I))*(1.0+S*SS(I))*
+(2.0+R*RR(I)+S*SS(I)-R*R-S*S)
 DUM=1.0/(4.0*AA)
 FX(I)=DUM*(1.0+S*SS(I))*(RR(I)*(2.0+R*RR(I)+S*SS(I)-R*R-S*S)+
+(1.0+R*RR(I))*(RR(I)-2.0*R))
 DUM=1.0/(4.0*B1)
 FY(I)=DUM*(1.0+R*RR(I))*(SS(I)*(2.0+R*RR(I)+S*SS(I)-R*R-S*S)+
+(1.0+S*SS(I))*(SS(I)-2.0*S))
 DUM=1.0/(2.0*AA*AA)
 FXX(I)=DUM*(RR(I)*(1.0+S*SS(I))*(RR(I)-2.0*R)+(1.0+S*SS(I))*
+(RR(I)**2-4.0*R*RR(I)-2.0))
 DUM=1.0/(2.0*B1*B1)
 FYY(I)=DUM*(1.0+R*RR(I))*(2.0*SS(I)*SS(I)-6.0*S*SS(I)-2.0)
 DUM=1.0/(2.0*AA*B1)
 FXY(I)=DUM*(4.0*RR(I)*SS(I)+2.0*R*RR(I)*RR(I)*SS(I)+
+2.0*S*RR(I)*SS(I)*SS(I)-3.0*R*R*RR(I)*SS(I)-
+3.0*S*S*RR(I)*SS(I)-2.0*R*SS(I)-2.0*S*RR(I))
 DUM=AA/16.0
 G(I)=DUM*RR(I)*(1.0+R*RR(I))**2*(1.0+S*SS(I))*(R*RR(I)-1.0)
 GX(I)=0.125*RR(I)*(1.0+R*RR(I))*(1.0+S*SS(I))*(3.0*R*RR(I)*
+RR(I)-RR(I))
 DUM=1.0/(2.0*AA)
 GXX(I)=DUM*RR(I)**3*(1.0+S*SS(I))*(3.0*R*RR(I)+1.0)
 DUM=1.0/(4.0*B1)
 GXY(I)=DUM*RR(I)*RR(I)*(1.0+R*RR(I))*SS(I)*(3.0*R*RR(I)-1.0)
 DUM=AA/(8.0*B1)
 GY(I)=DUM*RR(I)*SS(I)*(1.0+R*RR(I))**2*(R*RR(I)-1.0)
 GYY(I)=0.0
 DUM=B1/16.0
 H(I)=DUM*SS(I)*(1.0+R*RR(I))*(1.0+S*SS(I))**2*(S*SS(I)-1.0)
 DUM=B1/(8.0*AA)
 HX(I)=DUM*RR(I)*SS(I)*(1.0+S*SS(I))**2*(S*SS(I)-1.0)
 HXX(I)=0.0
```

```
      DUM=1.0/(4.0*AA)
      HXY(I)=DUM*RR(I)*SS(I)*SS(I)*(1.0+S*SS(I))*(3.0*S*SS(I)-1.0)
      HY(I)=0.125*SS(I)*SS(I)*(1.0+R*RR(I))*(1.0+S*SS(I))*
     +(3.0*S*SS(I)-1.0)
      DUM=1.0/(2.0*B1)
335   HYY(I)=DUM*SS(I)**3*(1.0+R*RR(I))*(3.0*S*SS(I)+1.0)
345   FORMAT(5F10.5)
      DO 350 INODE=1,4
      M=INODE-1
      N=M*7
      BB(1,N+1)=CARTD(1,INODE)
      BB(2,N+2)=CARTD(2,INODE)
      BB(3,N+1)=CARTD(2,INODE)
      BB(3,N+2)=CARTD(1,INODE)
      BB(4,N+3)=SHAPE(INODE)
      BB(4,N+5)=FX(INODE)
      BB(4,N+6)=GX(INODE)
      BB(4,N+7)=HX(INODE)
      BB(5,N+4)=SHAPE(INODE)
      BB(5,N+5)=FY(INODE)
      BB(5,N+6)=GY(INODE)
      BB(5,N+7)=HY(INODE)
      BB(6,N+3)=CARTD(1,INODE)
      BB(7,N+4)=CARTD(2,INODE)
      BB(8,N+3)=CARTD(2,INODE)
      BB(8,N+4)=CARTD(1,INODE)
      BB(9,N+3)=C2*SHAPE(INODE)
      BB(9,N+5)=C2*FX(INODE)
      BB(9,N+6)=C2*GX(INODE)
      BB(9,N+7)=C2*HX(INODE)
      BB(10,N+4)=C2*SHAPE(INODE)
      BB(10,N+5)=C2*FY(INODE)
      BB(10,N+6)=C2*GY(INODE)
      BB(10,N+7)=C2*HY(INODE)
      BB(11,N+3)=C3*CARTD(1,INODE)
      BB(11,N+5)=C3*FXX(INODE)
```

```
      BB(11,N+6)=C3*GXX(INODE)
      BB(11,N+7)=C3*HXX(INODE)
      BB(12,N+4)=C3*CARTD(2,INODE)
      BB(12,N+5)=C3*FYY(INODE)
      BB(12,N+6)=C3*GYY(INODE)
      BB(12,N+7)=C3*HYY(INODE)
      BB(13,N+3)=C3*CARTD(2,INODE)
      BB(13,N+4)=C3*CARTD(1,INODE)
      BB(13,N+5)=2.0*C3*FXY(INODE)
      BB(13,N+6)=2.0*C3*GXY(INODE)
      BB(13,N+7)=2.0*C3*HXY(INODE)
350   CONTINUE
      DO 360 I=1,28
      DO 360 J=1,13
360   BT(I,J)=BB(J,I)
      DO 370 I=1,13
      DO 370 J=1,28
      DO 370 K=1,13
370   DB(I,J)=DB(I,J)+D(I,K)*BB(K,J)
      DO 380 I=1,28
      DO 380 J=1,28
      DO 380 K=1,13
380   BTDB(I,J)=BTDB(I,J)+BT(I,K)*DB(K,J)
      RETURN
      END
      SUBROUTINE LOAD(RI,SI,DJACB,WX,WY)
C     .....................................................................
C     .   ROUTINE TO GENERATE ELEMENT LOAD VECTOR FOR SINUSOIDAL         .
C     .                          LOADING                                  .
C     .....................................................................
      DOUBLE PRECISION PI,Q,ALPHA,BETA
      COMMON/GAUS/XG(4,4),WGT(4,4),NINT,TH
      COMMON/ELT/NUMNP,NE,NEDOF,IID(7,100),LM(28,100),MAXA(1000)
     +,NWK,SK(10000),S(28,28),R(150),ELD(28),NEQ,MHT(1000),NEQ1,ND
      COMMON/MAT/CARTD(2,4),DERIV(2,4),Q0(5,5),Q90(5,5)
     #,SHAPE(4),BTDB(28,28),F(4),GX(4),HY(4),D(13,13)
```

```
      COMMON/TRY/BB(13,28),B2(5,13),B(5,28),DB(13,28),
     #BTD(28,5),BT(28,13),FX(4),FXX(4),FXY(4),FYY(4),FY(4),GY(4),
     #GXX(4),GYY(4),GXY(4),HX(4),HXX(4),HYY(4),HXY(4),G(4),H(4)
      COMMON/DIM/XX(2,4),X(100),Y(100),NODN(100,4)
      DIMENSION GPCOD(2)
      PI=4.D0*DATAN(1.D0)
      DO 401 IDIME=1,2
      GPCOD(IDIME)=0.0
      DO 401 INODE=1,4
      GPCOD(IDIME)=GPCOD(IDIME)+SHAPE(INODE)*XX(IDIME,INODE)
401   CONTINUE
      ALPHA=(PI/400.0)*GPCOD(1)
      BETA=(PI/400.0)*GPCOD(2)
      Q=DSIN(ALPHA)*DSIN(BETA)
      P=Q*WX*WY*DJACB
      DO 410 INODE=1,4
      K=(INODE-1)*7
      ELD(K+5)=ELD(K+5)+P*(F(INODE))
      ELD(K+6)=ELD(K+6)+P*(G(INODE))
410   ELD(K+7)=ELD(K+7)+P*(H(INODE))
      RETURN
      END
      SUBROUTINE UDL16(RI,SI,DJACB,WX,WY)
C     .....
C     .  ELEMENT LOAD VECTOR FOR UNIFORMLY DISTRIBUTED LOAD CASE  .
C     .....
      DOUBLE PRECISION PI,Q,ALPHA,BETA
      COMMON/DIM/XX(2,4),X(100),Y(100),NODN(100,4)
      COMMON/ELT/NUMNP,NE,NEDOF,IID(7,100),LM(28,100),MAXA(1000)
     +,NWK,SK(10000),S(28,28),R(150),ELD(28),NEQ,MHT(1000),NEQ1,ND
      COMMON/GAUS/XG(4,4),WGT(4,4),NINT,TH
      COMMON/MAT/CARTD(2,4),DERIV(2,4),QO(5,5),Q90(5,5)
     #,SHAPE(4),BTDB(28,28),F(4),GX(4),HY(4),D(13,13)
      COMMON/TRY/BB(13,28),B2(5,13),B(5,28),DB(13,28),
     #BTD(28,5),BT(28,13),FX(4),FXX(4),FXY(4),FYY(4),FY(4),GY(4),
     #GXX(4),GYY(4),GXY(4),HX(4),HXX(4),HYY(4),HXY(4),G(4),H(4)
```

```
      DIMENSION GPCOD(2)
      PI=4.D0*DATAN(1.D0)
      DO 401 IDIME=1,2
      GPCOD(IDIME)=0.0
      DO 401 INODE=1,4
      GPCOD(IDIME)=GPCOD(IDIME)+SHAPE(INODE)*XX(IDIME,INODE)
401   CONTINUE
      ALPHA=(PI/400.0)*GPCOD(1)
      BETA=(PI/400.0)*GPCOD(2)
      DO 420 I=1,29,2
      DO 420 J=1,29,2
      QMN=16.0/(PI*PI*I*J)
      Q=QMN*DSIN(I*ALPHA)*DSIN(J*BETA)
      P=Q*WX*WY*DJACB
      DO 410 INODE=1,4
      K=(INODE-1)*7
      ELD(K+5)=ELD(K+5)+P*F(INODE)
      ELD(K+6)=ELD(K+6)+P*G(INODE)
410   ELD(K+7)=ELD(K+7)+P*H(INODE)
420   CONTINUE
      RETURN
      END
      SUBROUTINE STRESS(TH)
C     ..................................................................
C     . CALCULATES STRESSES AT 2x2 GAUSS SAMPLING POINTS FOR EACH      .
C     .                          ELEMENTS                              .
C     ..................................................................
      COMMON/ELT/NUMNP,NE,NEDOF,IID(7,100),LM(28,100),MAXA(1000)
     +,NWK,SK(10000),S(28,28),R(150),ELD(28),NEQ,MHT(1000),NEQ1,ND
      COMMON/DIM/XX(2,4),X(100),Y(100),NODN(100,4)
      COMMON/MAT/CARTD(2,4),DERIV(2,4),Q0(5,5),Q90(5,5)
     #,SHAPE(4),BTDB(28,28),F(4),GX(4),HY(4),D(13,13)
      COMMON/TRY/BB(13,28),B2(5,13),B(5,28),DB(13,28),
     #BTD(28,5),BT(28,13),FX(4),FXX(4),FXY(4),FYY(4),FY(4),GY(4),
     #GXX(4),GYY(4),GXY(4),HX(4),HXX(4),HYY(4),HXY(4),G(4),H(4)
      DIMENSION Z(4),X1(4),Y1(4),ST(5),STR(5),SMU(4,4),Q(4,5,5)
```

```
     +,STRS(20),SIG(4),STRES(16,4,20),SIGN(4),RR(28)
      Z(1)=-TH/2.0
      Z(2)=-TH/4.0
      Z(3)=-TH/4.0
      Z(4)=0.0
      X1(1)=-0.57735
      X1(2)=0.57735
      X1(3)=0.57735
      X1(4)=-0.57735
      Y1(1)=-0.57735
      Y1(2)=-0.57735
      Y1(3)=0.57735
      Y1(4)=0.57735
      DO 1000 I=1,20
1000  STRS(I)=0.0
      DO 1112 I=1,NE
      DO 1112 J=1,4
      DO 1112 K=1,20
1112  STRES(I,J,K)=0.0
      DO 3 I=1,4
      DO 2 J=1,4
2     SMU(I,J)=0.0
3     SMU(I,I)=1.866
      SMU(1,2)=-.5
      SMU(1,3)=0.1339
      SMU(1,4)=-0.5
      SMU(2,3)=-0.5
      SMU(2,4)=0.1339
      SMU(3,4)=-0.5
      DO 4 I=1,4
      DO 4 J=1,4
4     SMU(J,I)=SMU(I,J)
      DO 11 I=1,5
      DO 11 J=1,5
      Q(1,I,J)=QO(I,J)
      Q(2,I,J)=QO(I,J)
```

```
      Q(3,I,J)=Q90(I,J)
11    Q(4,I,J)=Q90(I,J)
      DO 10 IELEM=1,16
      DO 501 I=1,28
501   RR(I)=0.0
      DO 20 I=1,28
      K=LM(I,IELEM)
      IF(K.EQ.0)GOTO 30
      RR(I)=R(K)
      GOTO 20
30    RR(I)=0.0
20    CONTINUE
      I1=NODN(IELEM,1)
      I2=NODN(IELEM,2)
      I3=NODN(IELEM,3)
      I4=NODN(IELEM,4)
      XX(1,1)=X(I1)
      XX(1,2)=X(I2)
      XX(1,3)=X(I3)
      XX(1,4)=X(I4)
      XX(2,1)=Y(I1)
      XX(2,2)=Y(I2)
      XX(2,3)=Y(I3)
      XX(2,4)=Y(I4)
      DO 12 IZ=1,4
      DO 502 I=1,5
      DO 502 J=1,13
502   B2(I,J)=0.0
      DO 6 I=1,5
6     B2(I,I)=1.0
      DO 7 I=1,3
      J=I+5
7     B2(I,J)=Z(IZ)
      DO 8 I=4,5
      J=I+5
8     B2(I,J)=Z(IZ)**2
```

```
      DO 9 I=1,3
      J=10+I
    9 B2(I,J)=Z(IZ)**3
      KGAUS=0
      DO 40 LX=1,4
      R1=X1(LX)
      S1=Y1(LX)
      KGAUS=KGAUS+1
      CALL SFR(R1,S1;DJACB)
      CALL BMAT(TH,R1,S1)
      DO 49 I=1,5
      DO 49 J=1,28
   49 B(I,J)=0.0
      DO 50 I=1,5
      DO 50 J=1,28
      DO 50 K=1,13
   50 B(I,J)=B(I,J)+B2(I,K)*BB(K,J)
      DO 505 I=1,5
  505 ST(I)=0.0
      DO 55 I=1,5
      DO 55 J=1,28
   55 ST(I)=ST(I)+B(I,J)*RR(J)
      DO 800 I=1,5
  800 STR(I)=0.0
      DO 70 I=1,5
      DO 60 J=1,5
   60 STR(I)=STR(I)+Q(IZ,I,J)*ST(J)
      K=(KGAUS-1)*5+I
   70 STRS(K)=STR(I)
   40 CONTINUE
      DO 80 I=1,5
      DO 53 K=1,4
   53 SIGN(K)=0.0
      SIG(1)=STRS(I)
      SIG(2)=STRS(I+5)
      SIG(3)=STRS(I+10)
```



36 lines *

```
      SIG(4)=STRS(I+15)
C     .....................................................
C     .  STRESSES ARE OBTAINED AT 2X2 GAUSS POINTS. THESE VALUES  .
C     .  ARE NORMALISED USING THE TECHNIQUE OF LOCAL STRESS SMOOTH- .
C     .  ENING AND THESE STRESSES WILL BE TRANSFERED TO THE CORNER  .
C     .  NODES IN THE FOLLOWING FEW STEPS                           .
C     .....................................................
      DO 90 I1=1,4
      DO 90 J1=1,4
 90   SIGN(I1)=SIGN(I1)+SMU(I1,J1)*SIG(J1)
      DO 100 I1=1,4
      K=(I-1)*4+I1
      STRES(IELEM,IZ,K)=SIGN(I1)
100   CONTINUE
 80   CONTINUE
 12   CONTINUE
 10   CONTINUE
      WRITE(2,*)'STRESS'
      DO 120 I=1,16,15
      DO 120 J=1,4
      WRITE(2,*)'ELEMENT & LEVEL ARE =',I,J
120   WRITE(2,999)(STRES(I,J,K),K=1,20)
999   FORMAT(4(E20.10,1X))
      RETURN
      END
```